Dissertation

Zur Erlangung eines Doktorgrades der Naturwissenschaften

Controlling Ras activity by manipulating its localization

vorgelegt von

Holger Vogel

bei der Fakultät für Chemie und Chemische Biologie

an der Technischen Universität Dortmund

November 2018

Diese Arbeit wurde am Max-Planck-Institut für molekulare Physiologie in Dortmund angefertigt.

1. Gutachter: Prof. Dr. Philippe I.H. Bastiaens

2. Gutachter: PD. Dr. Leif Dehmelt

Eidesstattliche Versicherung (Affidavit)

_____ _____

Name, Vorname
(Surname, first name)

Matrikel-Nr.
(Enrolment number)

Belehrung:

Wer vorsätzlich gegen eine die Täuschung über Prüfungsleistungen betreffende Regelung einer Hochschulprüfungsordnung verstößt, handelt ordnungswidrig. Die Ordnungswidrigkeit kann mit einer Geldbuße von bis zu 50.000,00 € geahndet werden. Zuständige Verwaltungsbehörde für die Verfolgung und Ahndung von Ordnungswidrigkeiten ist der Kanzler/die Kanzlerin der Technischen Universität Dortmund. Im Falle eines mehrfachen oder sonstigen schwerwiegenden Täuschungsversuches kann der Prüfling zudem exmatrikuliert werden, § 63 Abs. 5 Hochschulgesetz NRW.

Die Abgabe einer falschen Versicherung an Eides statt ist strafbar.

Wer vorsätzlich eine falsche Versicherung an Eides statt abgibt, kann mit einer Freiheitsstrafe bis zu drei Jahren oder mit Geldstrafe bestraft werden, § 156 StGB. Die fahrlässige Abgabe einer falschen Versicherung an Eides statt kann mit einer Freiheitsstrafe bis zu einem Jahr oder Geldstrafe bestraft werden, § 161 StGB.

Die oben stehende Belehrung habe ich zur Kenntnis genommen:

Official notification:

Any person who intentionally breaches any regulation of university examination regulations relating to deception in examination performance is acting improperly. This offence can be punished with a fine of up to EUR 50,000.00. The competent administrative authority for the pursuit and prosecution of offences of this type is the chancellor of the TU Dortmund University. In the case of multiple or other serious attempts at deception, the candidate can also be unenrolled, Section 63, paragraph 5 of the Universities Act of North Rhine-Westphalia.

The submission of a false affidavit is punishable.

Any person who intentionally submits a false affidavit can be punished with a prison sentence of up to three years or a fine, Section 156 of the Criminal Code. The negligent submission of a false affidavit can be punished with a prison sentence of up to one year or a fine, Section 161 of the Criminal Code.

I have taken note of the above official notification.

_____ _____

Ort, Datum
(Place, date)

Unterschrift
(Signature)

Titel der Dissertation:
(Title of the thesis):

_____

_____

_____

Ich versichere hiermit an Eides statt, dass ich die vorliegende Dissertation mit dem Titel selbstständig und ohne unzulässige fremde Hilfe angefertigt habe. Ich habe keine anderen als die angegebenen Quellen und Hilfsmittel benutzt sowie wörtliche und sinngemäße Zitate kenntlich gemacht.
Die Arbeit hat in gegenwärtiger oder in einer anderen Fassung weder der TU Dortmund noch einer anderen Hochschule im Zusammenhang mit einer staatlichen oder akademischen Prüfung vorgelegen.

I hereby swear that I have completed the present dissertation independently and without inadmissible external support. I have not used any sources or tools other than those indicated and have identified literal and analogous quotations.

The thesis in its current version or another version has not been presented to the TU Dortmund University or another university in connection with a state or academic examination.*

*Please be aware that solely the German version of the affidavit ("Eidesstattliche Versicherung") for the PhD thesis is the official and legally binding version.

_____ _____

Ort, Datum
(Place, date)

Unterschrift
(Signature)

Table of contents

1 Abstract

Proteins of the Ras family of small GTPases play a major role in the transduction of extracellular signals, especially growth factor signals, into the cell. Ras proteins thereby participate in the regulation of critical processes like cellular growth and proliferation. Due to this central role, gain-of-function mutations of these proteins can have severe consequences for the mutated cells including uncontrolled proliferation and these mutations are often connected to development of diseases including cancers of various tissues. Thereby, plasma membrane localization is crucial for the activity of Ras proteins. They not just recruit their effectors to the plasma membrane to facilitate their activation, the activation of Ras proteins is also highly dependent on plasma membrane localization.

Due to the dependence of Ras activity on plasma membrane localization, modified Ras proteins, whose localization within the cell can be controlled externally, could be useful tools to control Ras activity. Hence, in this work plasma membrane recruitable Ras proteins have been engineered that incorporate two different dimerization approaches based on chemically induced dimerization allowing translocation of either wild type or oncogenically mutated KRas proteins from the cytosol to the plasma membrane in a highly controllable manner. Contrary to the widespread believe that Ras carrying an oncogenic mutation is always in the GTP-bound active state, cytosolic recruitable Ras is just partially active. However, the inactive fraction of recruitable oncogenic Ras becomes activated upon plasma membrane recruitment suggesting that RasGEFs are necessary to maintain the activity of oncogenic Ras at the plasma membrane. Further, recruitment of oncogenic Ras to the plasma membrane sensitized the cellular ERK phosphorylation response to growth factor stimulation.

Using light-induced recruitment of oncogenic Ras to the plasma membrane, it could be shown that Ras activity can be propagated to surrounding cells highlighting a potential mechanism allowing Ras transformed cells to influence adjacent cells.

2 Zusammenfassung

Die Proteine der Ras Superfamilie gehören zu den kleinen GTPasen und erfüllen eine bedeutende Aufgabe bei der Weiterleitung biologischer Signale vom Zelläußeren ins Zellinnere, insbesondere von Wachstumsfaktorsignalen. Durch diesen Vorgang tragen sie zur der Regulierung äußerst wichtiger zellulärer Prozesse wie Wachstum und Proliferation bei und erhalten dadurch eine zentrale Bedeutung in der Steuerung zellulärer Prozesse. Aufgrund dessen führen *gain-of-function* Mutationen dieser Proteine zu ernsthaften Konsequenzen, sie können beispielsweise unkontrolliertes Zellwachstum sowie unterschiedlichste Krankheiten, einschließlich Krebserkrankungen verschiedenster Gewebe, auslösen. Hierbei ist die Lokalisation der Ras-Proteine an der Innenseite der Plasmamembran für deren Aktivität von herausragender Bedeutung: sie rekrutieren nicht nur ihre Effektoren zu deren Aktivierung an die Plasmamembran, sondern können selbst auch nur dort aktiviert werden.

Da die Aktivität von Ras-Proteinen stark von ihrer korrekten Lokalisation dieser Proteine an der Plasmamembran abhängt, könnten modifizierte Ras-Proteine, deren Lokalisation von außen beeinflusst werden kann, ein nützliches Werkzeug zur Kontrolle der Ras-Aktivität sein. Dazu sollen in dieser Arbeit zur Plasmamembran rekrutierbare Ras-Proteine auf Basis zweier verschiedener chemisch induzierbarer Dimerisierungstechniken erstellt werden, die sowohl die kontrollierte Translokation des Wildtyps als auch von onkogen mutiertem KRas aus dem Zytosol an die Plasmamembran erlauben.

Durch die Anwendung dieser neu generierten Werkzeuge zur Kontrolle der Ras-Aktivität, konnte gezeigt werden, dass – entgegen der weitverbreiteten Meinung – mutierte Ras-Proteine durchaus nicht immer im GTP-gebundenen aktiven Zustand innerhalb der Zelle vorliegen und zytosolisches onkogenes Ras nur partiell GTP-gebunden ist. Der inaktive Teil des onkogenen Ras wird jedoch bei Rekrutierung an die Plasmamembran aktiviert, was darauf hindeutet, dass RasGEFs notwendig sind um die Aktivität von onkogenem Ras an der Plasmamembran aufrechtzuerhalten. Des Weiteren führt die Rekrutierung von onkogenem Ras an die Plasmamembran zu einer Sensibilisierung der Antwort der zellulären ERK Phosphorylierung auf Stimulation mit Wachstumsfaktoren.

Bei der lichtinduzierten Rekrutierung von onkogenem Ras an die Plasmamembran konnte gezeigt werden, dass die dadurch induzierte Ras-Aktivität an benachbarte Zellen weitergeleitet werden kann. Hierdurch wird aufgezeigt, dass Ras transformierte Zellen in der Lage sind, andere Zellen in ihrer Umgebung zu beeinflussen.

3 Introduction

A key ability of living organisms is the ability to perceive their environment and being able to adapt to their surroundings in order to survive and to proliferate. Thereby, cells must be able to not just sense environmental cues like nutrition, but also other cells, and must be able to communicate with them. This ability to communicate with other cells is widespread in nature: it can be observed in bacteria, which are able to interact with each other for instance to form larger structures consisting of many individuals called biofilms (Bassler 2002), as well as in more complex plants and animals. In these multicellular organisms, cell-cell communication allows the control of behavior and function of the individual cells within an organism. This coordination is the basis for many important processes like development, wound healing and tissue homeostasis.

To be able to communicate with each other, a signal has to be able to cross the cellular boundary, in case of animal cells the plasma membrane, of both the transmitting cell as well as the receiving cell. This can be facilitated by either lipophilic molecules (e.g. hormones), which can pass the plasma membrane and reach their target molecule randomly by diffusion, direct contact between the cytoplasms of two adjacent cells mediated by gap junctions, or by release of molecules which cannot cross the plasma membrane by either exocytosis (e.g. neurotransmitters) or cleavage of membrane bound signaling molecules (e.g. growth factors like the epidermal growth factor EGF). Latter interact with cell surface receptors leading to a conformational change of the receptor allowing the transduction of the signal from the outside to the inside of the receiving cell. There are three types of cell surface receptors: Ion channels that form a pore permeable for specific ions upon interaction with extracellular ligands, G-protein coupled receptors that release a G-protein and enzyme-linked cell surface receptors that possess an enzymatic activity in their intracellular domain, which becomes active upon extracellular interaction with the signaling molecule (Alexander, Mathie et al. 2011). Most enzyme-linked receptors belong to the superfamily of receptor tyrosine kinases (RTKs). One subfamily of RTKs is the family of ErbB receptors containing the well-studied RTK ErbB1 also known as epidermal growth factor receptor (EGFR). Upon binding of the ligand EGF to EGFR, EGFR forms an asymmetric dimer leading to the activation of the intracellular kinase domain and phosphorylation of EGFR on several tyrosine residues (Zhang, Gureasko et al. 2006). The activation of the kinase domain of EGFR as well as the phosphorylation of tyrosine residues initiate a wide range of signaling processes (Schlessinger 2000). One of those is the recruitment of Grb2 whose SH2 domain binds a phosphorylated tyrosine residue of EGFR (Lowenstein, Daly et al. 1992). Grb2 can tether guanine nucleotide exchange factors (GEFs) of Rat sarcoma (Ras) proteins to the plasma membrane leading to their activation. These proteins are signaling hubs and an essential mechanism to spread the input information within the cell. Thereby the signal is processed and can result in a changed cellular behavior that then can be communicated to its neighbors.

3.1 Small GTPases of the Ras family

The research in the field of Ras proteins began when Harvey and Kirsten discovered in 1964 and 1967, respectively, that a virus collected from a leukemic rat could induce sarcoma in newborn rats (Harvey 1964, Kirsten and Mayer 1967). Later, it was found that a small GTPase of 21 kilo Dalton (kDa) can be found in these viruses and is responsible for this transformation. This ability to induce *ra*t *s*arcoma gave name to the Ras proteins. The early discovery also made Ras the founding member of the Ras superfamily having more than 150 members in human (Wennerberg, Rossman et al. 2005). The Ras superfamily can be divided in the subfamilies of Arf, Rab, Ran, Ras and Rho GTPases all sharing molecular similarities.

3.1.1 Activity cycle of Ras proteins

All members of the Ras subfamily share the catalytically active G-domain that is capable of hydrolyzing guanosine-5'-triphosphate (GTP) to guanosine-5'-diphosphate (GDP). The G-domain has a high picomolar affinity for GDP as well as GTP (John, Sohmen et al. 1990). The G-domain contains two switch regions – named switch I and switch II – that undergo conformational changes depending on the bound nucleotide: while the switch regions are more structured in the GTP-bound state when the crystal structures of several GTPases of the Ras superfamily are superimposed, the structure of these two regions is lost in the GDP-bound state (Vetter and Wittinghofer 2001). These conformational differences in the switch regions play an important role in the activity of the Ras GTPases: while it is impossible to interact with effector proteins in the unstructured GDP-bound state, they are able to interact with Ras-binding or Ras association domains of their effectors in the structured GTP-bound state (Nassar, Horn et al. 1995, Ponting and Benjamin 1996). Therefore, the GTP-bound form is considered the active "on" state, while the GDP-bound state of the GTPase is also referred to as inactive "off" state. Because Ras proteins can be in these two distinct states *in vivo*, they are often denoted as binary molecular switches.

In vivo, a rapid transient activation of Ras can be observed upon growth factor stimulation(Satoh, Endo et al. 1990, Osterop, Medema et al. 1993). However, an uncatalyzed transition between these two states is slow and does not match to the observed fast switching between the two states. In order to transition from the GDP-bound to the GTP-bound state, the GDP nucleotide has to be released so a different GTP molecule can replace it, which is present at a ten-fold excess over GDP in the cytoplasm (Trahey and McCormick 1987, Bos, Rehmann et al. 2007). Due to the picomolar affinity for GDP, this process is slow. Similarly, the transition from the active, GTP-bound state to the GDP-bound state is slow since Ras proteins possess a low catalytic rate constant of $2 \times 10^{-4}\ s^{-1}$ (Scheffzek, Ahmadian et al. 1997, Hall, Bar-Sagi et al. 2002). Two types of auxiliary proteins facilitate the transition between the two states: Ras guanine nucleotide exchange factors (RasGEFs) catalyze the transition between the GDP-bound state and the GTP-bound state, while GTPase activating proteins (GAPs) help transitioning from the active to the inactive state by increasing the

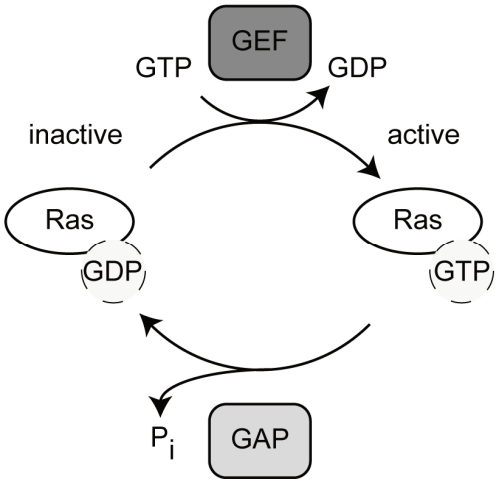

Figure 1: GTPase cycle of Ras family proteins.

Depending on external cues, Ras GTPases can cycle between the inactive, GDP-bound and the active, GTP-bound state. While RasGEFs facilitate the transition between the inactive and the active state, RasGAPs increase hydrolysis and the release of a phosphate ion (Pi) allowing transition from the active to the inactive state.

rate of GTP hydrolysis (Figure 1). This mechanism allows Ras proteins to cycle between the active and the inactive state.

3.1.2 Regulation of Ras protein activity by GEFs and GAPs

Ras protein activity is tightly regulated by GEFs and GAPs to prevent aberrant activity (Figure 1). The interaction between RasGEFs and Ras leads to an activation of the GTPase. Thereby, GEFs alter the nucleotide-binding site of Ras leading to the release of the Mg^{2+} co-factor necessary for nucleotide binding, which causes a decrease of the affinity and in the end release of the bound nucleotide (Boriack-Sjodin, Margarit et al. 1998). After dissociation of the GEF, Ras proteins quickly bind another nucleotide due to the picomolar affinity for them. Even though the affinity of Ras for GDP and GTP are almost equal, Ras protein become mostly GTP loaded since this nucleotide is about ten times more abundant in the cellular cytoplasm (Vetter and Wittinghofer 2001).

In human, there are three families of RasGEFs: the two members of the son of sevenless (SOS) family, Ras guanine nucleotide releasing proteins (RasGRPs) and Ras guanine nucleotide releasing factors (RasGRFs). While RasGEFs of the SOS family are ubiquitously expressed, GEFs of the RasGRP and RasGRF families are primarily expressed in the central nervous system and in B- and T-cells (Stone 2011, Jun, Rubio et al. 2013, Uhlen, Zhang et al. 2017).

All three families of RasGEFs share two protein domains responsible for the guanine nucleotide exchange: a Ras exchange motif (REM) and a Cdc25 homology domain. Other protein domains vary between the families and are involved in their regulation.

The SOS family of RasGEFs differs from the other families since these proteins possess a second allosteric Ras binding site within the REM/Cdc25 domains (Boriack-Sjodin, Margarit et al. 1998, Margarit, Sondermann et al. 2003). This allosteric site preferably binds GTP loaded active Ras over GDP bound Ras leading to a stabilization of the catalytically active binding site of SOS. It could be shown that the binding of active Ras at the allosteric site enhances the activity of SOS by approximately 75-fold (Freedman, Sondermann et al. 2006). This enhancement of catalytic activity by the reaction product resembles a positive feedback loop and leads to the switch-like activation of Ras (Boykevisch, Zhao et al. 2006).

Under resting conditions, SOS proteins are located in the cytosol where they form a complex with the adapter protein Grb2 via the interaction of a proline rich domain at the N-terminus of SOS with a SH3 domain of Grb2. In this case, SOS is locked in an auto-inhibited conformation to prevent spontaneous Ras activation by random encounters with Ras. Thereby, the N-terminal histone-like fold (HF), Dbl homology (DH) and pleckstrin homology (PH) domains of SOS are of importance. The DH-PH domains sterically block the allosteric site of the REM-Cdc25 domains and on top the HF domain stabilizes the auto-inhibited conformation by binding to the DH-PH domains as well as the REM-Cdc25 domains (Sondermann, Soisson et al. 2004, Gureasko, Kuchment et al. 2010).

Activation of SOS is facilitated by translocation to the plasma membrane upon growth factor stimulation leading to tyrosine phosphorylation of the cell surface receptors. The SH2 domains of Grb2 can interact with these phosphorylated tyrosine residues and thereby recruit SOS to the plasma membrane. There, the auto-inhibited conformation of SOS can be released by protein-lipid interaction of the N-terminal domains of SOS and phosphatidylinositol 4,5-bisphosphate (PIP_2) (Gureasko, Galush et al. 2008).

The intrinsic hydrolysis of GTP to GDP by Ras GTPases is slow (John, Schlichting et al. 1989). Therefore, auxiliary proteins (RasGAPs) enhancing the GTPase activity of Ras are needed. These proteins are able to increase the GTP hydrolysis of Ras by a factor of 10^5 (Gideon, John et al. 1992). The interaction between the GAP and Ras leads to a rearrangement of the active site of the GTPase (Scheffzek, Ahmadian et al. 1997). Glutamine 61 is involved in the coordination of the water molecule required for hydrolysis. This allows a nucleophilic attack of a water molecule leading to the hydrolysis of GTP to GDP putting Ras proteins in the inactive state.

3.1.3 Ras isoforms and their cellular localization

Of the 35 genes of the Ras family, three Ras genes are ubiquitously expressed and therefore considered the major isoforms: *HRAS*, *KRAS* and *NRAS*. While *HRAS* and *NRAS* each encode one protein, *KRAS* transcripts contain two variants of exon 4 that can be alternatively spliced resulting in two different proteins named after the respective exon: KRas4A and KRas4B. KRas4B is usually expressed at higher levels when compared to KRas4A. However, there are tissue dependent variations of the expression ratio (Plowman, Berry et al. 2006, Tsai, Lopes et al. 2015, Newlaczyl, Coulson et al. 2017). Further, differential expression of the splice variant can be observed in cancer cell lines of the same tissue. Since KRas4B is usually dominantly expressed, it is often abbreviated to KRas.

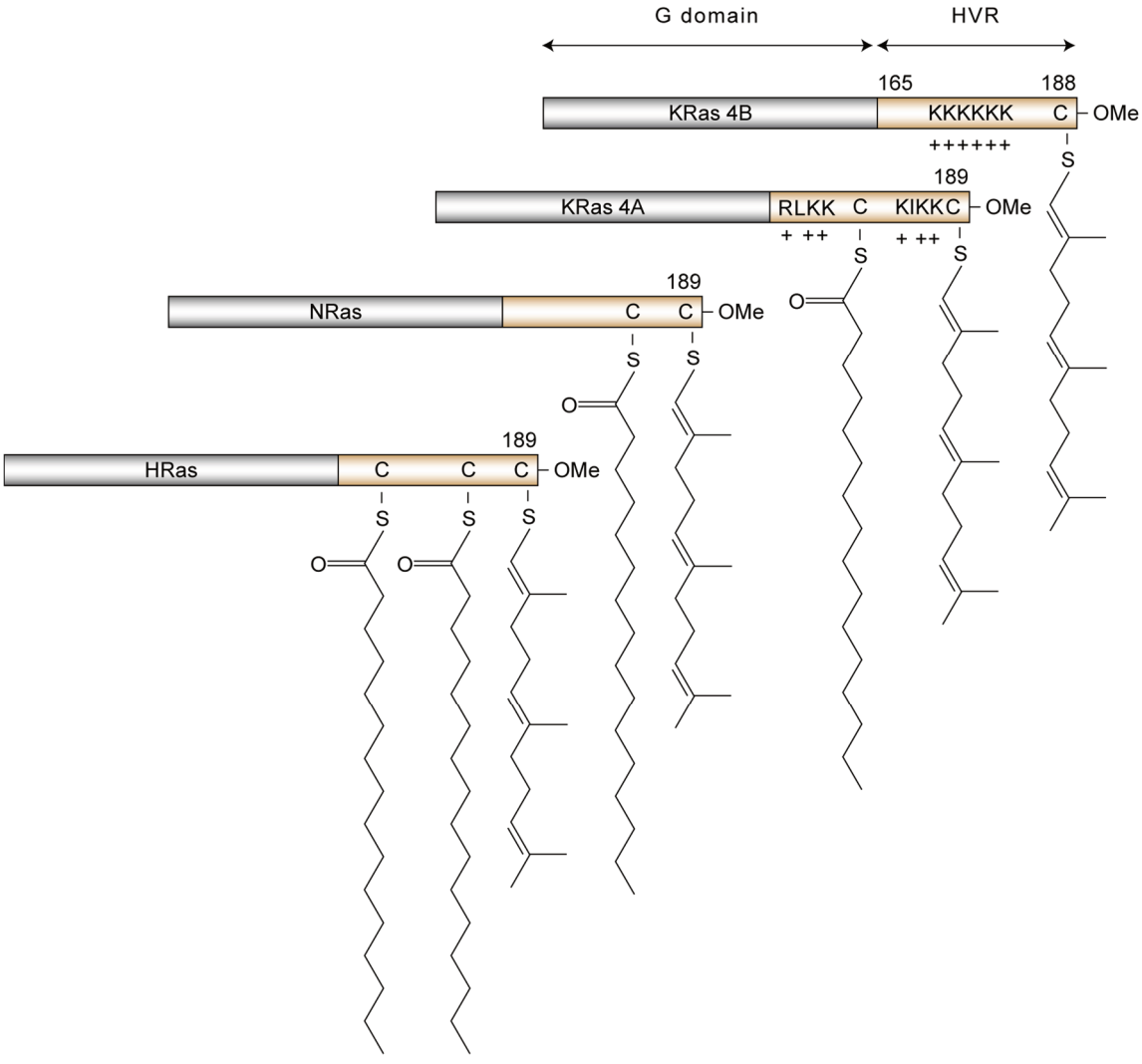

Figure 2: Posttranslational modifications of the different Ras isoforms.

While the first 165 amino acids (grey background) between the different isoforms are homologous the last 23 to 24 amino acids vary between the isoforms and are therefore called hypervariable region (HVR). This HVR is posttranslationally modified and tethers Ras proteins to membranes. All isoforms are farnesylated, the two splice variants of KRas contain positively charged residues. KRas4A, NRas and HRas are also palmitoylated to increase membrane affinity.

3.1.3.1 Posttranslational modifications of Ras

The products of the three major Ras genes share a high degree of similarity. They all encode a protein of 188 - 189 amino acids with a molecular weight of approximately 21 kDa. The first 167 amino acids of the different isoforms are homologous (94 % identical) and encode the catalytically active GTPase-domain. The C-terminal amino acids lack this homology and vary a lot between the three Ras isoforms. Therefore, this region of the Ras proteins is called hypervariable region (HVR). Despite the variability, the HVR is fulfilling the same function in all isoforms: targeting the Ras proteins to membranes (Figure 2) (Willumsen, Christensen et al. 1984). All isoforms share a common CAAX motif at the C-terminus. This motif consisting of a cysteine (C), two aliphatic amino acids (A) and any amino acid (X) is widespread and undergoes S-prenylation *in vivo* (Wang and Casey 2016). In the case of Ras proteins, the cysteine residue is irreversibly S-farnesylated by a farnesyl transferase, subsequently the AAX amino acids are cleaved by the Ras converting enzyme 1 (RCE1) and the carboxy-terminus is transformed into the methylester by the protein-S-isoprenylcysteine O-methyltransferase (ICMT) (Wright and Philips 2006, Ahearn, Haigis et al. 2011). The added hydrophobic farnesyl moiety increases the affinity of Ras proteins for membranes. Further, methoxylation of the C-terminus decreases electrostatic repulsion between the protein and negatively charged lipids.

Besides the farnesylation, all Ras proteins have a second membrane-targeting motif that differs between the isoforms. While NRas and KRas4A have one additional cysteine residue in their HVR, HRas two additional cysteine residues (Buss and Sefton 1986, Hancock, Magee et al. 1989). These cysteine residues can be reversibly S-palmitoylated by the palmitoyl-S-transferases DHHC9 and GCP16 at the Golgi apparatus (Magee, Gutierrez et al. 1987, Swarthout, Lobo et al. 2005). The hydrophobicity of the fatty acid added to the protein increases the affinity for membranes. KRas4B has no further cysteine residues in its HVR that could be modified. However, this isoform contains a polybasic stretch consisting of six lysine residues in its HVR. Under physiological pH, lysine residues are positively and can electrostatically interact with negatively charged lipids of membranes (Hancock, Paterson et al. 1990). Besides the palmitoylation, KRas4A possess two small polybasic stretches containing lysine and arginine residues.

3.1.3.2 Maintaining the localization of Ras at the plasma membrane

Unlike proteins containing a transmembrane domain, the posttranslational modifications of Ras lead to a rather weak interaction with membranes allowing frequent dissociation and re-association (Leventis and Silvius 1998, Silvius, Bhagatji et al. 2006). Further Ras proteins are depleted from the plasma membrane by endocytosis. During trafficking through the endosomal compartments, the lipid composition of the endosomes changes resulting in a lower density of negative charge. This allows KRas4B to dissociate more easily from the membrane. Palmitoylated

Ras proteins can be depalmitoylated by acyl protein thioesterases (APTs) acting in this area of the cell decreasing their membrane affinity (Rocks, Peyker et al. 2005, Vartak, Papke et al. 2014).

In equilibrium, this would lead to a distribution of Ras proteins over all cellular membranes the majority being endomembranes (Schmick, Vartak et al. 2014). If the Ras localization is observed *in vivo*, Ras proteins are primarily localized at the plasma membrane despite the excessive volume of endomembranes. Therefore, there has to be an energy driven process that is counteracting this tendency (Schmick, Kraemer et al. 2015).

Main drivers of the process that keeps Ras proteins at plasma membrane are the δ-subunit of the phosphodiesterase 6 (PDEδ) as well as two members of the Arf-like family of GTPases (Arl) Arl2 and Arl3 (Figure 3). When Ras proteins dissociate from membranes, the farnesylated C-terminus can be bound by farnesyl-binding pocket of PDEδ (Zhang, Liu et al. 2004, Chandra, Grecco et al. 2011, Dharmaiah, Bindu et al. 2016). This shielding of the farnesyl moiety from the cytosol prevents re-association of Ras proteins with membranes. GTP-bound Arl2 and Arl3 can interact with PDEδ at an allosteric site resulting in a conformational change of PDEδ that is most dramatic in the region of the farnesyl-binding pocket (Ismail, Chen et al. 2011). This conformational change closes this pocket and releases the Ras GTPase from PDEδ. It has been hypothesized, that Arl2 activity is restricted to the perinuclear area. Upon release, Ras proteins are able to dynamically interact with any endomembrane in their proximity (Schmick, Kraemer et al. 2015). In certain regions of the perinuclear region, the Ras proteins can be trapped increasing their dwell time in

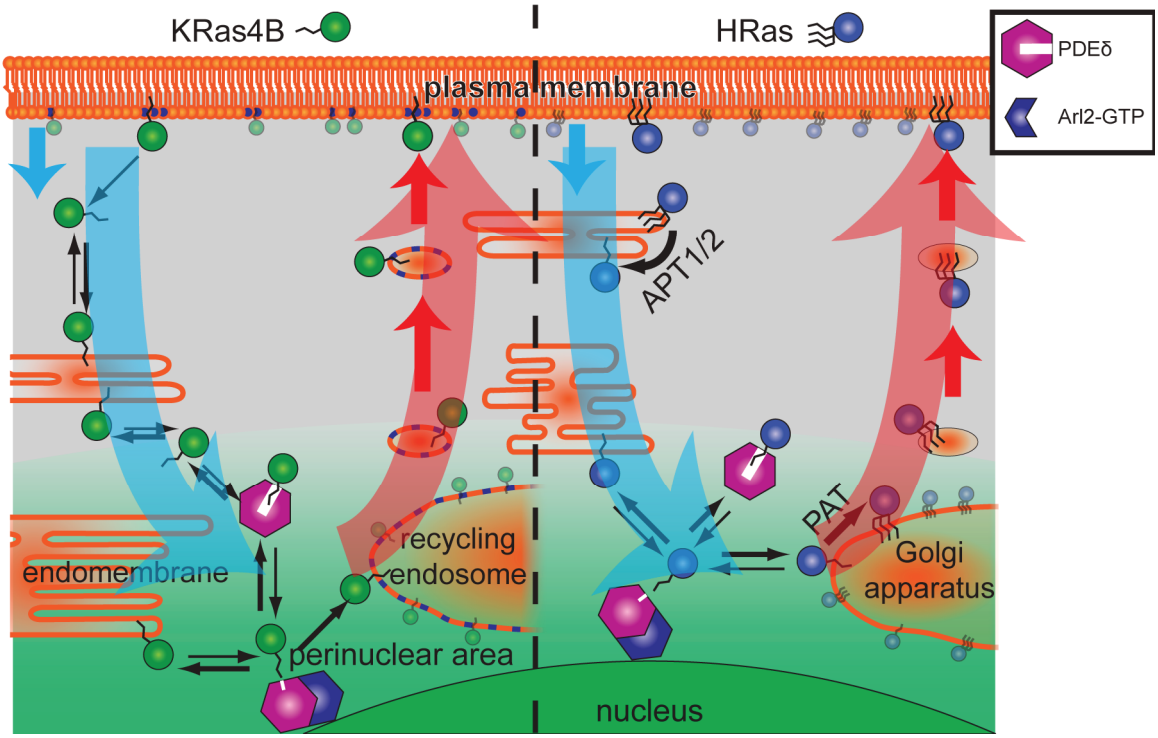

Figure 3: PDEδ/Arl mediated cycle to maintain Ras proteins at cellular compartments (Schmick, Kraemer et al. 2015).

these compartments: KRas4B with its polybasic stretch can be electrostatically trapped at the surface of the recycling endosome having a higher density of negative charges than other compartments of the perinuclear area (Schmick, Vartak et al. 2014, Schmick, Kraemer et al. 2015). In contrast, Ras isoforms that become palmitoylated can be trapped at the Golgi complex, where protein acyl transferases are localized that palmitoylate Ras and thereby palmitoylation increase its affinity for membranes. From the recycling endosome and the Golgi apparatus, the vesicle associated Ras proteins can be brought to the plasma membrane by directed vesicular transport leading to their enrichment in this cellular compartment.

3.1.4 The role of Ras in cellular signaling

The main role of Ras proteins in cellular signaling is to serve as a signaling hub, to relay and to amplify an input signal (Figure 4). Ras activation is usually dependent on an extracellular input signal that binds to a cell surface receptor. Often these receptors are RTKs like EGFR that become auto-phosphorylated and therefore activated by ligand binding. This leads to recruitment of SOS to the plasma membrane releasing it from its autoinhibited conformation. Active SOS can exchange the bound nucleotide of Ras leading to its activation. Besides RTKs, G-protein coupled receptors (GPCRs) can induce Ras activation as well. However, this can be dependent on the activation of RTKs (Daub, Weiss et al. 1996, Downward 2003). Ras cannot just be activated by cell surface receptors: Proteins of the Src family are also able to activate Ras proteins either directly or indirectly (van der Geer, Wiley et al. 1996, Bunda, Heir et al. 2014).

3.1.4.1 Ras in MAPK signaling

The first discovered and most well studied effectors of Ras are the Raf family kinases (Moodie, Willumsen et al. 1993, Vojtek, Hollenberg et al. 1993, Warne, Viciana et al. 1993, Zhang, Settleman et al. 1993). These kinases are an integral part of the mitogen activated protein kinase (MAPK)

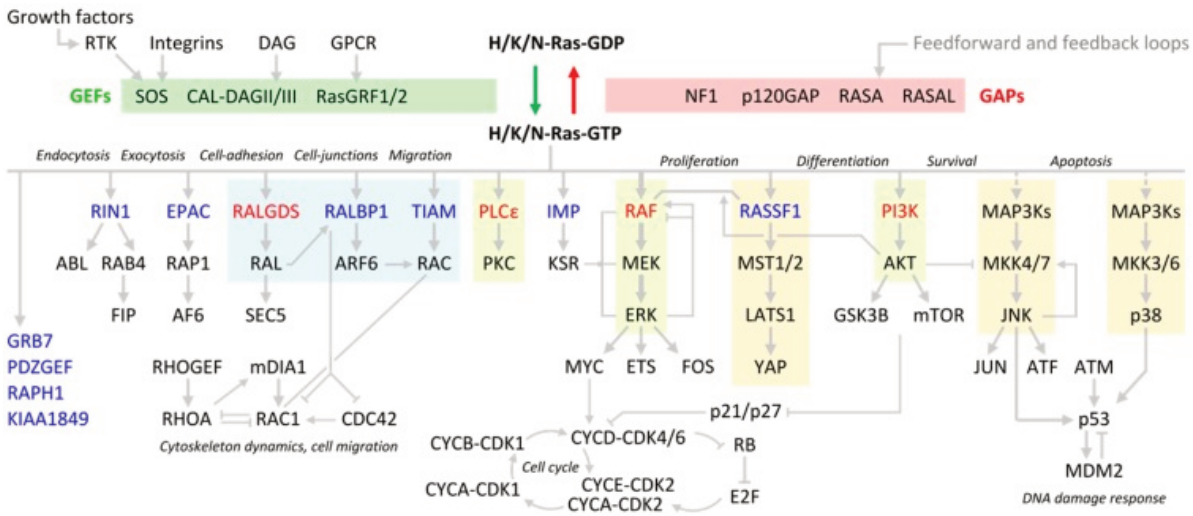

Figure 4: Simplified scheme of the Ras signaling network. Well-established Ras effectors are depicted in red, putative effectors in blue (Fey, Matallanas et al. 2016).

signaling network. The GTP-loading of Ras and the resulting conformational change within the switch regions creates an interface allowing the binding of Raf family kinases resulting in Raf recruitment to the plasma membrane. This recruitment leads to an effective concentration increase since the proteins that were distributed in a three-dimensional volume are now located on a two-dimensional surface. Further, the diffusion speed of Raf is reduced since it is now in complex with membrane anchored Ras. These factors increase the probability for formation of Raf dimers that is needed for the transactivation of Raf (Yarden and Tarcic 2013). Thereby, two Raf molecules, which can be different isoforms, form an asymmetric dimer consisting of an activator and a receiver kinase, in which the former activates the latter by cis-autophosphorylation (Hu, Stites et al. 2013). The activation of Raf kinases leads to subsequent phosphorylation of kinases of the MEK family. These kinases can phosphorylate and thereby active ERK. ERK can phosphorylate a variety of substrates. While some of these substrates are cytosolic, many of them are nuclear proteins (e.g. transcription factors) that become phosphorylated after ERK translocation to the nucleus (Yoon and Seger 2006).

The duration and magnitude of ERK signaling is influenced by negative feedback regulation. Many MAPK signaling components can be directly phosphorylated by ERK in order to shut down their activity (Lake, Correa et al. 2016). To terminate Ras signaling particularly, SOS1 can be phosphorylated on several serine residues directly by ERK. This leads to the dissociation of the Grb2/SOS complex (Corbalan-Garcia, Yang et al. 1996, Porfiri and McCormick 1996, Kamioka, Yasuda et al. 2010). Further, Raf proteins can be phosphorylated by ERK in two distinct regions at the N-terminus as well as at the C-terminus. Upon these phosphorylation events, Raf proteins are unable to interact with GTP bound Ras impairing their activation at the plasma membrane (Dougherty, Muller et al. 2005).

Besides the regulation of Ras/MAPK signaling by posttranslational modifications, signal termination can also be achieved by induced expression of regulatory proteins such as MAP kinase phosphatases (MKPs) or dual-specificity MAP kinase phosphatases (DUSPs) (Zhang, Kobayashi et al. 2010, Kidger and Keyse 2016). These phosphatases can dephosphorylate ERK and therefore terminate its activity. SPRY are another family of proteins negatively regulating MAPK signaling. Upon growth factor stimulation these proteins become phosphorylated, translocate to the plasma membrane and bind Grb2 preventing the formation of the Grb2/SOS complex (Hanafusa, Torii et al. 2002, Kim and Bar-Sagi 2004).

3.1.4.2 Ras signaling outside the MAPK network

Beside its role in MAPK signaling, Ras is involved in several other signaling networks. Direct interaction with phosphatidylinositide 3-kinases (PI3K) leads to activation of Akt that is involved in survival signaling and metabolism. Further, Ras can activate proteins of the RAL guanine

nucleotide dissociation stimulator (RALGDS) family leading to cell cycle progression. Interaction with phospholipase Cε (PLCε) stimulates calcium signaling.

3.1.5 Ras signaling in disease

Ras proteins are frequently mutated in human cancer of different tissues. Overall Ras proteins of all isoforms possess an activating mutation in 27 % of all human cancer (Hobbs, Der et al. 2016). However, the frequency of Ras mutations differs dramatically between different tissues and isoforms: Generally, *KRAS* is the most frequent mutated Ras gene. For instance, over 95 % of all pancreatic ductal adenocarcinoma contain mutated KRas. Similarly, KRas mutations are also often observed in colorectal and lung adenocarcinoma. On the other hand, *NRAS* is frequently mutated in melanoma (Forbes, Beare et al. 2017).

The mutations of Ras observed are single nucleotide missense mutations resulting in a gain of function on protein level. Most abundant are mutations of amino acid 12, followed by codon 13 and 61. These three amino acids are located in the active site of the GTPase domain and mutations of these residues impair the hydrolysis of GTP (Kotting, Kallenbach et al. 2008). At the positions 12 and 13 all Ras proteins have glycine residues. This amino acid has the smallest side chain and a substitution by any other amino acid leads to a steric inhibition of the GTP hydrolysis. Gln 61 coordinating the water molecule required for hydrolysis is directly involved in enzymatic activity. Besides the intrinsic GTP hydrolysis rate, also the GAP assisted GTP hydrolysis is dramatically reduced by these mutations. Being unable to hydrolyze GTP, Ras proteins mutated at these positions become constitutively active breaking the GTPase activity cycle (Figure 1). In turn, constitutively active Ras leads to a hyperactivation of its effectors initiating or contributing to the development and maintenance of the tumor.

Besides the oncogenic mutation of Ras proteins, an increased Ras signaling can also be achieved by alteration of Ras regulators. Loss-of-function mutations of neurofibromin, a Ras GAP, are frequently observed in certain kinds of cancers including lung adenocarcinoma, melanoma, squamous cell carcinoma and glioblastoma (Verhaak, Hoadley et al. 2010, Cancer Genome Atlas Research 2012, Brennan, Verhaak et al. 2013, Cancer Genome Atlas Research 2014, Cancer Genome Atlas 2015). Loss of the GAP function can result in activity levels of wild type Ras that are comparable to Ras harboring an oncogenic mutation (Nissan, Pratilas et al. 2014). Besides neurofibromin, the RasGAP DAB2IP can also be down regulated in cancers lacking Ras mutations (Min, Zaslavsky et al. 2010).

The most common up-regulation of a RasGEF is overexpression of RASGRP1. Overexpression of this GEF that is primarily expressed in T-cells is linked to the development of leukemia and results in high levels of GTP-bound active Ras (Ksionda, Limnander et al. 2013). SOS1 mutations are rarely observed rendering its contribution to cancer development insignificant (Swanson, Winter et al.

2008). Oncogenic Ras signaling can also be promoted by the loss of negative regulators like DUSPs and SPRY proteins.

3.1.6 Interaction of oncogenic Ras with wild type Ras

In the background of an oncogenic activating mutation of a Ras protein, the remaining wild type Ras proteins are often neglected. However, it is getting more and more clear, that wild type Ras still plays an important role in tumor development and maintenance. When studying the role of wild type Ras, one must differentiate between the role of the wild type counterpart of the mutated Ras isoform expressed by the other allele (e.g. KRas wt in the background of mutated KRas) and the role of wild type Ras proteins of the other isoforms (e.g. NRas/HRas wt with mutated KRas).

3.1.6.1 Wild type Ras of the corresponding isoform of mutated Ras

It is frequently observed in mouse models of tumor genesis that the cognate wild type allele of the mutated Ras isoform is lost during cancer development (Zhou, Der et al. 2016). Therefore, a tumor suppressive role of the wild type allele has been proposed, which would be overcome by the loss of heterozygosity. This can be observed in tumors driven by all three major Ras isoforms (Guerrero, Villasante et al. 1985, Bremner and Balmain 1990, Zhang, Wang et al. 2001, To, Rosario et al. 2013).

The evidence that wild type protein of the same isoform as the mutated Ras possesses a tumor suppressive function has further been substantiated by studies where the transformed phenotype of Rat fibroblasts harboring oncogenic HRas has been suppressed by transfection of wild type HRas (Spandidos and Wilkie 1988, Spandidos, Frame et al. 1990).

The loss of the corresponding wild type allele of the mutated Ras isoform is not just observed in mouse models but also in human tumors as well as in cancer cells lines and xenografts derived from human cancer (Li, Zhang et al. 2003, Wan, Li et al. 2006, Qiu, Sahin et al. 2011).

Besides phenotypic observations that the loss of the remaining wild type allele promotes tumor progression and metastasis, little is known about the molecular background. However, it could be shown that the amount of active GTP-bound Ras of all isoforms is increased and enhances cytokine signaling upon loss of wild type KRas in KRas mutant cells (Kong, Chang et al. 2016).

3.1.6.2 The role of wild type Ras of the non-mutant isoforms

In contrast to the corresponding wild type alleles of the mutated Ras isoform, the wild type Ras proteins of the other isoforms are often considered as tumor promoting factors especially in KRas mutant cell lines. For instance, ectopic expression of mutant KRas in KRas wild type Caco-2 cells can induce the expression of HRas and increase its activity while knock down of HRas reversed proteomic changes induced by expression of mutant KRas (Ikonomou, Kostourou et al. 2012). However, this could be a result of the ectopic expression of mutant KRas since neither a reduction of expression nor of activity of the other Ras isoforms is observed upon knock down of the

oncogenic Ras in other Ras mutant cell lines (Young, Lou et al. 2013). Further, it has been shown that knock down of wild type HRas in cell harboring oncogenic KRas decreases survival upon radiosensitization (Cengel, Voong et al. 2007).

Mechanistically, several links between the oncogenic Ras of one isoform and wild type Ras of the others were found. On the level of Ras itself, oncogenic KRas can increase the amount of active wild type Ras. The GTP-bound oncogenic KRas can interact with the allosteric site of the RasGEF SOS and thereby enhance its catalytic activity (see 3.1.2). This increased exchange activity of SOS leads to a higher fraction of GTP-bound wild type Ras of the other isoforms. Expression of a modified SOS protein carrying a mutation in the allosteric site can inhibit the cross-activation of wild type Ras by oncogenic Ras (Jeng, Taylor et al. 2012).

Another way how oncogenic KRas can lead to activation of wild type Ras is mediated by Akt signaling. Activation of PI3K by the oncogenic KRas leads to phosphorylation of Akt and subsequently to generation of nitric oxide by nitric oxide synthases (NOS). Nitric oxide can react with C118 of wild type HRas and NRas and thereby increase their respective GTP-bound active fraction (Lim, Ancrile et al. 2008).

In ERK signaling, oncogenic and wild type Ras have distinct roles: knock down of oncogenic Ras isoform leads to a reduction of basal ERK phosphorylation. Nevertheless, these cells still show an increase in phosphorylation upon stimulation with the growth factor EGF. Almost the opposite is observed when the wild type Ras isoforms are knocked down: while the basal ERK phosphorylation is just slightly decreased upon knock down of the wild type Ras isoforms, no increase upon stimulation with EGF is observed since all the remaining Ras proteins are already in the GTP-bound active state (Young, Lou et al. 2013).

In general, these results show a complex relationship between the oncogenic and the wild type Ras isoforms that can be tissue and isoform specific.

3.2 Inducible protein dimerization

Inducible protein dimerization is a powerful tool to precisely control proteins in space and time. Since being at the right place at the right time is often a feature of protein regulation, these dimerization approaches can allow controlling the activity of a protein.

In general, inducible protein dimerization systems share a common mode of action: One dimerization domain is localized to a cellular compartment where the protein of interest is active using a compartment specific targeting motif, while another dimerization domain of the system is fused to the protein of interest lacking its natural compartmental targeting motif. Upon an external cue, the two dimerization domains form a heterodimer. Despite the common principle, the protein

domains and cues used to achieve inducible dimerization vary vastly between different systems leading to a variety of different approaches with unique properties.

One major class of inducible protein dimerization approaches is based on chemically induced dimerization (CID). Here, the dimer-inducing cue is a cell permeable chemical compound added to the medium. The compound can bind to two protein domains of the respective CID system simultaneously and thereby inducing heterodimerization. Widely used are CID systems based on the heterodimerization of FRB and FKBP12 by the addition of rapamycin (Ho, Biggar et al. 1996, Rivera, Clackson et al. 1996, Putyrski and Schultz 2012). However, the use of rapamycin has the drawbacks that the high affinity of the dimerizer to the proteins renders the dimerization almost irreversible and it can perturb endogenous mTOR (mammalian target of rapamycin) signaling. To reduce the interaction with endogenous proteins of the host and to increase reversibility, rapamycin derivatives have been developed. Some of them are even cleavable by light to dissociate the induced dimer allowing some degree of reversibility. Furthermore, bioorthogonal approaches have been developed to minimize interaction with the host cells. For example, a CID approach based on a mutated FKBP and the *E. Coli* dihydrofolate reductase (eDHFR) and a synthetic ligand (SLF'-TMP) was developed (Liu, Calderon et al. 2014). In contrast to other CID systems, the induced dimer can be dissociated by addition of TMP due to a comparably weak interaction of TMP and the eDHFR.

To further increase spatial control, CID approaches using photo caged dimer-inducing agents have been engineered (Voss, Klewer et al. 2015). To generate this, the dimerizer is modified in a way that it can just bind one of the two protein domains used for dimerization while a photo-cleavable group blocks the other binding interface. Upon illumination with light of a specific wavelength, the protection group is split and heterodimerization can occur in the illuminated area. Thus, it is possible to restrict the dimerization to a small region of interest with subcellular dimensions. To avoid diffusion after uncaging, dimer-inducing compound, protein domains that can be covalently modified like HaloTag or SNAPTag can be used (Ballister, Aonbangkhen et al. 2014, Chen, Venkatachalapathy et al. 2017).

Besides CID, protein dimerization can be induced using optogenetic tools (Muhlhauser, Fischer et al. 2017, Rost, Schneider-Warme et al. 2017). These are often derived from naturally occurring photo-responsive proteins needless of an external chemical compound. Comparable to the CID approach, optogenetic systems usually consist of two different protein domains. Upon illumination with light of the appropriate wavelength, one of these domains undergoes a conformational change creating an interaction interface.

4 Objectives

Biological systems like cells, tissues or entire organisms must be able to sense their environment and quickly adapt to changes quickly to survive and procreate in constantly changing settings. Yet, this is a challenging task since the cells must deal with a noisy background and often with low input signals. This also transfers to cell-to-cell communication mediated by secreted molecules like growth factors. To achieve a robust response, cells therefore have to be able to amplify a low input signal and have to adapt to persistent background noise. Further, this leads to a behavior that constant input signals independent of the strength of the signal are often ignored. Instead, the cells respond to a dynamic change of a given input signal.

Proteins of the Ras family have a major role in the transduction of extracellular signals mediated by growth factor receptors to intracellular signaling networks by cycling between an active and an inactive state. Thereby, in their active state, they are involved in the amplification of the incoming signal by an engagement in a positive feedback loop with their GEF SOS. Oncogenic gain-of-function mutations of Ras proteins are known to result in constant activation of the mutated Ras protein as well as in hyperactivation of Ras effectors either by activating effectors independently of growth factors or due to higher sensitivity to lower changes in growth factor concentrations.

Ras activity is highly dependent on its localization to the plasma membrane. Due to this dependence, it can be hypothesized that controlling the localization of Ras proteins within a cell is also a way to control its activity. Hence, tools have to be developed which could allow the precise control of both wild type and oncogenic Ras localization within the cell. These tools must be characterized thoroughly in terms of activation of Ras itself upon translocation to the plasma membrane as well as the activation of downstream effectors and the positive feedback via its GEF SOS. The putative engagement in the positive feedback mechanism could also result in activation of endogenous Ras proteins.

The relationship between oncogenic and wild type Ras is of exceptional interest since the presence of oncogenic Ras could alter the growth factor concentration dependent cellular response with severe consequences for the cell expressing the oncogenic Ras as well as other cells in the vicinity via cell-to-cell communication. Further, these newly developed tools will be used to study the importance of activators and inhibitors of Ras activity for wild type and oncogenic Ras.

5 Results

5.1 Design of an activatable KRas to study the interaction with wild type Ras

Proteins of the Ras superfamily are lipid anchored plasma membrane proteins that transmit intracellular signals by recruiting their effector proteins upon an upstream signal from the cytosol to the plasma membrane where the effectors get activated. Therefore, the proper localization of Ras to the plasma membrane is important for their function. Interfering with the plasma membrane localization of Ras proteins has been shown to a viable approach to reduce Ras-mediated signaling (Zimmermann, Papke et al. 2013, Papke, Murarka et al. 2016, Martin-Gago, Fansa et al. 2017). We hypothesize that controlling the localization of Ras proteins by other means should also be a way to control the activity and the function of these GTPases. To control Ras localization, a previously developed chemically induced dimerization approach allowing the precise control of protein localization within cells by small organic compounds, was applied to KRas (Liu, Calderon et al. 2014).

The FKBP'/eDHFR recruitment system is based on a bivalent small-molecule SLF'-TMP inducing heterodimerization (Figure 5). The SLF' (modified synthetic ligand of FKBP) moiety of the molecule is able to bind to the FKBP' domain, whereas the TMP (trimethoprim) moiety non-covalently binds to the eDHFR domain. A polyethylene glycol linker joins both functional parts of this molecule. This versatile recruitment system can be applied to any protein of interest. The FKBP' domain contains a F37V mutation reducing interaction with endogenous FKBP protein (Clackson, Yang et

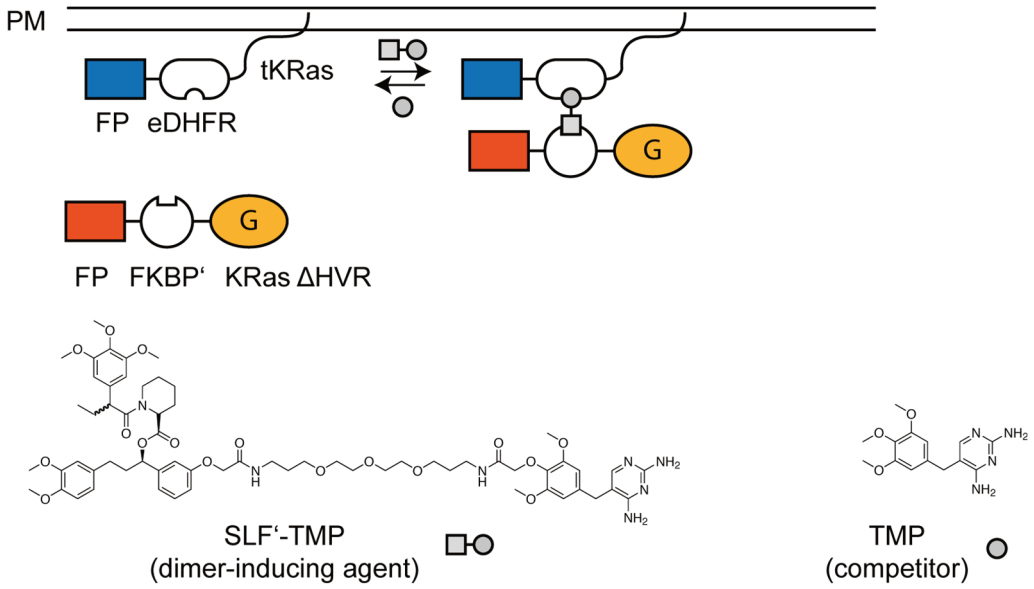

Figure 5: Schematic representation of the recruitable KRas design.

KRas is split into two parts – KRas ΔHVR and tKRas – and fused to a tandem of FKBP' or eDHFR domains, respectively. Upon addition of the cell permeable dimerizer SLF'-TMP the FKBP' and the eDHFR domain form a dimer resulting in PM recruitment of KRas ΔHVR. The recruitment can be reverted by addition of TMP. Both parts of the recruitable KRas are labeled with a fluorescent protein (FP) with a distinct fluorescence spectrum.

al. 1998).

If one of the dimerization domains is confined to a cellular compartment and the other is freely diffusing in the cytosol, the soluble domain will be recruited to the localized one upon addition of the dimer-inducing agent. Since the recruitment is based on non-covalent interactions, it can be reversed by addition of excess monovalent ligand of one of the dimerization domains like TMP. Several rounds of dimerization and dissociation of the heterodimer can be performed by alternating the administration of SLF'-TMP and TMP.

In order to generate a plasma membrane recruitable KRas4B, the protein was split into two parts:

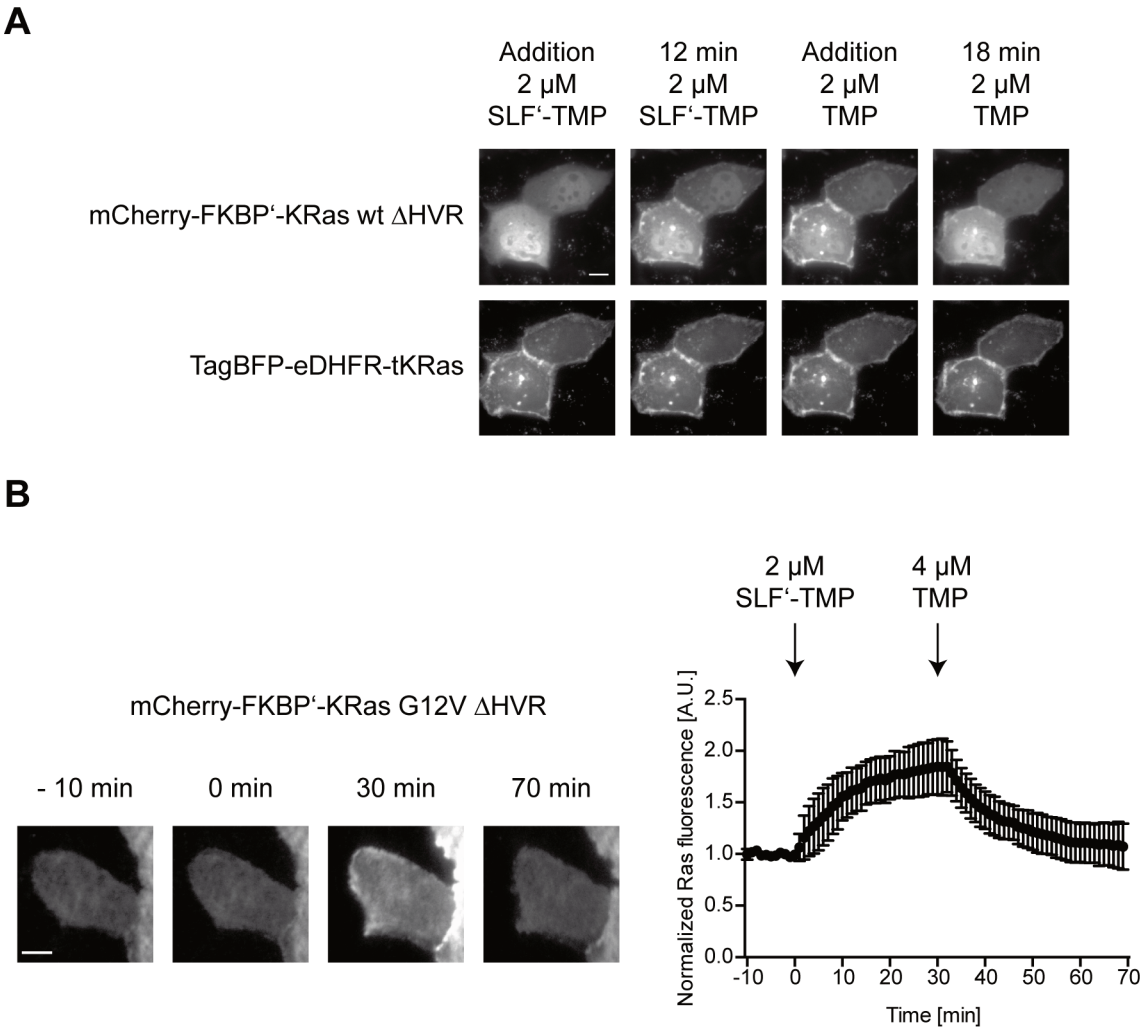

Figure 6: Plasma membrane translocation of mCherry-2xFKBP'-KRas ΔHVR upon SLF'-TMP addition, which can be reverted by TMP.

***A.** Fluorescence distribution of mCherry-2xFKBP'-KRas wt ΔHVR (top row) and TagBFP-2xeDHFR-tKRas (bottom row) expressed in MDCK cells upon SLF'-TMP and TMP addition observed by fluorescence microscopy. **B.** mCherry-2xFKBP'-KRas G12V ΔHVR fluorescence intensity upon addition of SLF'-TMP (at 0 min) and TMP (addition at 30 min) measured by TIRF microscopy (left panel). Right panel: Normalized fluorescence intensity ± s.d. measured by TIRF microscopy over time (n = 12 cells). The arrows indicate the administration of 2 µM SLF'-TMP and 4 µM TMP to induce (at 0 min) and reverse (at 30 min) Ras PM translocation, respectively. Scale bars: 10 µm*

the N-terminal catalytically active G-domain (KRas4B amino acids 1 - 168, named KRas ΔHVR) and the C-terminal hypervariable region (HVR) (KRas4B amino acids 169 - 188, named tKRas) responsible for the PM localization of KRas. KRas ΔHVR was N-terminally fused to a fluorescent protein (mCherry or mTFP) as well as two copies of a FKBP' domain. Since the lacking HVR of KRas is responsible for the plasma membrane localization of the full-length protein, mCherry-2xFBKP'-KRas ΔHVR is soluble in the cytosol and does not interact with any membranes (Figure 6A, top row). It can be observed that the fusion protein gets slightly enriched in the nucleus.

The tKRas part of KRas was N-terminally fused to the blue fluorescent protein TagBFP and two copies of the *E. Coli* dihydrofolate reductase (eDHFR). The hypervariable region (HVR) of KRas is sufficient to target TagBFP-2xeDHFR-tKRas to the PM (Figure 6A, bottom row). Further, the localization of TagBFP-2xeDHFR-tKRas is not influenced by the addition of SLF'-TMP or TMP.

The recruitment of mCherry-2xFKBP'-KRas ΔHVR to the plasma membrane can also be observed by total internal reflection fluorescence (TIRF) microscopy. In TIRF microscopy the excitation light only penetrates about 100 nm of the sample. This allows studying of processes that happen in the proximity of the basal plasma membrane. Therefore, this technique is well suited to study the recruitment of mCherry-2xFKBP'-KRas ΔHVR from the cytosol to the basal plasma membrane (Figure 6B). The translocation of the G-domain of KRas to the plasma membrane upon administration of 2 µM SLF'-TMP was observed by fluorescence microscopy. This concentration proved to be optimal for fast recruitment of the soluble G-domain to the plasma membrane (Liu, Calderon et al. 2014). While lower concentrations lead to a slower recruitment, higher concentrations do not accelerate recruitment. Higher concentrations could also interfere with recruitment by saturating the protein interaction domains with individual ligand molecules.

5.1.1 Characterization of KRas activity upon recruitment to the plasma membrane

As shown before, mCherry-2xFKBP-KRas ΔHVR can be effectively recruited to plasma membrane bound TagBFP-2xeDHFR-tKRas by addition of SLF'-TMP. However, plasma membrane localization alone does not provide any information about the nucleotide binding and therefore activation state of KRas. Further, it has to be made sure that the introduced modifications – the N-terminal addition of the fluorescent protein and the dimerization domains as well as the removal of the C-terminal HVR – do not impair the ability to facilitate activation of downstream effectors.

5.1.1.1 Oncogenic KRas gets activated when recruited to the plasma membrane

To determine the activation state, the Ras binding domain of CRaf (CRafRBD), a Ras effector, can be utilized: this domain just binds to Ras proteins if those are in the active, GTP bound state and not, if GDP is bound.

To study dynamics of the activation of wild type and oncogenic Ras upon recruitment to the plasma membrane with high temporal resolution, total internal reflection fluorescence (TIRF)

microscopy was performed (Figure 7 and Figure 8). Therefore, MDCK cells were transiently transfected with TagBFP-2xeDHFR-tKRas and mCherry-2xFKBP'-KRas wt ΔHVR (Figure 7) or oncogenic mCherry-2xFKBP'-KRas G12V ΔHVR (Figure 8), the two components of the recruitable KRas system, as well as CRafRBD-EYFP to measure the activity of the recruited Ras.

The fluorescence of mCherry-2xFKBP'-KRas wt ΔHVR at the basal plasma membrane increases

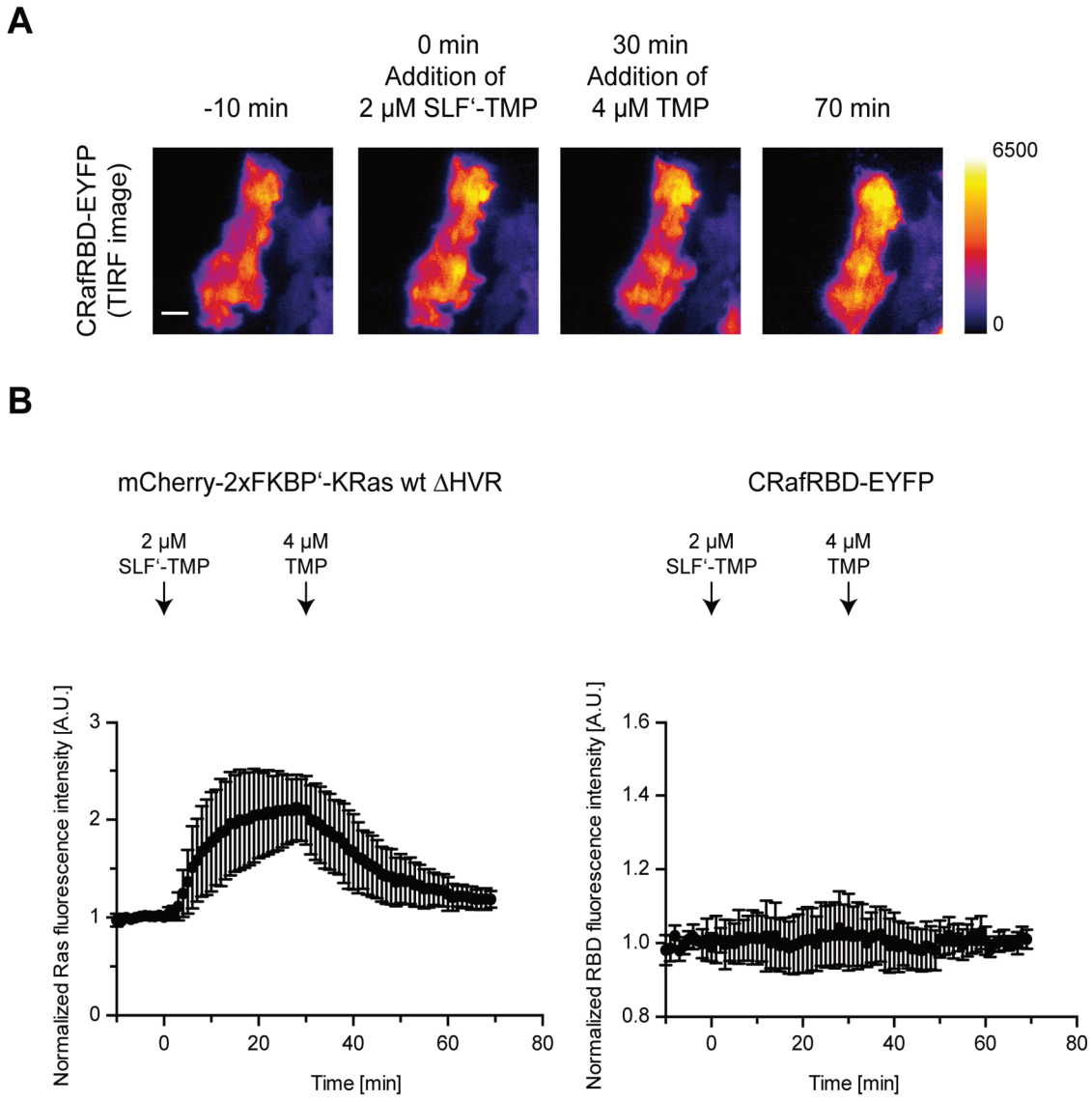

Figure 7: Recruitment of mCherry-2xFKBP'-KRas wt ΔHVR to the plasma membrane does not lead to CRafRBD-EYFP co-recruitment.

***A**. TIRF microscopy images of MDCK cells transiently expressing mCherry-2xFKBP'-KRas wt ΔHVR (not shown), TagBFP-2xeDHFR-tKRas (not shown) and CRafRBD-EYFP (false colored). 2 µM SLF'-TMP were added at 0 min to induce recruitment of mCherry-2xFKBP'-KRas wt ΔHVR to the plasma membrane. At 30 min, 4 µM TMP were added to displace mCherry-2xFKBP'-KRas wt ΔHVR from the PM to the cytosol. **B**. Single cell quantification of the fluorescence intensity of mCherry-2xFKBP'-KRas wt ΔHVR (left graph) and CRafRBD-EYFP (right graph) over time. Arrows indicate the administration of 2 µM SLF'-TMP and 4 µM TMP, respectively. Error bars: s.d., n = 8 cells, scale bar: 10 µm*

upon addition of 2 µM SLF'-TMP showing recruitment of the protein from the cytosol to the PM (Figure 7A). Upon addition of 4 µM TMP 30 minutes after recruitment, mCherry-2xFKBP'-KRas wt ΔHVR is released from the plasma membrane to the cytosol as observed by a decreased fluorescence in TIRF. However, the amount of CRafRBD-EYFP fluorescence in the TIRF field does not vary over time (Figure 7B).

In contrast to the recruitable wild type KRas, addition of 2 µM SLF'-TMP to the medium leads to increased fluorescence intensity detected by TIRF microscopy of both mCherry-2xFKBP'-KRas G12V ΔHVR and CRafRBD-EYFP in the TIRF field after the recruitment of oncogenic KRas to the plasma membrane (Figure 8A). A steady fluorescence signal was reached 10 to 15 minutes after

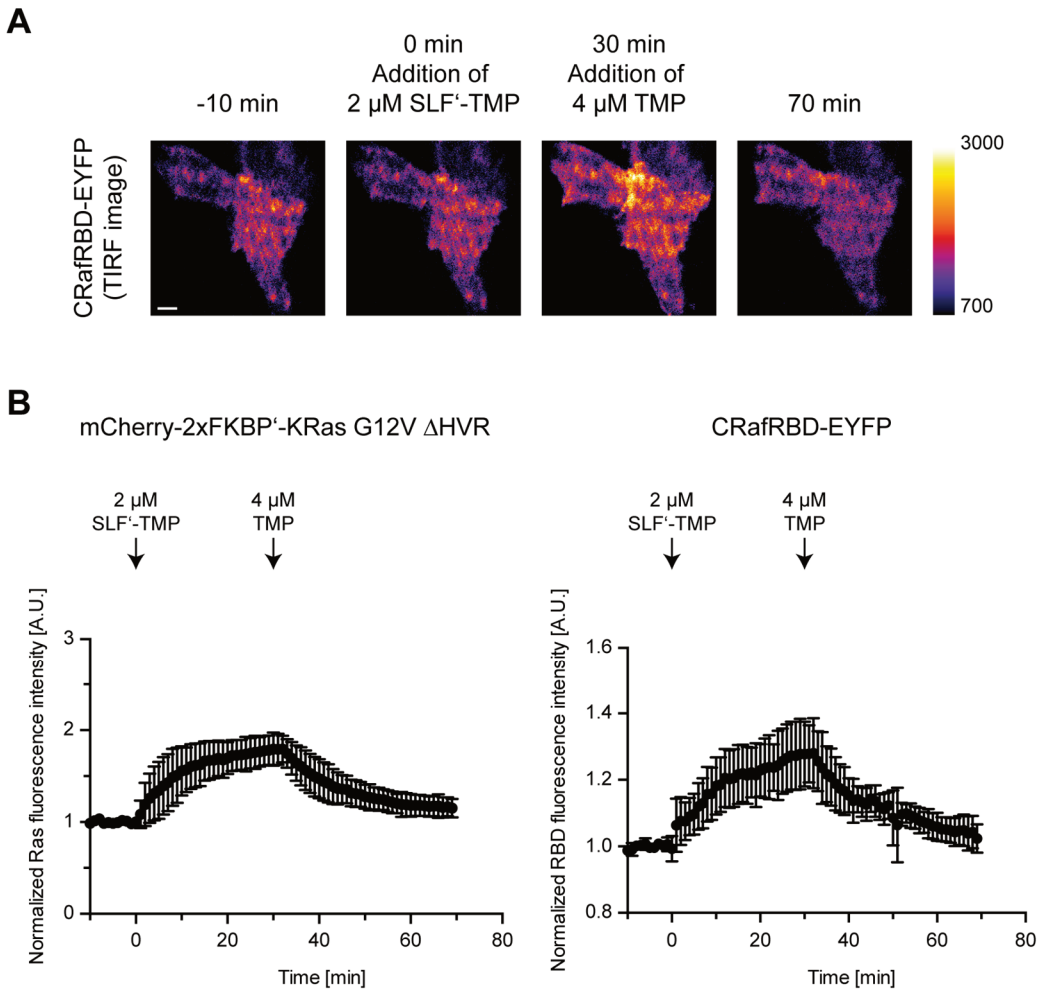

Figure 8: Activation of recruitable oncogenic KRas after translocation to the PM.

***A.** TIRF microscopy images of MDCK cells transiently expressing mCherry-2xFKBP'-KRas G12V ΔHVR (not shown), TagBFP-2xeDHFR-tKRas (not shown) and CRafRBD-EYFP (false colored). 2 µM SLF'-TMP were added at 0 min to induce recruitment of mCherry-2xFKBP'-KRas G12V ΔHVR to the plasma membrane. At 30 min, 4 µM TMP were added to displace mCherry-2xFKBP'-KRas G12V ΔHVR from the PM to the cytosol. **B.** Single cell quantification of the fluorescence intensity of mCherry-2xFKBP'-KRas G12V ΔHVR (left graph) and CRafRBD-EYFP (right graph) over time. Arrows indicate the administration of 2 µM SLF'-TMP and 4 µM TMP, respectively. Scale bar: 10 µm*

addition of the dimer-inducing compound (Figure 8B). Addition of the competitor TMP leads to a decrease in mCherry-2xFKBP'-KRas G12V ΔHVR and CRafRBD-EYFP fluorescence over time.

Single cell fluorescence intensity of mCherry-2xFKBP'-KRas G12V ΔHVR and CRafRBD-EYFP for the recruitment to the plasma membrane after SLF'-TMP addition and the dissociation after TMP administration was fitted using an exponential function. This yielded a $t_{1/2}$ (95% confidence interval) for mCherry-2xFKBP'-KRas G12V ΔHVR 5.97 min (4.64 min to 8.39 min) for the association and 9.57 min (7.40 to 13.5 min) for the dissociation. The half time of the association and the dissociation of the CRafRBD-EYFP were delayed compared to the recruitable Ras with 7.68 min (5.32 min to 13.8 min) and 12.6 min (7.46 min to 40.4 min), respectively.

A correlation between the amount of recruited oncogenic KRas and the amount of recruited CRafRBD could not be observed (Figure 9, Pearson correlation coefficient -0.20, p = 0.58). Since the recruitment of the CRafRBD-EYFP to the plasma membrane seems to be slower compared to the recruitment of mCherry-2xFKBP'-KRas G12V ΔHVR, this hints at an activation of the recruitable KRas G12V rather than the recruitment of a preformed complex of mCherry-2xFKBP'-KRas G12V ΔHVR and CRafRBD-EYFP.

So far, it has been established that recruitment of mCherry-2xFKBP'-KRas G12V ΔHVR to the plasma membrane leads to its activation. To investigate, if this recruitment leads to full activation of the recruited oncogenic GTPase or whether it can be further activated by addition of growth factors, recruitable oncogenic KRas G12V was recruited to the plasma membrane by addition of 2 µM SLF'-TMP for 30 min before 200 ng·mL^{-1} EGF were added to the medium (Figure 10). 30 minutes after EGF administration, 4 µM TMP were added to revert dimerization of displace

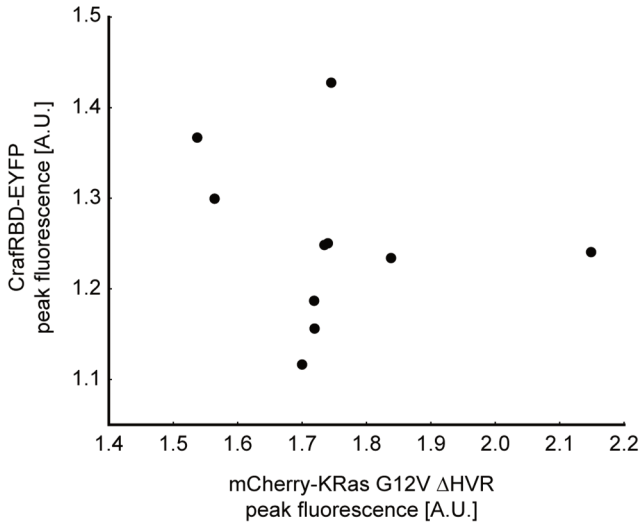

Figure 9: Correlation of the mean fluorescence of mCherry-KRas G12V ΔHVR and CRafRBD-EYFP fluorescence.

The values represent the calculated averages of the fluorescence intensities between 20 and 30 minutes after recruitment to the plasma membrane.

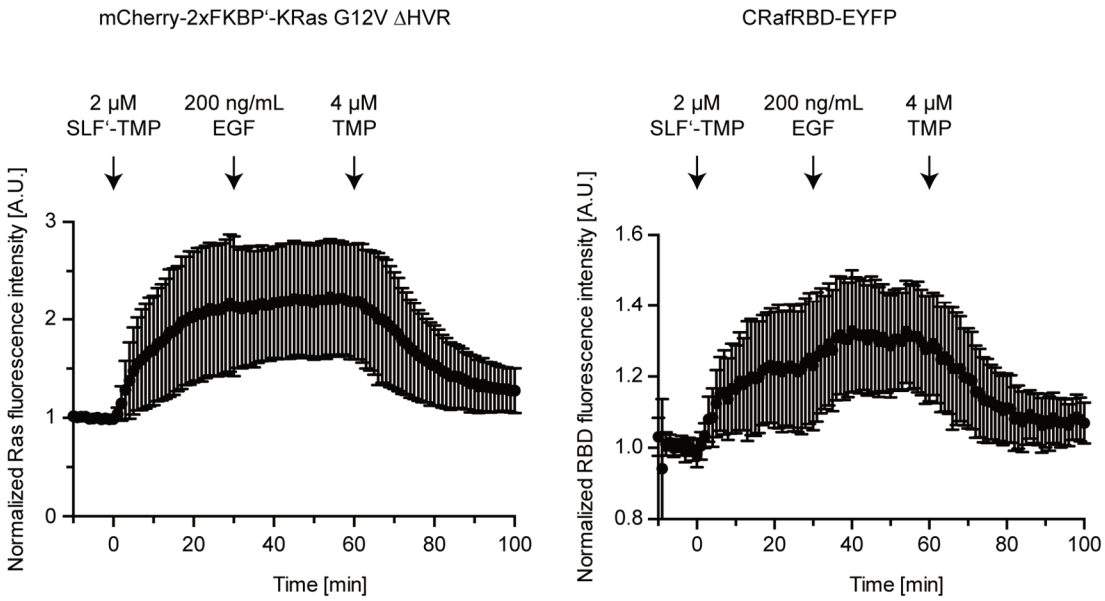

Figure 10: EGF administration after recruitment of oncogenic KRas to the PM further increases Ras activity.

Quantification of TIRF microscopy images of MDCK cells transiently transfected with mCherry-2xFKBP'-KRas G12V ΔHVR (left graph), TagBFP-2xeDHFR-tKRas (not shown) and CRafRBD-EYFP (right graph). Arrows indicate the time points of administration of SLF'-TMP to induce PM translocation of recruitable oncogenic KRas, EGF and TMP to revert PM translocation of KRas. Error bars: s.d., n = 9 cells

mCherry-2xFKBP'-KRas G12V ΔHVR to the cytoplasm. The fluorescence intensity of mCherry-2xFKBP'-KRas G12V ΔHVR and CRafRBD-EYFP were measured by TIRF microscopy.

As observed before (Figure 8), after administration of 2 µM SLF'-TMP the amount of mCherry-2xFKBP'-KRas G12V ΔHVR and CRafRBD-EYFP at the plasma membrane increases. After the addition of 200 ng·mL^{-1} EGF, the amount of CRafRBD-EYFP and therefore the Ras activity further increases 10 min after the administration of the growth factor while the amount of recruited mCherry-2xFKBP'-KRas G12V ΔHVR does not increase further. This increase in CRafRBD-EYFP fluorescence is sustained until 4 µM TMP are added to release mCherry-2xFKBP'-KRas G12V ΔHVR from the plasma membrane into the cytosol, which results in a lower TIRF fluorescence of both observed fluorescently labeled proteins. However, it is impossible to distinguish whether the additional recruitment of CRafRBD-EYP to the plasma membrane is due to increased activation of mCherry-2xFKBP'-KRas G12V ΔHVR or due to activation of endogenous wild type Ras molecules upon growth factor stimulation.

5.1.1.2 *Recruitment of oncogenic KRas to the PM induces ERK phosphorylation*

So far, it could be shown by membrane recruitment of CRafRBD that oncogenic recruitable KRas gets into it GTP bound active state after recruitment to the plasma membrane. However, this does not prove that the recruitable KRas is able to engage in cellular signaling. One major downstream effector of Ras is the MAP kinase ERK. Upon growth factor stimulation, ERK becomes

phosphorylated in a Ras dependent manner. To investigate, if ERK gets phosphorylated upon recruitment of mCherry-2xFKBP'-KRas ΔHVR to the PM, quantitative Western Blot analysis was performed using NIH3T3 cells stably expressing mTFP-2xFKBP'-KRas wt ΔHVR-P2A-TagBFP-2xeDHFR-tKRas or mTFP-2xFKBP'-KRas G12D ΔHVR-P2A-TagBFP-2xeDHFR-tKRas (Figure 11).

Western blot analysis shows that the basal amount of phosphorylated ERK does not differ between the cell lines expressing wild type recruitable KRas or recruitable oncogenic KRas G12D (Figure 11, 0 min time point). When mTFP-2xFKBP'-KRas wt is recruited to the plasma membrane, the fraction of phosphorylated ERK does not increase. This matches the observation that recruitable wild type KRas does not get activated upon recruitment to the plasma membrane as measured by plasma membrane translocation of CRafRBD-EYFP (Figure 7).

If instead oncogenic KRas is recruited to the PM, the fraction of phosphorylated ERK increases by a factor of three starting 10 minutes after the addition of the dimer-inducing compound. However, for longer periods of oncogenic KRas recruitment to the PM, an adaptive response of the cells can be observed as the fraction of phosphorylated ERK slowly decreases over time (Figure 11, 20 and

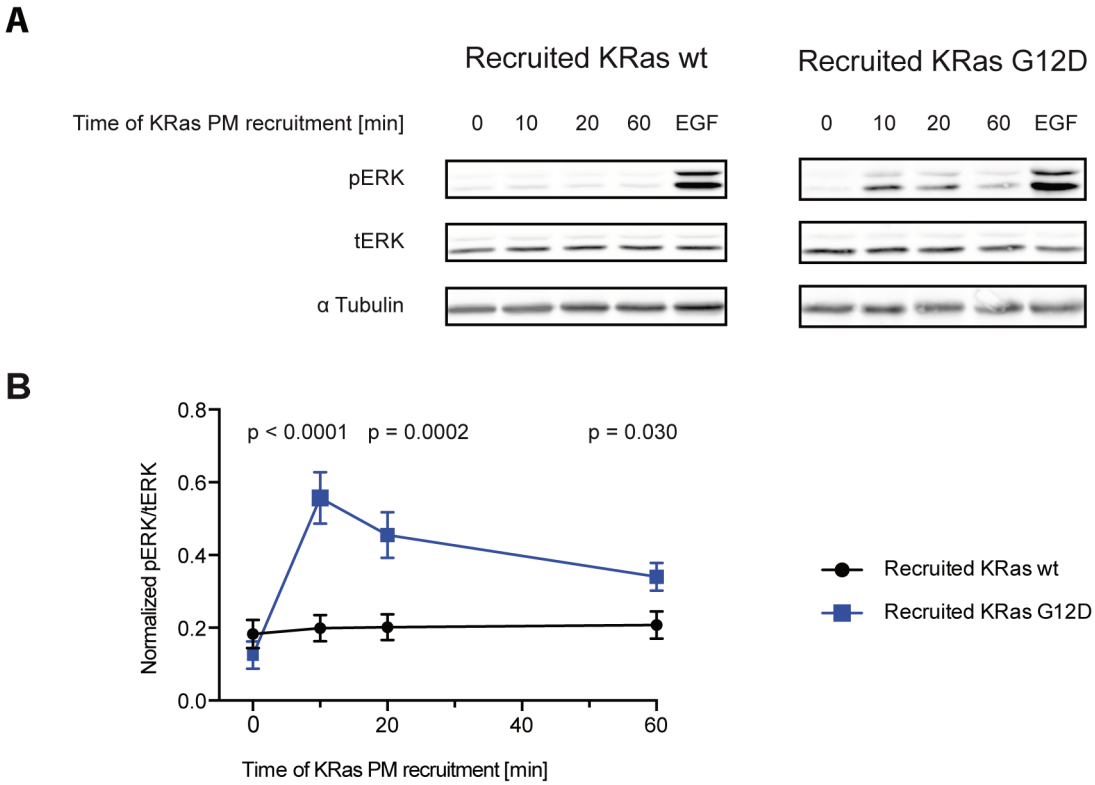

Figure 11: Recruitment of oncogenic KRas to the plasma membrane leads to ERK phosphorylation.

A. *Western Blot analysis of phosphorylated ERK in NIH3T3 cells stably expressing mTFP-2xFKBP'-KRas wt ΔHVR-P2A-TagBFP-2xeDHFR-tKRas or mTFP-2xFKBP'-KRas G12D ΔHVR-P2A-TagBFP-2xeDHFR-tKRas. Serum starved cells were incubated with 2 μM SLF'-TMP for the indicated time spans or for 5 min with 100 ng·mL^{-1} EGF (EGF). From top to bottom row: phosphorylated Erk on Thr202 and Tyr204 (pERK), total level of Erk (tERK) and loading control (α Tubulin).* ***B.*** *Quantification of pERK/tERK ± s.e.m. at each time point normalized to EGF (wt: n = 7, G12D: n = 5). p values noted above the curves were determined by applying a two-way ANOVA.*

60 min time points). The amplitude of the ERK phosphorylation after the recruitment of oncogenic KRas to the PM for 10 minutes is about 55 % of a saturating EGF stimulus with 100 ng·mL^{-1} EGF for 5 minutes.

In conclusion, it could be shown that the recruitment of oncogenic KRas to the plasma membrane leads to a nucleotide exchange and thereby to its activation. Oncogenic plasma membrane recruited KRas can interact with Ras effectors and leads to phosphorylation of the ERK kinase. On the other hand, wild type KRas does not get activated when recruited to the plasma membrane and thus does not lead to activation of Ras effector proteins.

5.1.2 Characterization of the interaction between recruited KRas and wild type Ras

The interaction of recruitable KRas and endogenous Ras cannot be studied with the previously applied imaging techniques using the TIRF fluorescence signal of a fluorescently labeled CRafRBD since the resulting images are always a convolution of the amount of active endogenous Ras and GTP-bound recruitable KRas. Pulldown assays using a recombinantly expressed CRafRBD as bait can be utilized to overcome this limitation since endogenous Ras and recruitable KRas differ in molar mass and can therefore be separated in SDS PAGE. Further, the fractions of active Ras of the different cell lines expressing either wild type or oncogenic recruitable KRas can be directly compared if treated in the same manner and simultaneously analyzed by Western blot.

Therefore, a fusion-protein of three copies of CRafRBD fused to glutathione-S-transferase (GST) was recombinantly expressed in *E. Coli*, purified and bound to glutathione beads. These beads were then used to pull down all active Ras species (endogenous as well as ectopically expressed recruitable Ras) from cell lysates treated with 2 µM SLF'-TMP for 0, 10, 20 or 60 minutes (Figure 12).

The input controls show that the levels of ectopically expressed recruitable KRas are equal between the two different cells lines allowing a direct comparison of the activities of endogenous as well as ectopically expressed recruitable KRas.

In the absence of the dimer-inducing ligand SLF'-TMP (0 min time point), the recruitable oncogenic KRas displays a fivefold higher active fraction compared to recruitable wild type KRas in serum-starved NIH3T3 cells (Figure 12A and B). When mTFP-2xFKBP'-KRas ΔHVR harboring the oncogenic G12D mutant is recruited to the plasma membrane, the amount of active ectopically expressed KRas doubles within 20 minutes of recruitment and the activation persists over a time span of at least 60 minutes. In contrast to the oncogenic recruitable KRas mutant, recruitment of wild type mTFP-2xFKBP'-KRas ΔHVR to the plasma membrane does not lead to an increased GTP-bound fraction. This highlights that the measurement of the recruitment time dependent Ras activity by CRafRBD pulldowns is yielding similar results compared to measurements obtained TIRF microscopic techniques (Figure 7 and Figure 8).

Besides active recruitable mTFP-2xFKBP'-KRas ΔHVR, active endogenous Ras is also pulled down by the CRafRBD (Figure 12A and C). Due to the separation by molecular weight during electrophoresis, the amount of active Ras of all endogenous Ras isoforms can be studied independently. The amount of active endogenous Ras is elevated in the cells expressing the recruitable oncogenic mTFP-2xFKBP'-KRas G12D ΔHVR by a factor of two, compared to the cells expressing recruitable wild type KRas. Interestingly, the amount of active endogenous Ras does not change upon recruitment of either mTFP-2xFKBP'-KRas ΔHVR species to the plasma

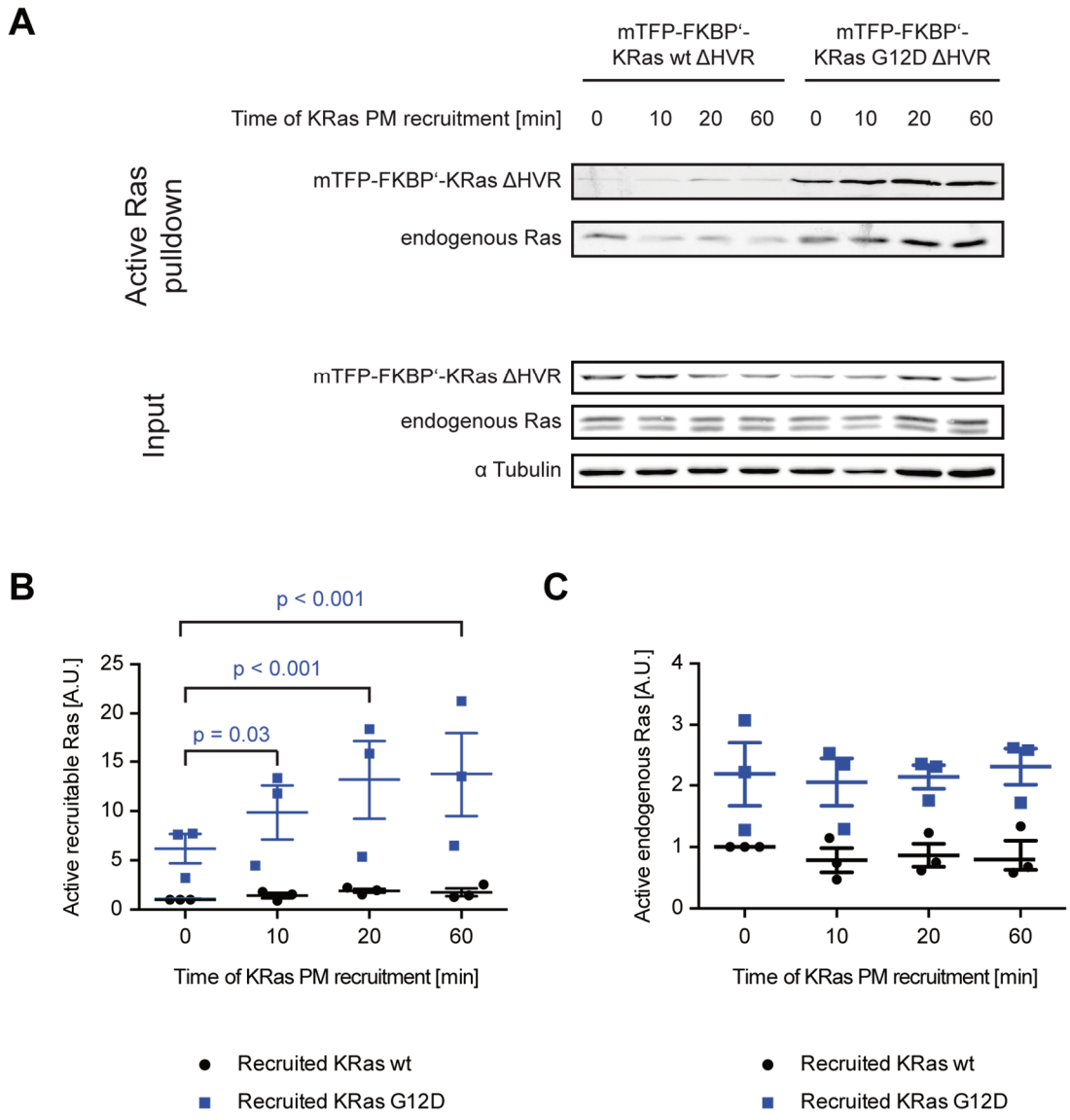

Figure 12: Recruitment of oncogenic KRas to the PM leads to its activation.

A. *Representative Western blot analysis of a 3xRafRBD-GST active Ras pulldown and the respective input controls of NIH3T3 cells stably expressing mTFP-2xFKBP'-KRas ΔHVR and TagBFP-2xeDHFR-tKRas after different recruitment periods.* ***B.*** *Quantification of the activity of the recruitable wild type and oncogenic KRas in dependence on recruitment time.* ***C.*** *Analysis of the activity of endogenous wild type Ras in dependence on length of recruitment of wild type or oncogenic KRas to the PM. Error bars: s.e.m., n = 3, p values noted were determined by two-way ANOVA with Bonferroni correction for multiple comparisons.*

membrane (Figure 12C).

So far, no activation of recruitable wild type KRas could be observed (Figure 7 and Figure 12). Since the recruitable oncogenic KRas gets activated upon PM recruitment and the difference of the two proteins is just one amino acid, it is unlikely that the addition of the N-terminal fluorescent protein and the dimerization domains are causing the difference in activation. Further, after observing that the recruitable oncogenic KRas is partially active in the cytosolic state and becomes fully active upon PM translocation, it could be hypothesized that the active fraction of the recruitable oncogenic KRas is involved in the activation process. Since the recruitable wild type KRas is lacking this fraction of active cytosolic KRas, it does not get activated upon recruitment if this hypothesis is valid.

To test this, an active KRas species (full-length mKate2-KRas G12V) was co-expressed in NIH3T3 cells stably expressing recruitable wild type KRas. Again, GST-tagged 3xCRafRBD was utilized to pull down the fraction of active Ras (Figure 13A). The difference in molecular weight of all three Ras species (endogenous Ras, mKate2-KRas G12V and mTFP-2xFKBP'-KRas wt ΔHVR) allows the quantification of the activity of the individual proteins in this assay. The co-expression of full-length mKate2-KRas G12V does not influence the basal amount of active recruitable wild type KRas (Figure 13, 0 min time point). However, upon recruitment of mTFP-2xFKBP'-KRas wt ΔHVR to the plasma membrane, the amount of active mTFP-2xFKBP'-KRas wt ΔHVR increases 3-fold

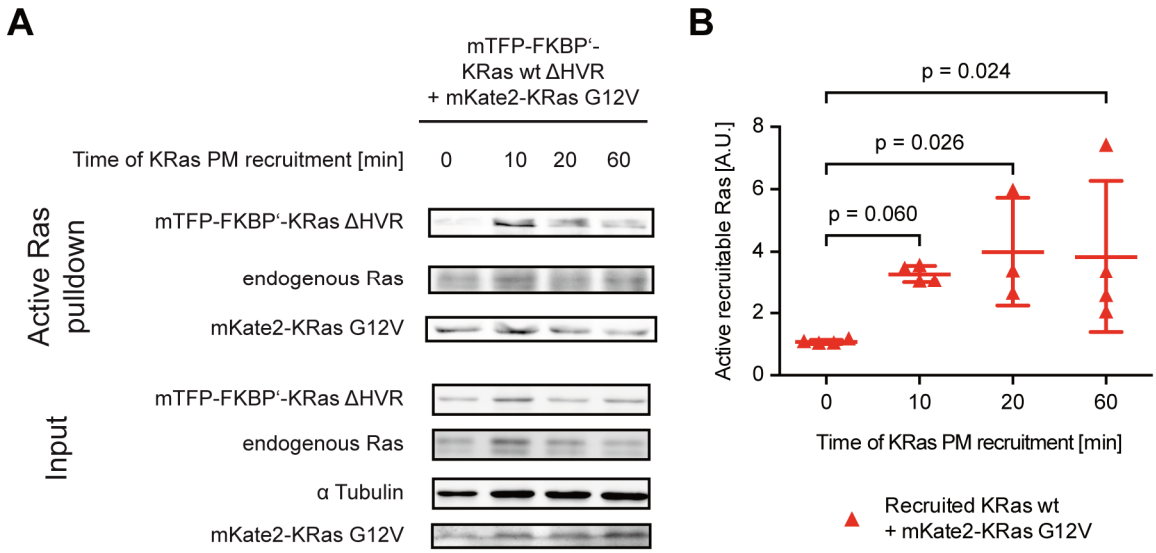

Figure 13: Activation of recruitable KRas wt upon PM recruitment is dependent on the presence of full-length oncogenic mKate2-KRas G12V.

***A.** Representative Ras activity pulldown and subsequent Western blot analysis of NIH3T3 cells stably expressing mTFP-2xFKBP'-KRas wt ΔHVR transiently transfected with full-length mKate2-KRas G12V and respective input controls as well as α Tubulin as loading control. **B.** Quantification of the band intensity of mTFP-2xFKBP'-KRas wt ΔHVR normalized to NIH3T3 cells just expressing mTFP-2xFKBP'-KRas wt ΔHVR in dependence on duration of PM recruitment. Error bars: s.e.m., n = 4 independent experiments, one-way ANOVA with uncorrected Fisher's LSD test*

after 10 minutes (Figure 13B). Further, the recruitment of wild type KRas to the plasma membrane does not influence the activity of the full-length oncogenic mKate2-KRas G12V.

In summary, these experiments show that mTFP-2xFKBP'-KRas G12D ΔHVR displays a higher active fraction in the cytosolic state compared to the recruitable wild type KRas. The fraction of active mTFP-2xFKBP'-KRas ΔHVR increases upon recruitment to the plasma membrane, if an active Ras species is present in the cell. This species could either be mTFP-2xFKBP'-KRas G12D ΔHVR or full-length oncogenic mKate2-KRas G12V.

5.1.3 Influence of recruitable KRas on the cellular response to growth factors

The previous characterization of the recruitable KRas showed that recruitment of oncogenic mTFP-2xFKBP'-KRas G12D ΔHVR to the plasma membrane leads to activation of the recruitable

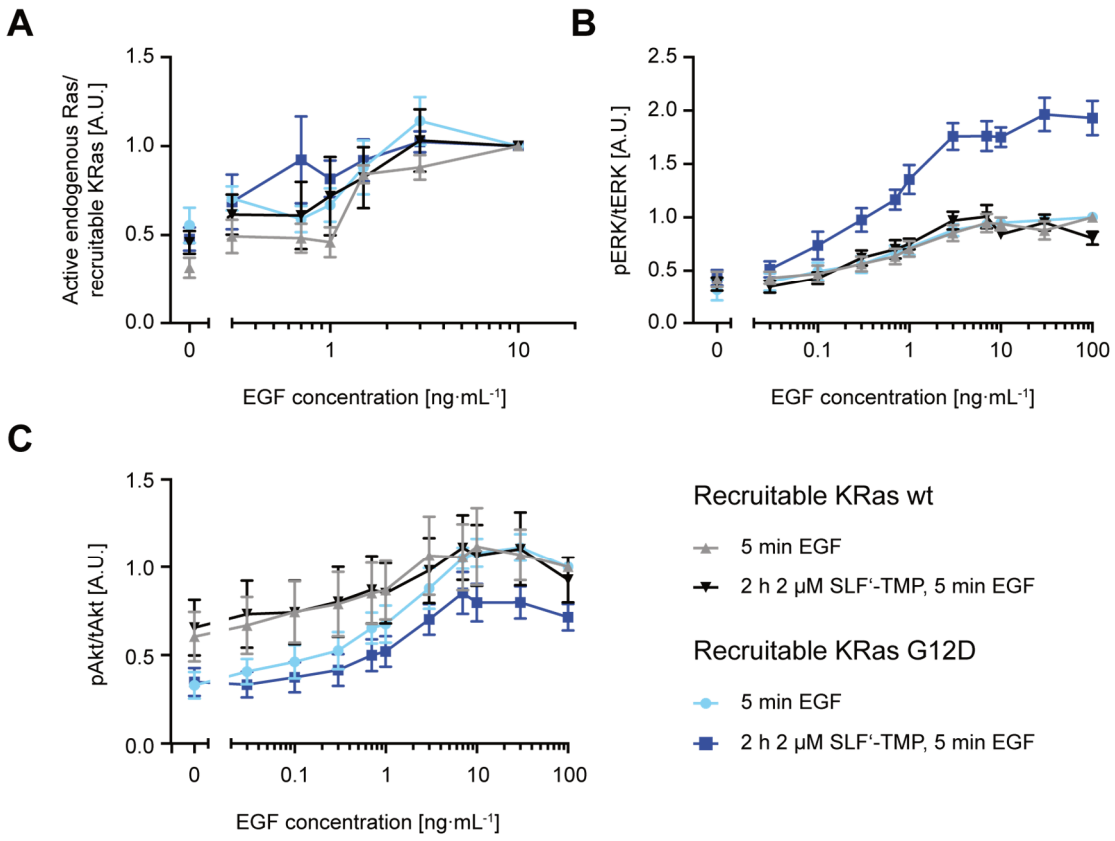

Figure 14: Influence of recruitable KRas on different cellular responses to epidermal growth factor

***A.** Analysis of endogenous wild type Ras activity in the presence and absence of recruitable KRas at the plasma membrane after stimulation with increasing doses of EGF. Pull-down experiments were performed using recombinant 3xCRafRBD-GST. Error bars: s.e.m., n = 4 independent experiments **B.** Analysis of ERK phosphorylation in dependence on recruitable KRas localization and EGF concentration. Error bars: s.e.m., n = 5 independent experiments **C.** Quantification of Akt phosphorylation response upon stimulation with increasing EGF doses in dependence on KRas localization. Error bars: s.e.m., n = 5 independent experiments*

KRas as well as to phosphorylation of ERK, but not to the activation of endogenous wild type Ras. However, all these observations have been made under serum-starved conditions in the absence of growth factors. Due to the activity of plasma membrane recruited oncogenic KRas, we hypothesize that this activity could have an influence on the cellular signaling response to growth factors like EGF.

To study this, the amount of active endogenous Ras was measured by GST-3xCRafRBD pulldown. In addition, the phosphorylation of the Ras activated kinases Akt and ERK was determined by In-Cell Western (ICW) assays to read out the activities of two major components of the Ras signaling network in the presence of the growth factor EGF. The recruited oncogenic Ras could either affect the activation threshold or the amplitude of the signal. Therefore, measurements were performed in dependence on increasing growth factor concentrations 5 min after stimulation either with mTFP-2xFKBP'-KRas ΔHVR recruited to the plasma membrane or with the recruitable KRas localized in the cytosol as the respective control. These experiments were performed with both NIH3T3 cell lines either expressing wild type or oncogenic recruitable KRas (Figure 14).

NIH3T3 cells expressing the wild type recruitable KRas show a sigmoidal increase of the amount of active endogenous Ras (Figure 14A), as well as ERK (Figure 14B) and Akt (Figure 14C) phosphorylation with increasing concentrations of EGF. It can be observed that the amount of active endogenous Ras increases more drastic over a smaller concentration range when compared to ERK and Akt phosphorylation, which are gradually activated over a wider EGF concentration range. Here, no significant difference in the dose-response profiles of all three readouts between the cells in which wild type Ras was recruited to the plasma membrane for 2 hours prior to the 5-minute-long EGF stimulus (black) or where the recruitable wt KRas is localized in the cytosol (grey) was observed.

When the oncogenic recruitable KRas is localized in the cytosol (light blue curves), the dose-response profiles of the amount of active endogenous Ras and ERK phosphorylation follow a similar sigmoidal activation curve when compared to the ones of the wild type recruitable KRas Figure 14A and B, respectively). However, the comparison of the fraction of phosphorylated Akt (Figure 14C) shows lower phosphorylation levels of Akt compared to the cells expressing recruitable wild type KRas up to an EGF concentration of 7 $ng \cdot mL^{-1}$.

The dose-response profile of active endogenous Ras when oncogenic mTFP-2xFKBP'-KRas G12D ΔHVR is recruited to the plasma membrane does not significantly differ from the one where mTFP-2xFKBP'-KRas G12D ΔHVR is located in the cytosol (Figure 14A). However, a significant difference between cytosolic and PM recruited mTFP-2xFKBP'-KRas G12D ΔHVR in EGF dependent phosphorylation of ERK Figure 14B) can be observed: the amplitude of the signal increases by a factor of 2 after stimulation with EGF for 5 minutes when the recruitable oncogenic

KRas is localized at the plasma membrane. When recruitable oncogenic KRas is at the plasma membrane, a 10-fold lower concentration of EGF (0.3 ng·mL^{-1}) is sufficient to reach the ERK phosphorylation levels, which are comparable to saturated ERK phosphorylation in the absence of oncogenic KRas at the PM. Notably, the basal phosphorylation of ERK does not differ between the cytosolic and PM recruited oncogenic KRas. Further, the overall shape of the curve is similar to the one without oncogenic recruitable KRas at the plasma membrane: ERK phosphorylation starts to increase at 0.1 ng·mL^{-1} EGF and starts to saturate at 1.5 ng·mL^{-1} EGF.

The dose-response curve of Akt phosphorylation is not significantly affected by the recruitment of oncogenic KRas to the plasma membrane prior to stimulation with EGF. However, when the two cell lines containing recruitable wt KRas Figure 14C, black and grey curves) or the recruitable oncogenic KRas G12D Figure 14B, blue and light blue curves) are compared, the Akt phosphorylation curve is lower in the cells containing the oncogenic recruitable KRas G12D while maintaining the overall shape.

5.2 Influence of oncogenic cells on their surrounding cells

We further wanted to study, if and how an oncogenic KRas mutation influences its neighboring cells. Therefore, it would be ideal to have a way to precisely manipulate the activity of oncogenic KRas in either single cells or small groups of cells in a given colony both in time and space. This is hard to achieve using the recruitment system based on chemically induced dimerization described in section 5.1, since this always leads to a global activation of oncogenic KRas and would therefore require a lower number of cells expressing the recruitable KRas, which can be hard to achieve. To accomplish spatially precise recruitment of KRas to the plasma membrane and activity of oncogenic KRas within a cluster of cells, light can be used as cue for dimerization in a modified recruitment system.

5.2.1 Design of a light controlled recruitable KRas

In order to restrict KRas activity locally even down to single cell level, a modified version of the recruitment system using a HaloTag and an eDHFR domain for hetero-dimerization can be used (Ballister, Aonbangkhen et al. 2014, Chen, Venkatachalapathy et al. 2017). To enable local activation, the TMP moiety of the bivalent dimer-inducing agent (TMP-Chlorohexyl) is chemically caged by an Nvoc group preventing the binding to the eDHFR domain. This group is cleavable by irradiation with violet or ultra-violet light in a wavelength range of 360 to 410 nm. Upon cleavage, the eDHFR domain can interact with the free TMP-Chlorohexyl. In contrast to the previously discussed chemically induced dimerization system, the FKBP'-domain is replaced by a HaloTag. HaloTag protein domains react with chloroalkyl groups *in vivo* under formation of a covalent modification of the HaloTag. Due to this covalent binding the dimer-inducing agent is not freely diffusing restricting heterodimerization to the area illuminated with light. Still, the dimerization can be reverted by the addition of free TMP competing for the eDHFR domain. To restore

dimerization after TMP administration, TMP can be washed out allowing for several cycles of recruitment.

To generate an optically plasma membrane recruitable KRas, the same approach as for the chemically activatable KRas (see 5.1) was chosen (Figure 15A): the C-terminal HVR of KRas serving as a membrane hub was N-terminally modified with a blue fluorescent protein (TagBFP) and the HaloTag dimerization domain (TagBFP-Halo-tKRas). The catalytically active domain of KRas4B (KRas ΔHVR) was N-terminally fused to a red fluorescent protein (mCherry) and the eDHFR domain used for recruitment. Additionally, a nuclear export sequence (NES) was added to the protein to avoid its accumulation in the nucleus yielding mCherry-NES-eDHFR-KRas ΔHVR.

To demonstrate that the light induced KRas recruitment can be performed in single cells, MDCK cells were transiently transfected with TagBFP-Halo-tKRas as well as mCherry-NES-eDHFR-KRas

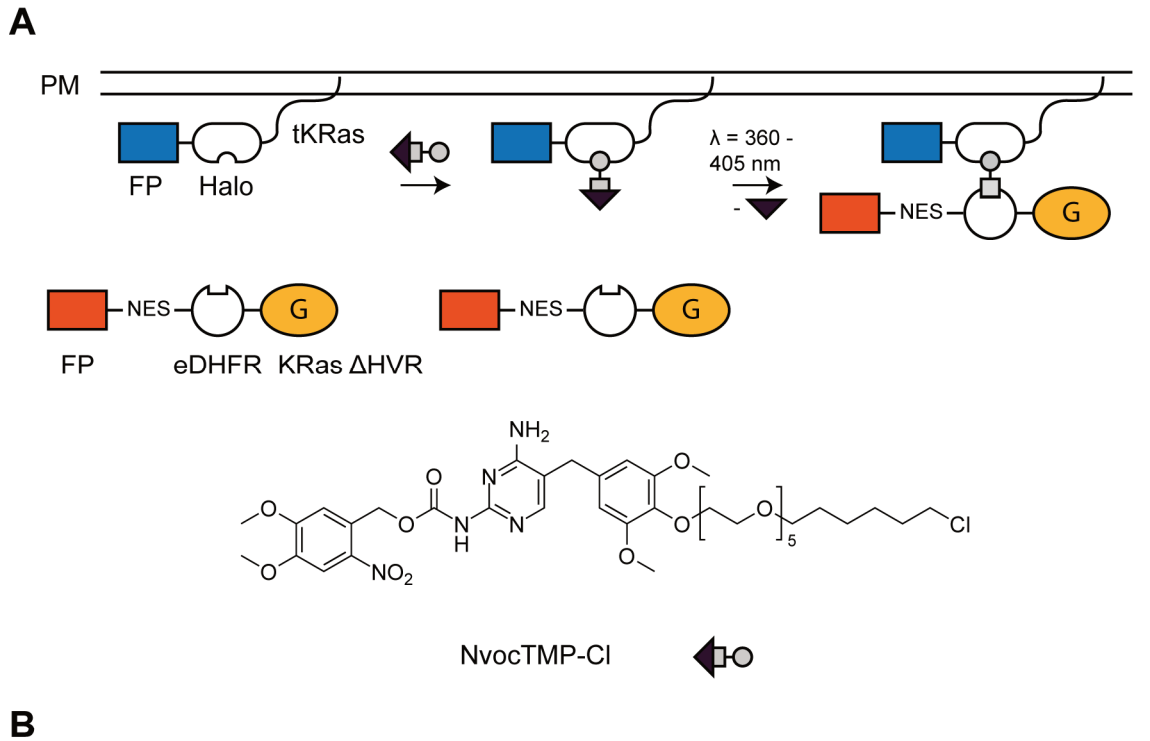

Figure 15: Design of light controlled recruitable KRas.

A. *Schematic drawing of the components of the light-controlled PM recruitable KRas.* ***B.*** *Example of light induced plasma membrane translocation of mCherry-NES-eDHFR-KRas G12V ΔHVR in a single cell (red outline). Scale bar: 10 µm.*

G12V ΔHVR (Figure 15B). A single cell was illuminated with high intensity 405 nm laser light to cleave the Nvoc protection group (Figure 15B, red outline). Within 1 minute after illumination with the 405 nm laser light, mCherry-NES-eDHFR-KRas G12V ΔHVR translocates to the plasma membrane. This shows that the light induced recruitment of mCherry-NES-eDHFR-KRas ΔHVR to the PM is significantly faster compared to the chemically induced recruitment of mCherry-2xFKBP'-KRas ΔHVR.

The altered domain structure of the optically recruitable KRas compared to the chemically recruitable KRas could have an influence on the activity of the PM recruited protein. To verify that

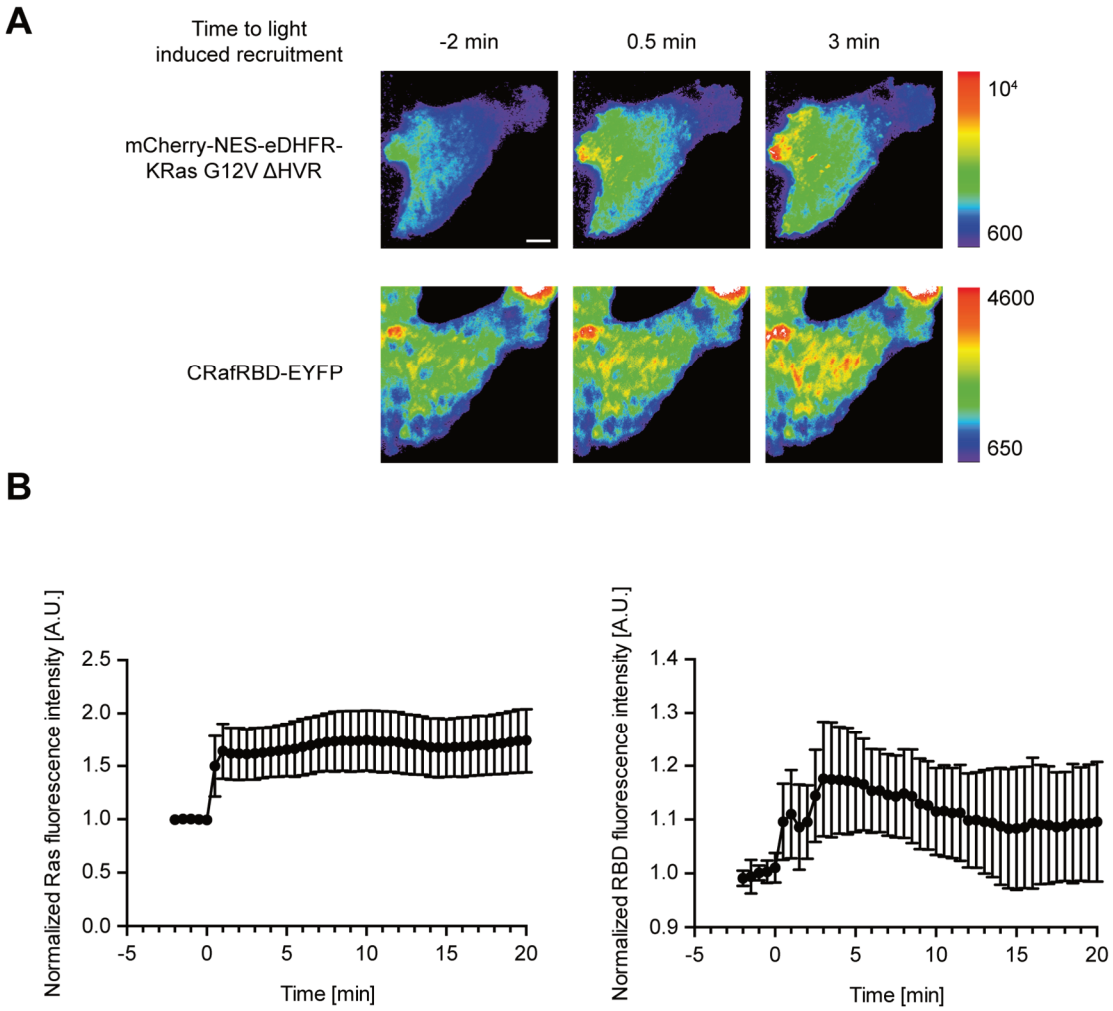

Figure 16: Light induced translocation of oncogenic KRas to the PM leads to its activation.

***A.** TIRF microscopic images of MDCK cells stably expressing CRafRBD-EYFP (bottom row, false colored) and transiently transfected with TagBFP-Halo-tKRas (not shown) and mCherry-NES-eDHFR-KRas G12V HVR (top row, false colored). Plasma membrane translocation of mCherry-NES-eDHFR-KRas G12V HVR was initiated by illumination with violet light at time point 0 min. **B.** Single cell analysis of the normalized TIR fluorescence intensity of mCherry-NES-eDHFR-KRas G12V HVR (left graph) and CRafRBD-EYFP (right graph). n = 9 cells, error bars: s.d., scale bar 10 µm*

the light induced recruitment of mCherry-NES-eDHFR-KRas G12V ΔHVR to the plasma membrane leads to its activation, MDCK cells stably expressing CRafRBD-EYFP were transiently transfected with TagBFP-Halo-tKRas and mCherry-NES-eDHFR-KRas G12V ΔHVR (Figure 16). Illumination with violet light leads to an increase in TIRF fluorescence of mCherry-NES-eDHFR-KRas G12V ΔHVR. Maximal recruitment is achieved 1 minute after cleavage of NvocTMP-Cl with light. Quantification of the TIRF fluorescence shows that after light induced recruitment, the fluorescence intensity does not further increase or decrease over time indicating a stable interaction between the membrane bound tKRas and the PM recruited G-domain of KRas (Figure 16B, left graph). In contrast, the TIRF fluorescence of CRafRBD-EYFP increases in two distinct steps after light induced PM recruitment of mCherry-NES-eDHFR-KRas G12V ΔHVR (Figure 16B, right panel). First, directly after recruitment of oncogenic KRas to the plasma membrane, the CRafRBD-EYFP fluorescence increases by about 10 %. After 2 minutes of KRas recruitment, the CRafRBD-EYFP fluorescence further increases by 10 % reaching the highest intensity 3 minutes after recruitment of oncogenic KRas to the plasma membrane. This is followed by a slow decrease of CRafRBD-EYFP fluorescence over a time span of 10 minutes.

To conclude, the enrichment of the Ras activity sensor CRafRBD-EYFP at the plasma membrane after light induced recruitment of oncogenic mCherry-NES-eDHFR-KRas G12V ΔHVR to the PM shows that the GTPase becomes active after translocation. When compared to the chemically induced dimerization, the KRas recruitment as well as the activation of KRas of this system is remarkably faster.

Further, it needs to be made sure if the light induced recruitment of mCherry-NES-eDHFR-KRas G12V ΔHVR to the PM leads to activation of downstream effectors of KRas. The Western blot approach used to characterize the phosphorylation of ERK in dependence on recruitment of mTFP-2xFKBP'-KRas G12D ΔHVR cannot be easily transferred to the light induced recruitment system, since it is based on measuring the ERK phosphorylation of the whole cell population and would require homogenous KRas recruitment. This however, is hard to achieve, since the cleavage of the Nvoc group is dependent on high light intensity, which is hard to ensure in a bigger area.

Therefore, the single cell measurement of ERK activity is advantageous. This could either be achieved using an ERK activity sensor usually containing a sequence that is phosphorylated by ERK and undergoes a change upon this phosphorylation, or, by fluorescently labeled ERK. Upon activation, ERK translocates to the nucleus where it can phosphorylate nuclear substrates like the transcription factors of the ETS family. Latter has the disadvantage that ectopic expression of ERK could influence cellular signaling and is connected to proliferation of cancer cells.

To examine if the recruitment of oncogenic mCherry-NES-eDHFR-KRas G12V ΔHVR to the plasma membrane leads to activation of targets downstream of Ras – for example ERK – MDCK cells stably expressing the Förster resonance energy transfer (FRET) based ERK activity sensor EKAREV-NES were used (Figure 17). Upon light induced plasma membrane recruitment of mCherry-NES-eDHFR-KRas G12V ΔHVR (Figure 17A), a heterogeneous change of the EKAREV sensor's FRET signal is observed: most cells show no change in the FRET ratio of the ERK activity sensor or a non-significant increase or decrease of the FRET ratio. Only 2 out of 11 cells show a significant increase of the ratiometric FRET signal corresponding to an increased activity of ERK (Figure 17B, red and blue curve). While the blue curve shows an almost immediate and sustained increase in ERK activity, the red one shows highest ERK activity 15 minutes after recruitment of Ras to the plasma membrane and decreases after 30 min post recruitment. If compared to the recruitable oncogenic KRas based on chemically induced dimerization (Figure 11), the activation of

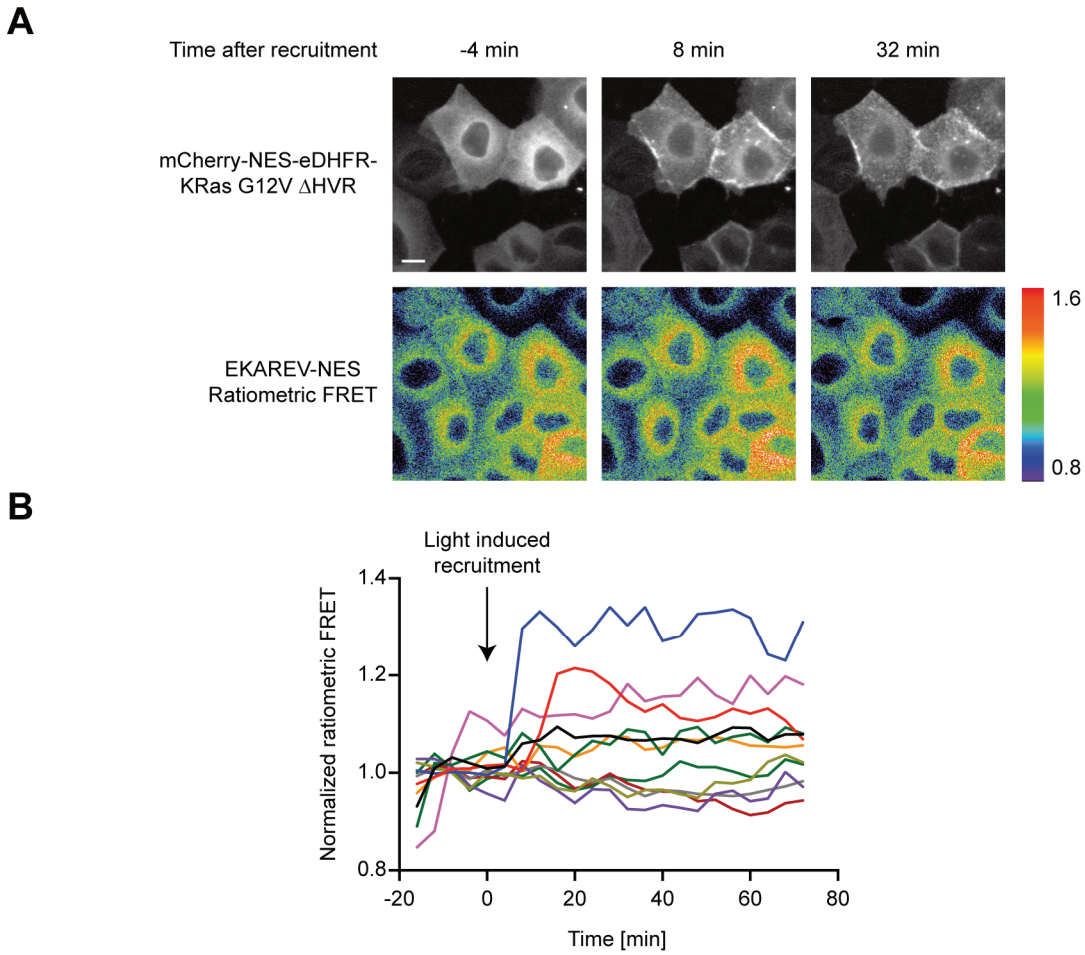

Figure 17: Activation of Ras the Ras effector ERK upon recruitment of oncogenic mCherry-NES-eDHFR-KRas G12V HVR to the PM

***A.** Fluorescence microscopic images of MDCK cells stably expressing the EKAREV-NES ERK activity sensor (bottom row, false colored) transiently transfected with Halo-tKRas (unlabeled) and mCherry-NES-eDHFR-KRas G12V ΔHVR. PM translocation of mCherry-NES-eDHFR-KRas G12V ΔHVR (top row) was induced by illumination with violet light at time point 0 min. **B.** Single cell quantification of the EKAREV-NES ERK activity sensor. Scale bar 10 µm*

ERK would be slower despite faster recruitment and activation of oncogenic KRas based on light induced recruitment. All in all, these results suggest, that the EKAREV ERK activity sensor might not be able to reliably measure changes in ERK activity upon recruitment of mCherry-NES-eDHFR-KRas G12V ΔHVR to the plasma membrane. Further, the spectral overlap between the high intensity violet light used for translocation of KRas to the plasma membrane and the absorption spectrum of the cyan fluorescent protein used as donor fluorophore of the EKAREV FRET sensor is problematic since light induced recruitment of KRas can lead to photobleaching of the sensor offsetting the measured FRET values.

Therefore, the translocation of fluorescently labeled ERK2-mCitrine from the cytosol to the nucleus was used as an alternative readout for ERK activity (Figure 18). After light induced plasma membrane recruitment of mCherry-NES-eDHFR-KRas G12V ΔHVR (Figure 18A, top row), a

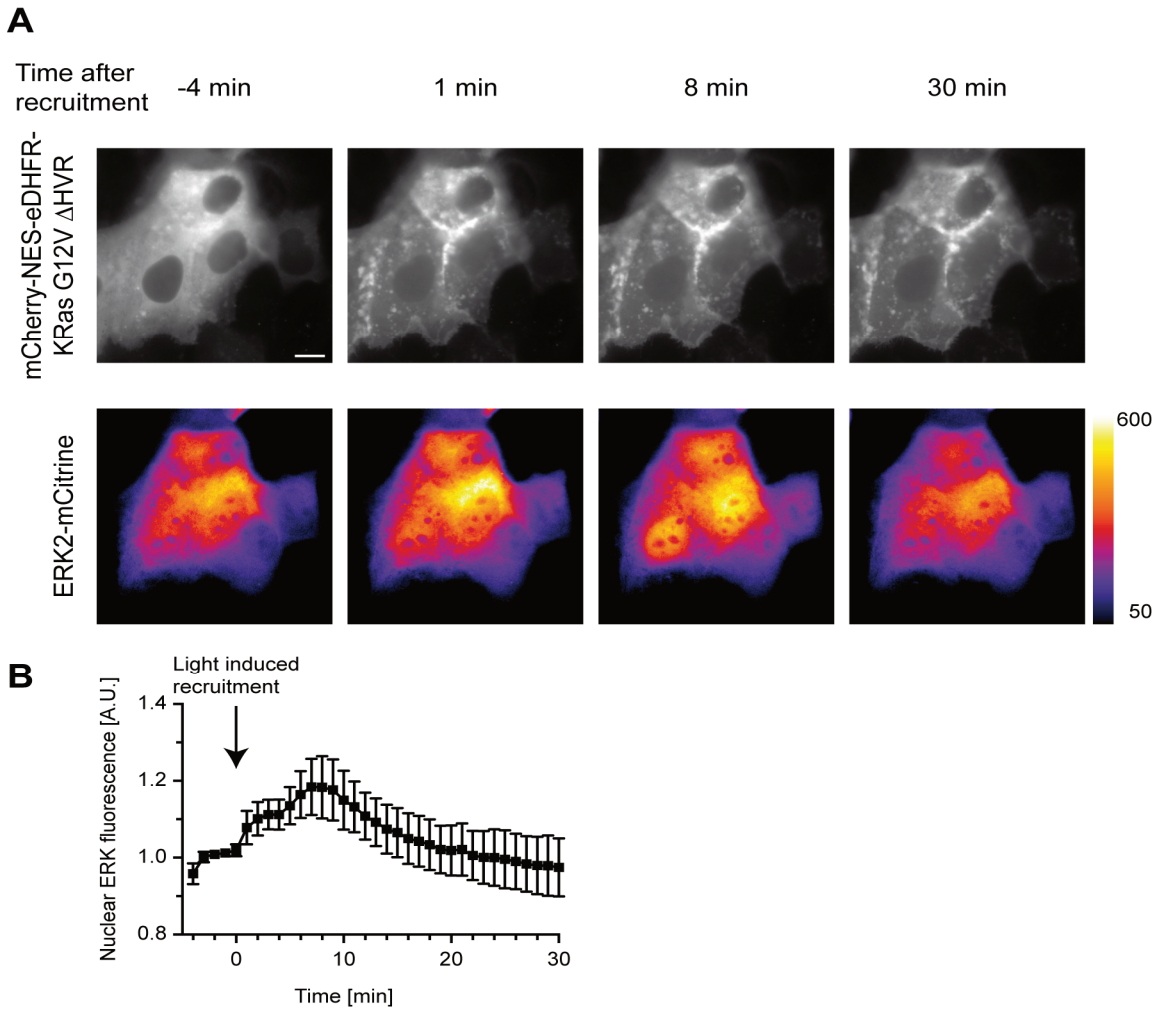

Figure 18: Recruitment of oncogenic mCherry-NES-eDHFR-KRas G12V ΔHVR to the plasma membrane leads to a transient ERK translocation to the nucleus.

***A.** Fluorescence microscopy images of MDCK cells expressing Halo-tKRas (unlabeled), mCherry-NES-eDHFR-KRas G12V ΔHVR (top row) and ERK2-mCitrine (bottom row, false colored). mCherry-NES-eDHFR-KRas G12V ΔHVR was recruited to the plasma membrane by illumination with UV light at time point 0 min. **B.** Average normalized nuclear ERK fluorescence ± s.d. (n = 10 cells). Scale bar 10 µm*

transient increase of nuclear ERK2-mCitrine can be observed (Figure 18A, bottom row). Similar to the recruitment of CRafRBD-EYFP to the plasma membrane (Figure 16B), fluorescently labeled ERK is transitioning from the cytosol to the nucleus in distinct two steps. Already after 1 minute of PM recruited oncogenic KRas an initial rise of nuclear ERK2-mCitrine is observed (Figure 18B). After 5 minutes of recruitment, the nuclear fluorescence intensity further increases and the maximal amount of nuclear ERK is observed after 8 minutes of oncogenic KRas recruitment to the plasma membrane. The amount of nuclear ERK2-mCitrine starts to decrease shortly after peak nuclear accumulation. About 20 minutes after recruitment of oncogenic KRas to the plasma membrane, the nuclear fraction of ERK is comparable to the levels before light induced PM recruitment of oncogenic KRas.

Overall, the recruitment of oncogenic KRas to the plasma membrane by light induces a transient enrichment of ERK in the nucleus indicating a transient ERK activity. Similarly, a transient ERK activity upon KRas PM recruitment can be observed using the chemically induced dimerization approach (Figure 11).

5.2.2 Oncogenic Ras influences neighboring cells

During the characterization of the activity of the recruitable Ras by co-translocation of fluorescently labeled CRafRBD, it could be noticed that, in a subset of cells, the light induced recruitment of oncogenic KRas to the plasma membrane is affecting the endogenous Ras activity in surrounding cells that do not express the recruitable oncogenic KRas (Figure 19A, arrows). However, differences to the cells transfected with the recruitable oncogenic KRas can be observed: while the cells expressing the recruitable oncogenic KRas show a sustained Ras activity (Figure 19B, black curve), in the adjacent cells a transient pulse of Ras activity with a duration of

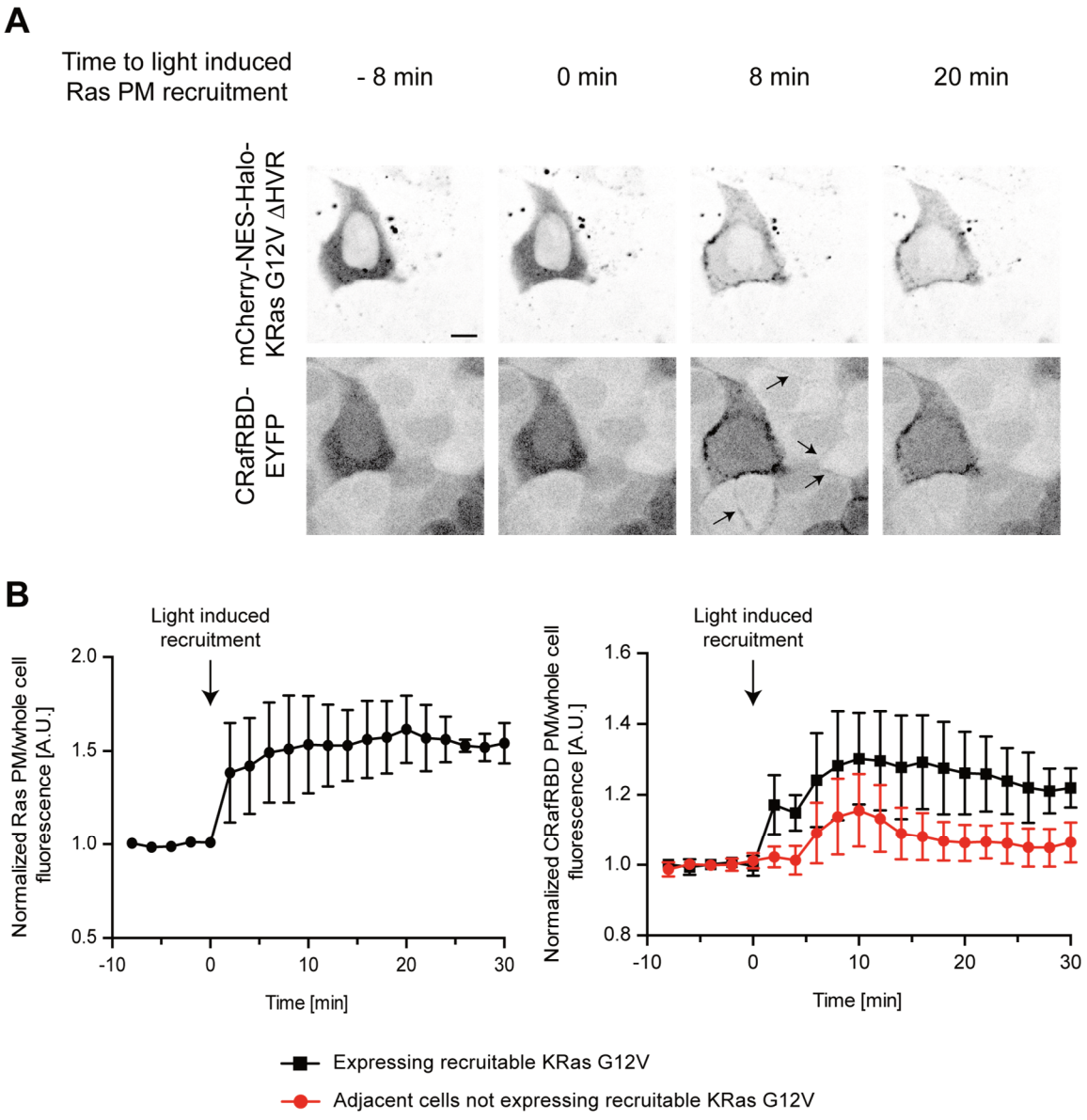

Figure 19: Recruitment of oncogenic KRas to the PM propagates to neighboring cells

A. *Fluorescence images of MDCK cells expressing mCherry-NES-eDHFR-KRas G12V ΔHVR, Halo-tKRas (unlabeled) and CRafRBD-EYFP. mCherry-NES-Halo-KRas G12V ΔHVR was recruited to the plasma membrane by illumination with UV light at time point 0 min.* ***B.*** *Quantification of normalized PM/whole cell median fluorescence of mCherry-NES-Halo-KRas G12V ΔHVR (left graph) and CRafRBD-EYFP (right graph) in cells containing mCherry-NES-Halo-KRas G12V ΔHVR (black, n = 3 cells) and not transfected adjacent cells (red, n = 9 cells). Scale bar: 10 µm*

approximately 10 minutes can be observed (Figure 19B, red curve). After the activity pulse, endogenous Ras activity is slightly elevated when compared to the activity prior to Ras recruitment in adjacent cells. Compared to the cells containing the recruitable oncogenic KRas, the recruitment of CRafRBD to the plasma membrane in the neighboring cells is delayed (Figure 19B). While the Ras activity in the cells expressing the recruitable Ras increases within a minute after recruitment (Figure 16 and Figure 19B, black curves), increase of Ras activity of surrounding cells can be observed 6 minutes after light induced recruitment of oncogenic KRas to the plasma membrane.

6 Discussion

6.1 Characterization of recruitable KRas

In this study, two tools based on chemically induced dimerization have been developed, which allow the control of Ras activity by controlling its localization within the cell. Therefore, KRas4B was split into two parts: the catalytically active N-terminus harboring the nucleotide binding pocket and the C-terminal hypervariable region responsible for the plasma membrane localization. Removal of the HVR results in a soluble Ras protein. Besides the cytosolic localization, a slight enrichment in the nucleus can be observed. This might be an artifact of the N-terminal fusion with a fluorescent protein (mCherry or mTFP) with the recruitable Ras lacking the HVR since fluorescent proteins show a slight enrichment in the nucleus (Seibel, Eljouni et al. 2007). This accumulation in the nucleus can be overcome by the addition of a nuclear export sequence to the fusion protein.

The kinetics of translocation of the recruitable KRas based on the FKBP'/eDHFR CID system to the plasma membrane are comparable to proteins of a similar size using this system (Liu, Calderon et al. 2014). Similarly, the kinetics of light induced KRas translocation to the plasma membrane based on a localized Halo-Tag and an eDHFR domain fused to the soluble protein match the values reported in the literature (Ballister, Aonbangkhen et al. 2014, Chen, Venkatachalapathy et al. 2017). In general, translocation of recruitable KRas from the cytosol to the plasma membrane is significantly faster when the light induction-based recruitment system is used. This is due to differences in the specific protocols: in the CID approach, which is using a tandem of FKBP'/eDHFR domains, the dimer inducing agent is added to the medium and first needs to pass the plasma membrane of the cells to induce dimerization. The for dimerization required concentration of the ligand can further lead to multiple ligand molecules binding to the dimerization domains resulting in a slowed down translocation. In contrast, the protocol for the light induced recruitment requires incubation and wash out of excess photocaged dimer inducing ligand prior to the uncaging event. This eliminates contribution of the previously mentioned processes and leads to faster most likely diffusion limited translocation of the protein from the cytosol to the plasma membrane. Further, the light induced PM recruitment approach allows a precise control of the amount of recruited protein by partially illumination of a cell. This makes the light induced translocation of KRas to the plasma membrane an ideal tool to observe processes in single cells while the chemically induced dimerization approach is better suited for population-based studies requiring KRas translocation in a large number of cells.

A noteworthy disadvantage of the light induced translocation of KRas is the high intensity light needed to cleave the Nvoc group of the photocaged dimerizer. On the one hand this short wavelength light could lead to phototoxicity, on the other hand it limits the use of blue and cyan

fluorescent proteins in microscopy experiments due to photobleaching. Photobleaching was indeed observed during the use of the EKAREV-NES ERK sensor based on FRET of an ECFP donor fluorophore.

6.1.1 Properties of cytosolic KRas

The removal of the membrane targeting motifs located in the HVR and addition of a CID system allows studying of the nucleotide binding of Ras in dependence on the cellular localization of Ras as well as mutagenic state. When the recruitable Ras is located in the cytosol, the fraction of active GTP-bound Ras is higher if the recruitable KRas is carrying an oncogenic Ras mutation compared to the wild type equivalent (Figure 12).

If wild type and oncogenic recruitable Ras are compared, the different fractions of active cytosolic Ras are most likely a result of the different hydrolysis rates. First, the oncogenic mutation reduces the intrinsic hydrolysis rate of Ras proteins by 2 orders of magnitude (Ahmadian, Zor et al. 1999). Further, RasGAPs like NF-1 or RASA1 – also known as RasGAP – are also localized in the cytosol (al-Alawi, Xu et al. 1993, Annibaldi, Michod et al. 2009, Stowe, Mercado et al. 2012). These proteins might be able to interact with recruitable wild type Ras in the cytosol enhancing GTP hydrolysis and therefore lead to its inactivation. The oncogenic Ras mutation impairs the interaction with GAPs, thereby impeding their acceleration of GTP hydrolysis. This might cause the observed elevated level of GTP-bound recruitable KRas harboring an oncogenic Ras mutation since these proteins solely rely on the slow intrinsic GTP hydrolysis.

Since the concentration of GTP in the cytosol exceeds the concentration of GDP by a factor of 10, it can be assumed that newly synthesized proteins become GTP loaded. Experiments, in which protein synthesis is inhibited, might show an increase of the fraction of GDP-bound soluble oncogenic Ras. Further, it is unknown whether RasGAPs are constitutively active in the cytosol or if they are subject to regulation of their activity, which would impact the hydrolysis rate of the recruitable wild type KRas (Maertens and Cichowski 2014).

6.1.2 Activation of recruitable KRas upon plasma membrane translocation

Upon membrane translocation of recruitable oncogenic KRas induced by SLF'-TMP administration, the fraction of GTP-bound Ras increases by a factor of 2 and reaches full activation (Figure 12). This activation is sustained since the oncogenic Ras cannot interact with GAPs and just slowly hydrolyzes GTP to GDP. The question arises what is causing of the increased activity of oncogenic KRas upon plasma membrane translocation. Due to the high picomolar affinity for GDP and GTP, it is highly unlikely that recruitment of oncogenic KRas to the plasma membrane leads somehow to the dissociation of the nucleotide followed by replacement with more abundant GTP. Further, only recruitable oncogenic KRas becomes activated upon plasma membrane recruitment while

wild type Ras stays inactive ruling out a mechanism based on spontaneous dissociation of the nucleotide.

Another possible activation mode would be that recruitment of oncogenic KRas to the plasma membrane enables the interaction with a RasGEF leading to nucleotide exchange and therefore to full activation of oncogenic Ras. The potential mechanism must be dependent on the presence of an active Ras species since in the absence of an oncogenic Ras species, wild type Ras does not get activated when recruited to the plasma membrane. However, it becomes GTP-loaded when oncogenic full-length KRas is co-expressed and might act as a stimulant of nucleotide exchange (Figure 12 and Figure 13).

In case of the recruitable KRas carrying an oncogenic mutation, about 50 % of the recruitable GTPase is GTP-bound under serum-starved conditions (Figure 12). Upon plasma membrane recruitment of the protein, this active fraction could serve as active Ras species at the plasma

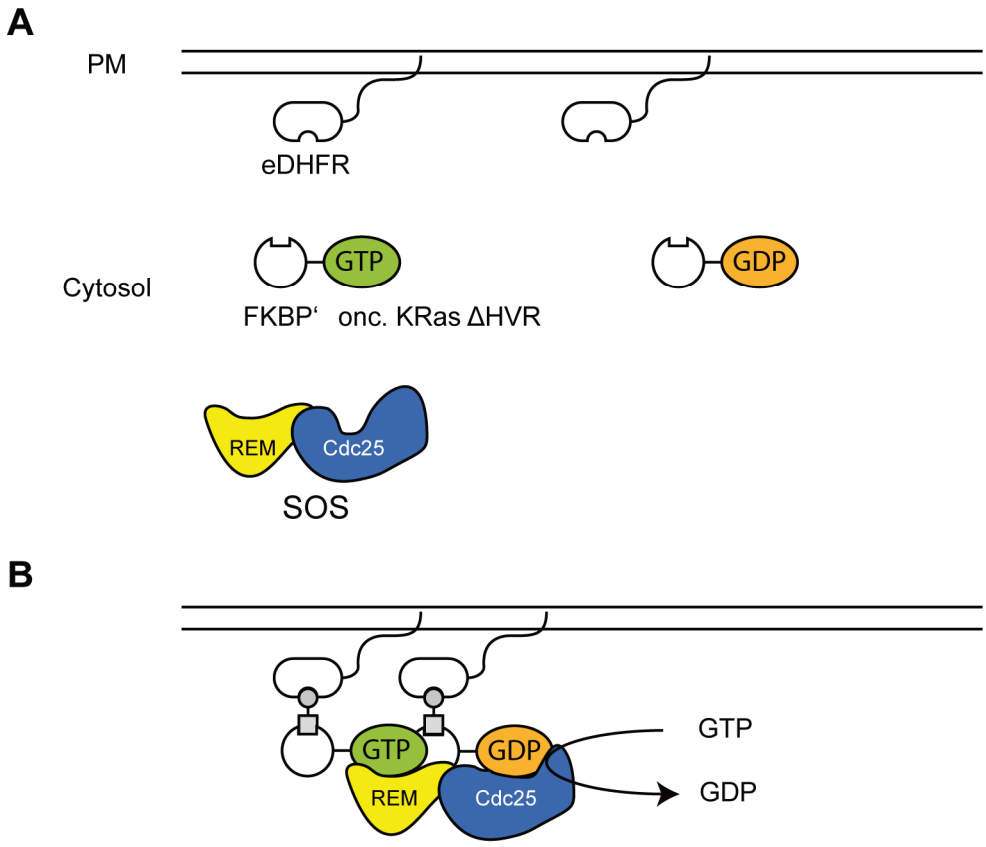

Figure 20: Potential activation of recruitable oncogenic KRas by SOS

A. *In the absence of the dimer-inducing ligand, the recruitable oncogenic KRas as well as the RasGEF SOS are located in the cytosol. The recruitable oncogenic KRas molecules are partially in the inactive, GDP-bound, partially in the active, GTP-bound state. SOS proteins are autoinhibited and cannot catalyze nucleotide exchange of Ras.* ***B.*** *Upon recruitment of recruitable oncogenic KRas to the plasma membrane by the addition of a small-molecule dimerizer, interaction of SOS with lipids of the membrane enables the active fraction of the PM recruited to bind to the allosteric site of SOS resulting in activation of the GEF. GEF activity leads to the exchange of GDP to GTP in the inactive fraction of recruited oncogenic KRas.*

membrane and initiate the nucleotide exchange by stimulation of GEF activity. Further, the translocation of CRafRBD-EYFP to the plasma membrane in two distinct steps after light induced recruitment of oncogenic KRas to the PM substantiates this model (Figure 16). In that case, the first increase of CRafRBD-EYFP co-recruitment to the plasma membrane would be caused by the fraction of PM recruited KRas already bound to GTP. If this active fraction can initiate GEF activity, this would lead to GTP-binding of the former inactive fraction of recruitable KRas. The now completely active recruited KRas can recruit additional molecules of the activity sensor to the plasma membrane resulting in the second observed increase of CRafRBD-EYFP fluorescence.

There are three differently regulated families of RasGEFs that could cause this activation: SOS, RasGRP and RasGRF. Best studied are the RasGEFs of the SOS family. RasGEFs of the SOS family possess two binding sites for Ras: The catalytically active site mediating the nucleotide release of bound Ras protein as well as a second allosteric site that preferentially binds GTP-bound Ras and increases the exchange activity of the GEF (Sondermann, Soisson et al. 2004). This would be sufficient to explain the observed activation of recruitable Ras upon plasma membrane recruitment in the presence of an active Ras species at the membrane. In this simplified consideration, the active Ras species – for example full length oncogenic KRas or the active fraction of the recruitable oncogenic KRas – would interact with the allosteric site of SOS resulting in increased exchange activity. This activity would result in activation of previously inactive Ras proteins at the plasma membrane (Figure 20). Further, this should again increase GEF exchange rate, resulting in a self-sustaining cycle of active Ras, independent of its mutation state. However, this simplistic consideration neglects the fact that SOS is autoinhibited. In the autoinhibited conformation the allosteric Ras binding site is blocked by the DH domain of SOS (Sondermann, Soisson et al. 2004). However, it has been shown that an increase in membrane surface density of Ras as well as membrane localization of SOS can enhance the activity of SOS even when autoinhibited by the N-terminal protein domains (Gureasko, Galush et al. 2008). Further, another study suggests that generation of a small pool of active Ras, in this case by RasGEFs of the RasGRP family, might be sufficient to prime the activity of SOS (Roose, Mollenauer et al. 2007). Since the recruitment of oncogenic Ras to the plasma membrane resembles such an increase in active Ras concentration, the recruitment could indeed lead to SOS activation and therefore to full activity of the recruited oncogenic Ras. This could explain why a nucleotide exchange does not occur when recruitable wild type Ras is translocated to the plasma membrane by chemically induced dimerization: the lack of an active Ras species prevents the activation of SOS. However, if an active Ras species is present, for instance full length oncogenic Ras, this species can prime the activation of SOS and therefore induce nucleotide exchange in recruitable wild type Ras, as observed (Figure 13).

RasGEFs of the RasGRP and RasGRF family are mainly expressed in certain tissues. If at all, these GEFs are expressed at low levels in the fibroblasts (NIH3T3) and epithelial kidney cells (MDCK)

used in this study, according to respective RNA expression data (Chadwick and Goode 2008, Uhlen, Fagerberg et al. 2015, Uhlen, Zhang et al. 2017). The activation of these GEFs is independent of active Ras but rather facilitated by protein-lipid interaction and Ca^{2+} ions. Therefore, GEFs of these two families are unlikely to contribute to the activation of recruitable KRas in the studied cell lines but might play a role in cells of other tissues. RasGEFs of the SOS family on the other hand are ubiquitously expressed and are therefore the prime candidate for initiation of recruitable Ras activation (Stone 2011). This should be verified by analysis of protein expression of the cell lines used in this study. Further, the RasGEFs expressed in these cells should be knocked-down or knocked-out prior to recruitment of KRas to the plasma membrane to specifically identify the GEF responsible for the activation of the recruited KRas proteins.

If these findings and the observations that soluble oncogenic KRas is just partially active are taken together, they show the importance of plasma membrane localization for KRas activity, especially if the active fraction proves to be newly synthesized protein. Therefore, to maintain the constitutive active state that is frequently observed for the full-length protein carrying an oncogenic mutation, activity of RasGEFs seems to be crucial, which was already claimed by a theoretical study (Kenney and Stites 2017). In most cell types, SOS proteins will fulfill the role of the activator since these RasGEFs are most active at the plasma membrane due to interaction with PIP_2.

6.1.3 Recruitment of oncogenic KRas to the PM influences Ras signaling

The differences in Ras activity of wild type and oncogenic species after recruitment to the plasma membrane are also reflected in the activity of downstream nodes of the Ras signaling network. Since recruitable wild type KRas does not get activated upon chemically induced translocation to the plasma membrane and does not show basal activity in the cytosol, no ERK response can be observed after addition of the dimer-inducing compound (Figure 11).

While recruitment of wild type KRas to the plasma membrane increases the overall KRas concentration at the plasma membrane, this higher KRas concentration does not influence the growth factor dose dependent phosphorylation of Akt and ERK (Figure 14).

In contrast, when oncogenic KRas is translocated to the plasma membrane, ERK phosphorylation increases 10 minutes post recruitment (Figure 11). After 20 minutes of oncogenic KRas plasma membrane recruitment, the fraction of phosphorylated ERK starts to decrease. Similarly, a transient translocation of fluorescently labeled ERK2 to the nucleus is observed upon light induced plasma membrane recruitment of soluble oncogenic KRas (Figure 18). This shows that the cells expressing the recruitable oncogenic Ras can adapt to the sudden increase of Ras activity resulting in phosphorylated ERK. Since Ras is activated by translocation to the plasma membrane in the absence of growth factor, the termination of the ERK signal also is independent of receptor

activity. ERK proteins are well known to be involved in negative feedback regulation in the MAPK signaling network (Lake, Correa et al. 2016). For instance, they can hyperphosphorylate proteins of the Raf family resulting in their inability to interact with active Ras and therefore in reduced plasma membrane localization (Wartmann, Hofer et al. 1997, Dougherty, Muller et al. 2005). Besides kinases of the Raf family, MEK1 is also phosphorylated by ERK. These phosphorylation events lead to inactivation of the upstream kinases terminating the signal.

Recruitment of oncogenic KRas to the plasma membrane not just directly induces ERK activity, but also alters the ERK phosphorylation response to growth factor stimulation drastically (Figure 14B). While the overall shape of the curve is maintained, the amplitude of the ERK signal increases by almost 2-fold at the highest doses of EGF. This ERK phosphorylation data was obtained by In-Cell Western analysis, a population-based measurement. Therefore, the increase in phosphorylated ERK can be interpreted in different ways: First, this could mean that cells with oncogenic KRas located at the plasma membrane have a higher fraction of phosphorylated ERK compared to those where the oncogenic KRas is located in the cytosol. If this was the case, this could have severe consequences for the cells. The activation of ERK by an EGF stimulus is described by a so-called "fold change detection" (Cohen-Saidon, Cohen et al. 2009, Adler and Alon 2018). As the name suggests, in fold change detection not the absolute amplitude of a signal but the relative change is detected. Since the amplitude of the ERK phosphorylation is higher when cells are stimulated with EGF and oncogenic KRas is translocated to the plasma membrane, a 10-fold lower EGF dose would be sufficient to induce the same relative change in ERK phosphorylation. This could result in activation of physiological processes like proliferation at growth factor concentration way below the threshold of a system without oncogenic KRas present at the PM.

Otherwise, the total number of cells responding to the added growth factor with ERK phosphorylation could be higher when oncogenic KRas is recruited to the plasma membrane. This phenomenon was observed in a study using a colorectal cancer cell line harboring oncogenic KRas and a derived cell line, in which oncogenic KRas is replaced by wild type KRas (Björn Koos, personal communication). At the same EGF concentration, more cells containing the mutated KRas showed ERK phosphorylation when compared to the isogenic cell line having only wild type KRas. This could result in more proliferative cells.

Despite the observed effects on Erk phosphorylation, Akt phosphorylation was not affected. Neither the recruitment of wild type nor oncogenic KRas to the plasma membrane did significantly alter the phosphorylation of Akt upon growth factor stimulation (Figure 14C). Akt is phosphorylated by phosphatidylinositol-4,5-bisphosphate 3-kinase (PI3K), which can be activated by active Ras, but also directly be activated by the phosphorylated EGF receptor (Castellano and Downward 2011). Therefore, it is possible that PI3K activation is independent on Ras activity and

concentration in the used NIH3T3 cells as also reported in other studies (Toettcher, Weiner et al. 2013).

Still, differences in the EGF dose dependent Akt phosphorylation can be observed. The basal Akt phosphorylation of the cells expressing the recruitable oncogenic KRas is decreased when compared to the cells expressing the wild type counterpart. This could have several reasons. First, these cell lines were subjected to clonal selection after the introduction of the respective recruitable KRas and this difference in basal Akt activity could be due to heterogeneity of the parental cell line. Further, the active cytosolic fraction of the recruitable oncogenic KRas might be able to induce the down-regulation of the basal Akt phosphorylation, which is independent of both Ras localization and growth factor stimulation.

6.1.4 Ras activation by light-induced plasma membrane recruitment of SOScat

To control the activity of Ras, one other recruitment-based approach is described in the literature (Toettcher, Weiner et al. 2013). In contrast to the recruitment of Ras as presented in this work, Toettcher and colleagues used reversible optogenetic recruitment of the catalytically active domains of the RasGEF SOS (SOScat) from the cytosol to the plasma membrane to indirectly induce Ras activity. The induced Ras activity subsequently leads to rapid translocation of the Ras effector ERK to the nucleus. This nuclear translocation is reversed upon light-induced displacement of SOScat from the plasma membrane into the cytosol. So, both recruitment of SOScat or oncogenic KRas to the plasma membrane induce activity of the Ras effector ERK. However, a different signaling response can be observed in the same cell line: while PM recruitment of SOScat leads to sustained ERK activity as long as SOScat is localized to the PM, a transient ERK response can be observed upon sustained PM recruitment of oncogenic KRas (Figure 11 and Figure 18).

As the recruitment of oncogenic KRas to the plasma membrane, SOScat PM recruitment also does not induce Akt phosphorylation in NIH3T3 cells, confirming that Akt activation in these cells in independent of Ras activity.

Since the recruitment of SOScat lacking all regulatory protein domains to the plasma membrane leads to activation of all Ras proteins, this approach is not feasible to study the interaction of wild type Ras with oncogenic Ras.

6.2 Interaction between endogenous wild type and recruitable oncogenic Ras

Due to the positive feedback loop of active Ras to its GEFs of the SOS family, the recruitment of KRas to the plasma membrane might not just activate Ras effectors but endogenous wild type Ras. The recruitment of active KRas to the plasma membrane could therefore result in higher basal activity of endogenous wild type Ras and influence the wild type Ras activity response curve to stimulation with growth factors like EGF.

6.2.1 Influence of oncogenic KRas on wild type Ras independent of growth factors

The expression of either wild type or oncogenic recruitable KRas has differential effects on endogenous wild type Ras. In comparison to the cells expressing wild type recruitable KRas, the amount of active endogenous Ras is 2-fold higher in the cells possessing recruitable oncogenic KRas even when the recruitable KRas is solely located in the cytosol (Figure 12A and C). However, the higher basal activity of the endogenous wild type Ras is not reflected in higher ERK phosphorylation in the absence of growth factors (Figure 11B and Figure 14B). Thus, the cells expressing recruitable oncogenic KRas seem to be able to adapt to the higher amount of active endogenous wild type Ras in terms of ERK signaling output.

As mentioned before, the Akt phosphorylation under serum-starved conditions is decreased in the cell line expressing the recruitable oncogenic KRas (Figure 14C). If this reduction is due to negative feedback induced by Ras activity, ERK activity would be more robust towards changes in Ras activity than Akt signaling. Further, the administration of growth factor still induces an increase of Ras activity (Figure 14A). Taken together, these results indicate that cells expressing recruitable oncogenic KRas in the cytosol are capable of adapting to the elevated levels of active endogenous wild type Ras at the plasma membrane and are still responsive to EGF stimulation.

Here, the activity of endogenous wild type Ras upon recruitment of either wild type or oncogenic recruitable KRas to the plasma membrane in the absence of growth factors has been studied. Neither in the cells expressing the recruitable wild type KRas nor in the cells expressing recruitable oncogenic KRas the amount of active endogenous Ras changes upon recruitment of KRas to the plasma membrane (Figure 11C). In case of the cells harboring the recruited wild type Ras, this is expected since the recruited KRas does not get GTP-loaded upon recruitment. On the other hand, it is surprising that just the recruitable oncogenic KRas but not the endogenous wild type Ras gets activated upon recruitment. It is unlikely that the activator of the recruitable oncogenic KRas can discriminate between wild type and oncogenic Ras, raising the question what is causing the difference in activity. Since – in contrast to oncogenic Ras – wild type Ras can be deactivated by the interaction with GAPs, a constitutive GAP activity could explain this phenomenon. Such a constitutive GAP activity is observed when active GTP-bound Ras is injected either in *Xenopus* oocytes or mammalian cells and quickly converted into inactive GDP-bound Ras (Trahey and McCormick 1987, Rubio and Wetzker 2000). Therefore, it might be necessary in this signaling network to temporarily decrease GAP activity upon growth factor stimulation to generate a robust Ras activity response to a stimulus. If such a mechanism exists, it has to be independent of Ras mediated signaling since the recruitment of active oncogenic KRas to the plasma membrane does not lead to the activation of wild type Ras. Rather, it is more likely dependent on the activity of the growth factor receptor. For instance, the RasGAP NF1 can be degraded by ubiquitination upon growth factor stimulation (Cichowski, Santiago et al. 2003,

McGillicuddy, Fromm et al. 2009, Hollstein and Cichowski 2013). However, this degradation might be depending on cell type and the specific growth factor (Mangoura, Sun et al. 2006, von Kriegsheim, Baiocchi et al. 2009). Further, down-regulation of RasGAPs independent of Ras might also occur via Src or PI3K signaling (Rubio and Wetzker 2000, Giglione, Gonfloni et al. 2001, Sasaki, Janetopoulos et al. 2007). In summary, a constitutive activity of RasGAPs might be a cellular mechanism to safeguard against aberrant wild type Ras activation and could lead to rapid deactivation of endogenous wild type Ras upon recruitment of oncogenic KRas to the plasma membrane.

6.2.2 Cellular response to growth factors in dependence on oncogenic KRas at the PM

In tissue culture as well as in a multicellular organism, cells are rarely isolated entities and form groups of interacting cells. Different chemical agents like growth factors or ions transfer signals between cells. In this noisy environment, activity thresholds can generate a robust input-output relationship. In Ras signaling, the positive feedback to its activator SOS can generate an “all or none” response. Since this feedback is dependent on the amount of active Ras at the plasma membrane, recruitable oncogenic KRas could therefore shift the threshold concentration for Ras to lower concentrations of growth factors, as observed here for EGF stimulation. Ultimately, this could lead to a phenotypic response for example in the form of proliferation initiated by a growth factor concentration that would be below the activity threshold in the absence of oncogenic KRas at the plasma membrane.

However, upon stimulation with increasing doses of the growth factor EGF, no significant shift of the activation threshold can be observed (Figure 14A). This might reinforce the hypothesis that the activity of endogenous wild type Ras is controlled by a constitutive GAP activity and that these proteins get deactivated upon activation of growth factor receptors independently of KRas since the GEF activity at the plasma membrane is sufficient to activate the recruitable oncogenic KRas.

Also, it must be questioned whether the concentration dependent activity of Ras is the decisive factor in oncogenic Ras signaling. Despite the same Ras activation threshold at EGF concentrations between 1 and 3 $ng \cdot mL^{-1}$, the phosphorylation and therefore the activity of the Ras effector ERK is increased at lower growth factor concentrations in the presence of recruitable oncogenic KRas at the plasma membrane. Though ultimately, the activity of Ras effectors like ERK and not activity of Ras itself initiate cellular processes like gene transcription and proliferation that could result in an oncogenic phenotype.

6.3 Propagation of Ras activity to other cells

Upon the recruitment of oncogenic KRas to the plasma membrane by utilizing the light inducible recruitment approach in MDCK cells, a spread of Ras activity to adjacent cells measured by plasma membrane translocation of fluorescently labeled CRafRBD as Ras activity sensor could be observed

(Figure 19). In contrast to the sustained Ras activity caused by the PM recruited oncogenic KRas, these cells, which were not transfected with the oncogenic recruitable KRas and just harbor endogenous wild type Ras, nonetheless show a transient Ras activity. Due to the six-minute delay of the Ras activity in the adjacent cells, it can be assumed that the Ras activity is first processed in the cell containing the recruitable oncogenic KRas and a Ras effector initiates the spread of the signal and in this event of cell-to-cell communication. Since increased ERK activity can be observed minutes after KRas recruitment to the plasma membrane, this kinase could be a candidate for the initiation of propagation of Ras activity. Further, a propagation of ERK activity between cells has been previously observed in various cell lines including the MDCK cells used here (Aoki, Kumagai et al. 2013). The most intensively characterized NRK-52E cells in the study by Aoki and colleagues are also cells of the epithelium of the kidney. However, these cells were isolated of rat kidneys while the MDCK cells are of canine origin. Nevertheless, both species are isolated from higher vertebrates. Therefore, it is reasonable to assume similarities in their cell-to-cell communication.

Remarkably, the measured delay of the ERK activity propagation in the NRK-52E cells was 5 to 8 minutes and matches the Ras activity delay observed here in MDCK cells. Using a panel of small molecule inhibitors, they were able to show that the ERK activity propagation between adjacent cells is dependent on several factors. The inhibition of EGFR as well as ADAM metalloproteinases leads to the most drastic reduction in ERK activity propagation, while inhibition of protein kinase C (PKC) and PI3K partially impairs propagation of ERK activity. From this, they propose a model, in which ERK activates ADAM proteases cleaving and thereby releasing membrane bound EGF ligand. Then, the free ligand can bind to EGF receptors of adjacent cells resulting in ERK activity in a PI3K and/or PKC dependent manner.

In contrast to the here shown propagation of Ras activity to neighboring cells by translocation of CRafRBD to the plasma membrane, they were not able to detect propagation of Ras activity using the FRET-based RaichuEV-Ras activity sensor. Therefore, the results of this study might be able to extend the model proposed by Aoki and colleagues. The activation of EGFR in cells surrounding cells, in which oncogenic KRas has been recruited to the plasma membrane, might not just lead to activation of PI3K and/or PKC, but also to activation of wild type Ras contributing to the activation of ERK.

Altered cell-to-cell communication between tumor and stroma cells is an important event in tumorgenesis and considered as one of the many hallmarks of cancer. Cancer cells can manipulate the surrounding stroma cells when they send out signals that deviate from the ones of normal cells. This can change the signaling of the stroma cells and therefore the factors they secrete. Due to this recursive interaction between stroma and cancer cells, these signals of the stroma cells can alter the state of the cancer cell, which is distinct of the one of an isolated cancer cell. The

propagation of Ras activity by oncogenic Ras could be part of such a recursive interaction between cancer and stroma cells. It is known for KRas to engage in such a recursive interaction: pancreatic cancer cells expressing oncogenic KRas can interact with surrounding stroma cells via sonic hedgehog signaling (Tape, Ling et al. 2016).

7 Material and methods

7.1 Material

7.1.1 Buffers, solutions and media

7.1.1.1 Molecular biology

SOC medium	20 g·L^{-1} Bacto-Trypton, 5 g·L^{-1} Bacto-yeast extract, 0.5 g·L^{-1} NaCl, 2.5 mM KCl, 10 mM $MgCl_2$, 20 mM glucose (ZE Biotechnologie, MPI Dortmund)
LB medium	10 g·L^{-1} Bacto-Trypton, 5 g·L^{-1} yeast extract, 10 g·L^{-1} NaCl, pH 7.4 (ZE Biotechnologie, MPI Dortmund)
TB medium	12 g·L^{-1} Trypton, 24 g·L^{-1} yeast-extract, 4 mL·L^{-1} glycerol, 17 mM KH_2PO_4, 72 mM K_2HPO_4 (ZE Biotechnologie, MPI Dortmund)
LB agar selection plates with antibiotics	15 g·L^{-1} agar in LB medium, autoclaved, supplemented with respective antibiotics: Kanamycin: 50 µg·mL^{-1}; Ampicillin: 100 µg·mL^{-1} (ZE Biotechnologie, MPI Dortmund)
TAE buffer	40 mM Tris/Acetate pH 7.5, 20 mM NaOAc, 1 mM EDTA
DNA sample buffer (10x)	50 % Glycerol, 0.1 % Orange G, 100 mM EDTA

7.1.1.2 Protein biochemistry

Bacterial lysis buffer	50 mM Tris-HCl pH 7.5, 400 mM NaCl, 1 mM DTT, 1 % Triton X-100, 1 mM EDTA, 1 tablet Roche cOmplete™ ULTRA, EDTA-free per 50 mL
GST-3xRafRBD wash buffer	50 mM Tris-HCl pH 7.5, 50 mM NaCl, 20 % Glycerol, 1 mM EDTA, 1mM DTT, 1 tablet Roche cOmplete™ ULTRA, EDTA-free per 50 mL
Active Ras pulldown buffer	50 mM Tris-HCl pH 7.5, 200 mM NaCl, 10 % Glycerol, 5 mM $MgCl_2$, 1% Triton X-100, 1 tablet Roche cOmplete™ ULTRA, EDTA-free per 50 mL
PBS	136 mM NaCl, 2.7 mM KCl, 10 mM Na_2HPO_4, 17 mM KH_2PO_4 pH 7.4
2x SDS sample buffer	150 mM Tris-HCl pH 6.8, 1.2 % SDS, 30 % Glycerol, 2.1 M β-mercaptoethanol, 0.1 % bromophenolblue
5x SDS sample buffer	60 mM Tris-HCl pH 6.8, 2 % SDS, 25 % Glycerol, 0.7 M β-mercaptoethanol, 0.1 % bromophenolblue
RIPA lysis buffer	1 % sodium deoxycholate. 150 mM sodium chloride, 0.5 mM EDTA, 20 mM Tris pH 7.4, 1 % (v/v) Igepal, 0.1 % phosphatase inhibitor cocktail 2, 0.1 % phosphatase inhibitor cocktail 3
SDS running buffer	25 mM Tris-base, 192 mM glycine, 0.1 % SDS
Transfer buffer	25 mM Tris-base, 192 mM glycine, 20 % methanol
TBS	50 mM Tris-HCl pH 7.5, 150 mM NaCl
TBS-Tween	50 mM Tris-HCl pH 7.5, 150 mM NaCl, 0.1 % Tween 20

7.1.2 Kits and commercially available reagents

7.1.2.1 Molecular biology

Monarch® Plasmid Miniprep Kit (#T1010L)	New England Biolabs
NucleoBond® Xtra Midi Plus EF (#740422.50)	Macherey-Nagel
UltraPure™ Agarose (#16500500)	Thermo Fisher Scientific
RedSafe Nucleic Acid Staining Solution (#21141)	JH Science
Zymoclean™ Gel DNA Recovery Kit (#D4001)	Zymo Research
Quick Ligation™ Kit (#M2200S)	New England Biolabs
DNA Clean & Concentrator™-5 (#D4003)	Zymo Research

7.1.2.2 Protein biochemistry

Pierce™ Glutathione Magnetic Agarose Beads (#78602)	Thermo Fisher Scientific
Micro BCA™ Protein Assay Kit (#23235)	Thermo Fisher Scientific
Precision Plus Protein™ Dual Color Standards (#1610374)	Bio-Rad
Odyssey® Blocking Buffer (PBS) (#927-40000)	LI-COR

7.1.2.3 Antibodies

Primary antibody	**Dilution**	**Supplier**
Ras Antibody, clone RAS10 (#05-516)	1:1000 (Western Blot)	Merck-Millipore
α-Tubulin (#T6074)	1:4000 (Western Blot)	Sigma-Aldrich
Phospho-p44/42 MAPK (Erk1/2) (Thr202/Tyr204) (#4370)	1:2000 (Western Blot), 1:200 (In-Cell Western)	Cell Signaling Technology
ERK1 + ERK2 antibody [9B3] (#ab36991)	1:2000 (Western Blot)	Abcam
p44/42 MAPK (Erk1/2) (L34F12) Mouse mAb (#4696)	1:200 (In-Cell Western)	Cell Signaling Technology
Phospho-Akt (Ser473) (D9E) XP® Rabbit mAb (#4060)	1:500 (In-Cell Western)	Cell Signaling Technology
Akt (pan) (40D4) Mouse mAb (#2920)	1:200 (In-Cell Western)	Cell Signaling Technology

Secondary antibody	**Dilution**	**Supplier**
IRDye® 800CW Donkey anti-Mouse IgG (H + L) (#926-32212)	1:10000 (Western Blot)	LI-COR
IRDye® 680RD Donkey anti-Rabbit IgG (H + L) (#926-68073)	1:10000 (Western Blot)	LI-COR
IRDye® 800CW Donkey anti-Rabbit IgG (H + L) (#926-32213)	1:500 (In-Cell Western)	LI-COR
IRDye® 680RD Donkey anti-Mouse IgG (H + L) (#926-68072)	1:500 (In-Cell Western)	LI-COR

7.1.2.4 Cell culture reagents

CO_2 Independent Medium (#18045-054)	Thermo Fisher Scientific

DPBS without Ca^{2+}/Mg^{2+} (#P04-361000)	PAN Biotech GmbH
Dulbecco's Modified Eagle's Medium (DMEM, #P04-03600)	PAN Biotech GmbH
Effectene® transfection reagent (#301427)	QIAGEN
Fetal calf serum (FCS, #F7524)	Sigma-Aldrich
FuGENE® 6 Transfection Reagent (#E2692)	Promega
L-Glutamine (#P04-80100)	PAN Biotech GmbH
Lipofectamine™ 2000 (#11668019)	Thermo Fisher Scientific
Trypsin/EDTA (#P10-023100)	PAN Biotech GmbH

7.1.3 Chemicals

2-Mercapto-ethanol	SERVA Electrophoresis GmbH
Acetic acid conc.	Sigma-Aldrich
Albumin bovine fraction V, pH 7.0 (BSA)	SERVA Electrophoresis GmbH
Ammonium persulfate (APS)	SERVA Electrophoresis GmbH
Ampicillin sodium salt	SERVA Electrophoresis GmbH
Blasticidin	Gibco
Bromophenolblue	Sigma-Aldrich
Dimethyl sulfoxide (DMSO)	SERVA Electrophoresis GmbH
Dithiothreitol (DTT)	Fluka® Analytical
Ethanol	J.T.Baker
Ethylenediaminetetracetic acid (EDTA)	Fluka® Analytical
Glycerol	GERBU Biotechnik GmbH
Glycine	Carl Roth GmbH
Guanosine 5′-[γ-thio]triphosphate tetralithium salt	Sigma-Aldrich
Guanosine 5′-diphosphate sodium salt	Sigma-Aldrich
Isopropanol	J.T.Baker
Isopropyl β-D-1-thiogalactopyranoside (IPTG)	Applichem
Kanamycin sulfate	GERBU Biotechnik GmbH
Magnesium chloride (MgCl2)	Merck KG
Methanol	Sigma-Aldrich
N,N,N',N'-Tetramethylene-diamine (TEMED)	Carl Roth GmbH
Puromycin	Sigma-Aldrich
Sodium chloride (NaCl)	Fluka® Analytical
Sodium dodecyl sulfate (SDS)	Carl Roth GmbH
Trimethoprim	Sigma-Aldrich
Tris-base	Carl Roth GmbH
Triton X-100	SERVA Electrophoresis GmbH
Tween 20	SERVA Electrophoresis GmbH
Roti®-Histofix 4 %	Carl Roth GmbH
SLF'-TMP	Courtesy of the lab of Dr. Yaowen Wu
2/4-NvocTMP-Cl	Courtesy of the lab of Dr. Yaowen Wu
2-log DNA Ladder (0.1 – 10 kb)	New England Biolabs

Precision Plus Protein™ Dual Color Standards	Bio-Rad

7.1.4 Plasmids

Plasmid name	**Vector**	**Id**
ERK2-mCitrine	mCitrine-N1	492
CRafRBD-EYFP	EYFP-N1	595
GST-3xCRafRBD	pGEX-6P-1	3388
TagBFP-D1-tKRas	TagBFP-C1	5296
mCherry-D2-KRas wt ΔHVR	mCherry-C1	5297
mCherry-D2-KRas G12V ΔHVR	mCherry-C1	5298
mTFP-D2-KRas wt ΔHVR	mTFP-C1	5386
mTFP-D2-KRas G12V ΔHVR	mTFP-C1	5387
mKate2-KRas G12V	mKate2-C1	5910
mTFP-D2-KRas wt dHVR-P2A-TagBFP-D1-tKRas	PiggyBac CAG IRES PuroR	6482
mTFP-D2-KRas G12D dHVR-P2A-TagBFP-D1-tKRas	PiggyBac CAG IRES PuroR	6483
TagBFP-Halo-tKRas	TagBFP-C1	6524
mCherry-NES-1xeDHFR-KRas wt ΔHVR	mCherry-C1	6753
mCherry-NES-1xeDHFR-KRas G12V ΔHVR	mCherry-C1	6754
EKAREV-NES	PiggyBac CAG IRES PuroR	6941

7.1.5 Enzymes

T4 DNA Ligase (#15224017)	Thermo Fisher Scientific
Restriction endonucleases and corresponding reaction buffers	New England Biolabs
CIAP (Calf Intestinal Alkaline Phosphatase) (#18009019)	Thermo Fisher Scientific

7.1.6 *E. Coli* Strains

BL21-CodonPlus(DE3)-RIL	Agilent Technologies
XL10 Gold	Agilent Technologies

7.1.7 Mammalian cell lines

NIH3T3	Kind gift of the Ziegler group, MPI Dortmund
MDCK	ATCC

7.2 Methods

7.2.1 Molecular biology

7.2.1.1 *Transformation of chemically competent* E. Coli

50 µL chemically competent *E. Coli XL10-Gold* (used for DNA amplification) or 100 µL *E. Coli BL21-CodonPlus(DE3)-RIL* (used for recombinant protein expression) were mixed with 10 ng plasmid DNA and DTT (final concentration 78 mM). This mixture was incubated on ice for 20 minutes. To transform the bacteria, a heat shock to 42 °C for 45 s was applied followed by an incubation on ice for 2 min. Afterwards, 200 µL SOC medium were added and the mixture was incubated at 37 °C for 1 h on a rotating shaker. Subsequently, the bacteria were plated on LB selection plates containing the respective antibiotic resistance encoded on the plasmid and incubated overnight at 37 °C.

7.2.1.2 *Cultivation of* E. Coli

5 mL LB medium (small scale plasmid preparation), 150 mL LB medium (large scale plasmid preparation) or 50 mL TB medium (recombinant protein expression) containing the respective antibiotic were inoculated with *E. Coli* of a single colony grown on a LB plate. The bacteria were incubated overnight at 37 °C and shook at 200 rpm.

7.2.1.3 *Isolation of plasmid DNA (small scale)*

Isolation and purification of plasmid DNA was done with the Monarch® Plasmid Miniprep Kit New England Biolabs) following the manufacturers guidelines. The DNA was eluted in 30 µL elution buffer.

7.2.1.4 *Isolation of plasmid DNA (medium scale)*

Endotoxin-free purification was performed using the NucleoBond® Xtra Midi Plus EF kit (Machery-Nagel) following the manufacturers guidelines. The plasmid DNA was eluted in 3 times 200 µL TE-EF buffer.

7.2.1.5 *Photometric determination of DNA concentration*

The concentration and purity of isolated DNA was determined by the absorption at 260 nm and the ratio of the absorption at 260 nm divided by the absorption at 280 nm, respectively. The UV absorption was determined by using a NanoDrop 1000 spectrophotometer (Thermo Fisher Scientific) and corrected for the absorption of the buffer.

7.2.1.6 *Agarose gel electrophoresis*

Agarose gel electrophoresis was performed to separate DNA fragment by molecular weight. 0.8 – 2 % low-melting UltraPure agarose was suspended in TAE buffer, supplemented with RedSafe Nucleic Acid Staining Solution, which can be excited by ultra-violet or blue light leading to orange fluorescence when bound to DNA, and heated until it melted. The solution was cast into a Midi gel chamber and a comb was added into the liquid agarose to generate the sample wells. After

solidification, the comb was removed and the gels were moved into an electrophoresis chamber and overlaid with TAE buffer. Samples were mixed with 10x DNA sample buffer and loaded into the wells. The 2-log DNA ladder (New England Biolabs) was used as a reference and loaded in a separate well of the gel. To separate the DNA fragments, a constant potential of 150 V was applied for 30 min. To visualize the DNA, the bound dye was either excited using a blue light Safe-Imager (Invitrogen) or ultra-violet light of the imager Gel Doc XR (Biorad) containing a digital camera.

7.2.1.7 Purification of DNA fragment from agarose gels

After electrophoresis, the bands of the desired DNA fragments were excised from the gel, transferred to a 1.5 mL reaction tube and weighed. The DNA was isolated using the Zymo Gel Extraction kit following the manufacturers recommendations and eluted in 15 µL elution buffer.

7.2.1.8 Digestion of DNA using restriction enzymes

Restriction enzymes were used to cut DNA at specific positions. Therefore, up to 2 µg DNA were diluted in 50 µL of a buffer in which the used enzyme possesses highest activity. The reaction was performed using 5 U enzyme per µg DNA for at least 1 h up to 16 h, if the used enzyme does not exhibit unspecific activity, and at the manufacturers recommended temperature. If the DNA was cut with two enzymes, the conditions recommended by the online tool "double digest finder" (NEB) were applied.

7.2.1.9 5'-Dephosphorylation of DNA fragments

Dephosphorylation of the 5'-ends of digested vector DNA fragments was done to inhibit self-ligation of the vector. Therefore, 1 U calf intestinal alkaline phosphatase (CIAP) was added to the restriction digest mixture and incubated at 37 °C for 1 h.

7.2.1.10 Ligation of insert with plasmid DNA

To ligate DNA inserts into plasmid backbones, 50 ng dephosphorylated vector DNA was mixed with the insert in a 4-fold molar excess. The amount of insert DNA (m_{Insert}) was estimated by the size (s) of the fragments assuming equal distribution of the four nucleobases:

$$m_{Insert} = \frac{m_{Vector} \times s_{Insert} \times excess}{s_{Vector}} \qquad (1)$$

Ligation was achieved by applying the QuickLigation kit following the manufacturers recommendations. The ligated DNA was subsequently transformed into competent *E.Coli XL10-Gold* (see 7.2.1.1).

7.2.1.11 Ligation independent cloning

For ligation independent cloning approaches, the plasmid backbone was linearized by digestion with a restriction endonuclease (7.2.1.8) and the desired insert created by polymerase chain

reaction (7.2.1.12). The DNA fragments were purified using agarose gel electrophoresis. To generate 5'-overlaps on the vector as well as the insert, the purified DNA was incubated with 0.6 U T4 DNA polymerase in NEB buffer 2.1 in a 20 µL reaction for 1 h at ambient temperature. The enzyme was heat inactivated at 75 °C for 20 min. 50 ng vector were incubated with a 2-fold molar excess of insert (see equation (1)) in T4 ligase buffer (Invitrogen) in a total reaction volume of 10 µL. Subsequently, 5 µL of the annealed DNA were transformed in chemically competent *E. Coli XL10-Gold* (see 7.2.1.1).

7.2.1.12 Polymerase chain reaction (PCR)

PCR primers were designed to bind the template DNA on both strands at regions of interest. Additionally, recognition sites for restriction endonucleases (for cloning using restriction enzymes and ligation) or to the plasmid backbone complementary sequences used in ligation independent cloning approaches were added to the 5'-end of the primer, if necessary. Annealing temperatures were calculated using equation (2):

$$T_A = 59.9 + 41\frac{C + G - 16.4}{A + C + G + T} \qquad (2)$$

Herculase II Fusion DNA Polymerase was used for standard PCR reactions using the conditions in Table 1 and Table 2.

Table 1: Pipetting schema for a standard PCR reaction

Template DNA	5 ng
Herculase II Fusion DNA Polymerase	1 µL
Forward primer	0.5 µM
Reverse primer	0.5 µM
dNTPs	250 µM each
Nuclease free water	Ad 50 µL

Table 2: Cycling conditions for a standard PCR reaction

Number of cycles	**Temperature [°C]**	**Duration [s]**
1	95	120
30	95	15
	T_A	20
	72	30 per kb
1	72	180

PCR reaction products were purified either by agarose gel electrophoresis, if the reaction yielded unspecific PCR products, or by column purification using the DNA Clean & Concentrator™-5 kit (Zymo research) according to the manufacturers recommendations.

7.2.1.13 In vitro *mutagenesis*

The Q5® Site-Directed Mutagenesis Kit was used to introduce point mutations into existing plasmids. PCR primers containing the desired mutations were designed with the help of the "NEBaseChanger" online tool. The mutagenesis was performed following the recommendation of the manufacturer and using the annealing temperatures for PCR reactions provided by the "NEBaseChanger" tool. 5 µL of the reaction product were transformed into chemically competent *E. Coli* XL10-Gold and plated on appropriate selection LB-agar plates (see 7.2.1.1).

7.2.1.14 *DNA sequencing*

DNA samples were sequenced by GATC Biotech AG using specific primers for the respective plasmids.

7.2.2 Protein biochemistry

7.2.2.1 *Whole cell lysate*

Whole cell lysates for protein analysis using Western blots or Ras activity pulldown assays were prepared from cells grown in 6 well plates or 6 cm petri dishes. The growth medium was aspirated, the cells were once washed with ice-cold TBS and subsequently lysed with RIPA- or Ras activity pulldown buffer containing protease and phosphatase inhibitors on ice. After an incubation period of 5 min, cells were scraped off the culture vessel and transferred to precooled 1.5 mL reaction tubes. Lysates were cleared by centrifugation at 20000 g, 4 °C for 20 min. The supernatant was transferred to fresh precooled tubes and either directly subjected to determination of protein concentration or stored at -80 °C.

7.2.2.2 *Photometric protein concentration determination*

To determine the protein concentration of whole cell lysates, the bicinchoninic acid (BCA) assay was applied. Aqueous solutions of bovine serum albumin (BSA) spanning a concentration range from 0.1 $\mu g \cdot \mu L^{-1}$ to 5 $\mu g \cdot \mu L^{-1}$ were used as standard. 4 µL BSA standard or sample were incubated with 80 µL BCA reagent prepared following the recommendations of the manufacturer in a 96 well plate format at 37 °C for 1 h. Afterwards, the absorption at 562 nm was determined using a plate reader.

7.2.2.3 *Sample preparation for SDS-PAGE*

Before samples were loaded onto the gel, they were mixed with 5x SDS sample buffer and heated to 95 °C for 5 min. After heating, the samples were centrifuged at 20000 g for 3 min.

7.2.2.4 *SDS-PAGE*

To separate proteins of whole cell lysates by their molecular weight, a denaturing SDS polyacrylamide gel electrophoresis was performed. Therefore, gels containing 12 % acrylamide for separation were cast and overlaid with a 4 % stacking gel into with a comb was introduced prior to polymerization. The polymerized gels were moved to a gel electrophoresis chamber filled with SDS

running buffer and the comb was removed. Equal amounts of sample were added to separate wells of the gel along with the protein standard Precision Plus Protein™ Dual Color (Bio-Rad). Electrophoresis was performed at constant potential of 80 V for 30 min followed by 130 V for 1 h 45 min.

7.2.2.5 Western blot analysis

Before the Western blot was performed, the stacking gel and the dye band of the SDS sample buffer were cut off and the polyvinylidene fluoride (PVDF) membrane was soaked in methanol for 1 min. The blotting chamber (XCell II™ Blot Module, Thermo Fisher Scientific) was assembled according to the manufacturers recommendation and filled with transfer buffer. The transfer of the proteins to the membrane was performed at constant potential of 40 V for 70 min. To block unspecific binding of the antibodies to the membrane, it was incubated with Odyssey® Blocking Buffer (PBS) for 1 h at ambient temperature. Primary antibodies were diluted in Odyssey® Blocking Buffer (PBS) and incubated with the blot overnight at 4 °C. To remove excess antibody, the membrane was washed 3 times with TBS-Tween for 5 min. Infrared-fluorophore labeled secondary antibodies binding antibodies of the species, in which the primary antibodies were produced, were diluted in Odyssey® Blocking Buffer (PBS) and added to the membrane. After an incubation period of 1 h, the blot was washed as before and subsequently scanned using a LI-COR Odyssey® CLx Imaging System. The digital Western blot images were analyzed using the "Gel analyzer" tool of the ImageJ (Schneider, Rasband et al. 2012) distribution Fiji (Schindelin, Arganda-Carreras et al. 2012). In the resulting band profiles, each peaks base was manually connected by a straight line and the area of each peak measured. To compare results of different blots, values were normalized to the respective control condition.

7.2.2.6 In-Cell Western™ assay

In-Cell Western™ assays can be used as an alternative to Western blot analysis and allow higher throughput. To increase cell adhesion to the plate, black 96 well plates with clear bottom were treated with 50 µL of a 100 $mg \cdot L^{-1}$ poly-L-lysine solution for 20 min. Afterwards, the plates were washed twice with 100 µL PBS and air dried. 8000 NIH3T3 cells were plated in each well of the plate and incubated for one day. Afterwards, the medium was exchanged for DMEM supplemented with L-Gln, non-essential amino acids and 0.5 % FCS and the cells were incubated for another day. Then, the medium was exchanged for DMEM just supplemented with L-Gln and non-essential amino acids and treated as desired. To fix the cells after treatment, the medium was removed and subsequently the cells were once washed with PBS and fixated in 50 µL of a stabilized 3.7 % paraformaldehyde solution was added for 10 min. Then, cells were washed 3 times with 100 µL TBS and permeabilized with TBS containing 0.1 % Triton X-100 for 5 min to permeabilize the cells. After rinsing the cells 3 times with 100 µL TBS, they were blocked with Odyssey® Blocking Buffer (PBS) for 30 min. The cells were incubated with 50 µL of the desired primary antibodies diluted in

Odyssey® Blocking Buffer (PBS) over night at 4 °C. Excess antibody was removed by washing the plate 3 times with TBS followed by incubation with 50 µL matching infrared-fluorophor labeled secondary antibodies diluted in Odyssey® Blocking Buffer (PBS) for 30 min at ambient temperature. The plates were then rinsed 3 times with TBS and the fluorescence intensity of the individual wells was measured using a LI-COR Odyssey® CLx Imaging System. The resulting images were imported into the ImageJ distribution Fiji. The mean fluorescence intensity was determined for each well by using the "Microarray Profile" plugin.

7.2.2.7 Recombinant GST-3xRafRBD expression

20 mL of an overnight grown culture (see 7.2.1.2) of *E. Coli* BL21-CodonPlus(DE3)-RIL transformed with the plasmid encoding the recombinant protein were added to 480 mL TB medium and incubated at 37 °C on a 200 rpm while the optical density at 600 nm (OD_{600}) was checked regularly. At an OD_{600} of 0.8, recombinant protein expression was induced by the addition of 0.1 mM IPTG. GST-3xRafRBD was expressed for 5 h at 30 °C. Afterwards, the bacteria were harvested by centrifugation at 4000 g for 30 min at 4 °C. Pellets were ether lysed directly or stored at -20 °C.

7.2.2.8 Lysis of E. Coli

To extract the GST-3xRafRBD from the bacteria, the harvested cells were resuspended in 20 mL bacterial lysis buffer and lysed by sonication (MS73 probe, cycle 5, 40 % power, 5 times 1 min with 30 s breaks in between). Solid bacterial components were removed by centrifugation at 17600 g at 4 °C for 20 min. The pellet was discarded and glycerol was added the supernatant to a final concentration of 20 % (v/v). The lysate was aliquoted and snap frozen in liquid nitrogen. Aliquots were stored at -80 °C.

7.2.2.9 Purification of GST-3xRafRBD

Prior to the purification of GST-3xRafRBD, glutathione magnetic agarose beads were washed twice with 1 mL bacterial lysis buffer to equilibrate them. Afterwards, 700 µL crude bacterial lysate was added to the beads and incubated for 30 min to 2 h at 4 °C on a rotating wheel. The beads were first washed four times with 1.5 mL GST-3xRafRBD wash buffer, then twice with 1.5 mL Active Ras pulldown buffer and resuspended in 300 µL Active Ras pulldown buffer.

7.2.2.10 In vitro nucleotide loading of GTPases in cell lysates

200 µg of whole cell lysates, as determined by colorimetric protein concentration determination (see 7.2.2.2), were diluted with Active Ras pulldown buffer to a total volume of 500 µL and EDTA was added to a final concentration of 10 mM to remove the bound nucleotides. 10 mM GTPγS or 100 mM GDP were added to artificially put all GTPases in an active or inactive conformation, respectively. The lysates were incubated at 30 °C for 15 min under constant agitation. Placing the samples on ice and adding 60 mM $MgCl_2$ terminated the reaction.

7.2.2.11 *Active Ras pulldown by immobilized GST-3xRafRBD*

Equal amounts (200 µg) of whole cell lysates were diluted to a total volume of 500 µL and mixed with 30 µL bead-bound GST-3xRafRBD (see 7.2.2.9). The solution was incubated at 4 °C for 30 min. Afterwards, the beads were washed 3 times 500 µL Active Ras pulldown buffer. After the last washing step, residual buffer was carefully removed using a 1 mL syringe and a G26 needle. To elude the bound protein from the beads, 50 µL 2x SDS sample buffer was added and the samples were heated to 95 °C for 10 min. The liquid phase was transferred to a clean 1.5 mL reaction tube and stored at -20 °C or directly subjected to Western blot analysis (see 7.2.2.5).

7.2.3 Mammalian cell culture

7.2.3.1 *Cultivation and passaging of mammalian cells*

Adherent mammalian cells were cultivated in 75 cm^2 cell culture flasks in Dulbecco's Modified Eagle's Medium DMEM high glucose medium supplemented with non-essential amino acids, L-Glutamine and 10 % fetal calf serum (complete growth medium, CGM) in a humidified 5 % CO_2 atmosphere at 37 °C. Cells were passaged when they occupied approximately 90 % of the flasks surface. Therefore, the medium was aspirated, the cells were washed twice with DPBS without Ca^{2+} and Mg^{2+} and 1 mL of a trypsin/EDTA solution was applied to detach the cells from the flasks surface. While trypsin cleaves cell surface proteins, EDTA complexes bivalent cations like Ca^{2+} mediating cell-cell contacts. Detachment was performed at 37 °C. The trypsin/EDTA solution was inactivated by addition of 5 mL growth medium after cells were detached and the cell solution was homogenized by pipetting up and down. After transferring the cells to a conical 25 mL vial, the cell concentration in the suspension was determined using an automated cell counter (Vi-Cell XR, Beckman Coulter). Cells were then seeded into fresh T75 flasks and dishes at appropriate numbers in complete growth medium.

7.2.3.2 *Long-term storage of cells under cryo-conditions*

Mammalian cells can be stored at temperatures below -80 °C for later used. To suppress the formation of ice crystals and thereby enhancing the viability of the cells, cryo-protectants like dimethyl sulfoxide (DMSO) have to be added to the medium before freezing the cells. Adherent cells were detached and the cell concentration was determined (see 7.2.3.1). Then, cells were pelleted by centrifugation at 200 g for 5 min at ambient temperature and the growth medium was aspirated. The cell pellet was resuspended in 90 % CGM/10 % DMSO to yield a suspension of 10^6 cells·mL^{-1}. This solution was divided into 1 mL aliquots in 2 mL CryoPure screw cap tubes. The tubes were moved into a CoolCell® LX cell freezing container which allows slow freezing of cells at a constant cooling rate of -1 °C·min^{-1} and placed in an -80 °C freezer overnight. For permanent storage, the frozen vials were moved to a -152 °C freezer.

7.2.3.3 Transient transfection of mammalian cells with plasmid DNA with Effectene®

Effectene was used to transiently transfect MDCK cells. To transfect MDCK cells in 1 well of a 6-well plate, 1.2 µg plasmid DNA were diluted in 360 µL buffer EC. 8 µL of Enhancer were added to the DNA solution. After 5 min incubation at ambient temperature, 15 µL Effectene was added, the solution was mixed using a vortex mixer and incubated for 10 min at ambient temperature. During this incubation step, the growth medium of the MDCK cells was aspirated, the cells washed once with PBS and 1 mL of CGM added to the well. After incubation, 1 mL of fresh CGM was added to the transfection complex, mixed and added to the cells dropwise. The plate was gently rocked to ensure proper mixing.

7.2.3.4 Transient transfection of mammalian cells with plasmid DNA with Lipofectamine™ 2000

To transfect NIH3T3 cells at 80 % confluency in one well of a 6-well plate using the transfection reagent Lipofectamine 2000, 1.25 µg plasmid DNA and 5 µL Lipofectamine 2000 each were diluted in 125 µL OptiMEM and incubated for 5 min at ambient temperature. Afterwards, the DNA solution was added to the solution containing the transfection reagent and incubated for 20 min at ambient temperature. The transfection complex was drop wise added to the cells and the plate carefully agitated to ensure proper mixing. On the next day, the growth medium containing the DNA and the transfection reagent was aspirated, the cells were washed with PBS once and further cultivated in fresh CGM.

7.2.3.5 Generation of stable cell lines using the piggyBac™ Transposon System

Besides viral transduction, the piggyBac™ Transposon System can be utilized to insert ectopic DNA into a host's genome via a "cut and paste" mechanism. Therefore, cells are co-transfected with a plasmid containing the CAG promoter, gene of interest and an antibiotic resistance gene flanked by internal terminal sequences (ITRs), which can be recognized by the transposase, as well as a plasmid encoding the piggyBac™ transposase. The transposase excises the ectopic DNA at the recognition sites from the plasmid and inserts this cut DNA into TTAA-chromosomal sites of the host.

To generate stable cell lines utilizing the piggyBac™ Transposon System, NIH3T3 or MDCK cells were seeded in 6-well plates at a density of 1 x 10^6 cells per well. On the next day, cells were co-transfected with a plasmid containing the transposon as well as with a plasmid encoding the transposase in a 1:1 ratio. One day later, the cells were passaged, seeded into a 25 cm^2 flask and grown in the presence of puromycin to select for cells, which incorporated the ectopic DNA. Expression of the introduced genes, all fused to a fluorescent protein, was verified by fluorescence microscopy.

7.2.3.6 *Incubation with 2/4-NvocTMP-Cl ligand for photo activation of Ras*

To label TagBFP-Halo-tKRas covalently with the photo-caged 2/4-NvocTMP-Cl ligand, a 50 µM solution (5x) of the ligand in the required growth medium was prepared. 20 % of the medium covering the cells was removed and replaced with the medium containing the photo-caged ligand. The cells were incubated with the ligand for 15 minutes at 37 °C in a humidified CO_2 incubator. To wash out excess amounts of 2/4-NvocTMP-Cl, the cells were washed three times with warm PBS and incubated with fresh medium for 30 minutes at the same conditions. Afterwards, the medium was replaced with medium without phenol red and the container was transferred to the microscope.

7.2.4 Microscopy

7.2.4.1 *Wide-field fluorescence microscopy*

Wide-field fluorescence images were obtained using an Olympus IX-81 fluorescence microscope with either a 63x/1.35 NA oil or 20x/0.75 NA air objective. The filter-sets used to detect the fluorescence of various fluorescent proteins are listed in Table 3.

Table 3: Excitation and emission bands used for wide-field microscopy

Fluorophor	Excitation band width [nm]	Emission band width [nm]
TagBFP	370 - 410	460 - 510
mCFP /mTFP	425 - 445	460 - 510
EYFP/mCitrine	490 - 500	515 - 560
FRET CFP/EYFP	425 - 445	515 - 560
mCherry	535 - 555	570 - 625
Nvoc cleavage	360 - 370	-

To remove the Nvoc protection group from NvocTMP-Cl, the field of view was illuminated with light of the wavelength of 360 nm - 370 nm for 5 seconds and with 100 % intensity of the halogen lamp.

7.2.4.2 *Total internal reflection fluorescence microscopy*

For TIRF imaging, an Olympus IX-81 fluorescence microscope equipped with a TIR-MITICO motorized TIRF illumination combiner and a 60x/1.45 NA oil TIRFM objective. Wide-field images were obtained using the filter-sets listed in Table 4. For the acquisition of TIRF microscopy images, a quadruple excitation filter for TBFP/TCFP/TYFP/TRFP was used with the respective emission filters.

Table 4: Filter-sets used for the acquisition of wide-field fluorescence microscopy images

Fluorophor	Excitation band width [nm]	Emission band width [nm]
TagBFP	370 - 410	460 - 510
EYFP/mCitrine	490 - 500	515 - 560

mCherry	535 - 555	570 - 625
Nvoc cleavage	360 - 370	-

To cleave the Nvoc group of NvocTMP-Cl, the sample was illuminated with a 360 nm - 370 nm band pass filter for 5 seconds using 100 % intensity of the fluorescence lamp.

7.2.4.3 *Confocal laser scanning microscopy*

Confocal live cell images were obtained using a Leica TCS SP5 or a Zeiss LSM 510 META confocal laser scanning microscope. The excitation light was focused on the cells using a 63x/1.4 NA oil objective. Fluorophores were imaged using excitation and emission settings given in Table 5 using sequential imaging.

Table 5: Excitation wavelength and emission band with used for confocal live cell imaging

Fluorophor	Excitation wavelength [nm]	Emission band width [nm]
TagBFP	405	420 - 480
mCFP mTFP	458	475 - 525
EYFP/mCitrine	514	530 - 600
mCherry	561	575 – 615
Nvoc cleavage	405	-

To cleave the Nvoc group of NvocTMP-Cl the FRAP wizard of the Leica TCS SP5 microscope was used: A polygonal ROI outlining a single cell was created manually. The fluorescence of the cytosolic light recruitable KRas was used to identify the outline of the cell. This ROI was illuminated twice with 405 nm laser light using 75 % of the lasers maximal power. To remove the Nvoc group of NvocTMP-Cl using the Zeiss LSM 510 META confocal microscope in single cells, a rectangular field stop and the DAPI filter set of the microscope's fluorescence lamp were used.

7.2.5 Image processing and data analysis

Images were processed using the ImageJ (Schneider, Rasband et al. 2012) distribution Fiji (Schindelin, Arganda-Carreras et al. 2012).

7.2.5.1 *Background correction of microscopy images*

After converting the gray scale images to 32-bit, the background was subtracted by measuring the mean fluorescence intensity in an area without cells and subtracting the resulting value from the whole image.

7.2.5.2 *Determination of single cells fluorescence values and normalization*

To determine the fluorescence intensity of single cells in TIRF image series, an ROI (region of interest) outlining the respective cell was manually drawn for each frame of the sequence. The median fluorescence intensity value of this ROI was obtained by the *measure* function of the

software ImageJ. The fluorescence intensity values of an image series were normalized by division of every single value by the mean fluorescence intensity of the first 5 to 10 frames of the series.

7.2.6 Statistics

Samples were compared with two-way ANOVA (analysis of variance) utilizing the Sidak test for multiple comparisons in GraphPad Prism 6. Pearson correlation coefficients were calculated using Origin 2018 by OriginLabs.

8 References

Adler, M. and U. Alon (2018). "Fold-change detection in biological systems." Current Opinion in Systems Biology **8**: 81-89.

Ahearn, I. M., K. Haigis, D. Bar-Sagi and M. R. Philips (2011). "Regulating the regulator: post-translational modification of RAS." Nat Rev Mol Cell Biol **13**(1): 39-51.

Ahmadian, M. R., T. Zor, D. Vogt, W. Kabsch, Z. Selinger, A. Wittinghofer and K. Scheffzek (1999). "Guanosine triphosphatase stimulation of oncogenic Ras mutants." Proc Natl Acad Sci U S A **96**(12): 7065-7070.

al-Alawi, N., G. Xu, R. White, R. Clark, F. McCormick and J. R. Feramisco (1993). "Differential regulation of cellular activities by GTPase-activating protein and NF1." Mol Cell Biol **13**(4): 2497-2503.

Alexander, S. P., A. Mathie and J. A. Peters (2011). "Guide to Receptors and Channels (GRAC), 5th edition." Br J Pharmacol **164 Suppl 1**: S1-324.

Annibaldi, A., D. Michod, L. Vanetta, S. Cruchet, P. Nicod, G. Dubuis, C. Bonvin and C. Widmann (2009). "Role of the sub-cellular localization of RasGAP fragment N2 for its ability to sensitize cancer cells to genotoxin-induced apoptosis." Exp Cell Res **315**(12): 2081-2091.

Aoki, K., Y. Kumagai, A. Sakurai, N. Komatsu, Y. Fujita, C. Shionyu and M. Matsuda (2013). "Stochastic ERK activation induced by noise and cell-to-cell propagation regulates cell density-dependent proliferation." Mol Cell **52**(4): 529-540.

Ballister, E. R., C. Aonbangkhen, A. M. Mayo, M. A. Lampson and D. M. Chenoweth (2014). "Localized light-induced protein dimerization in living cells using a photocaged dimerizer." Nat Commun **5**: 5475.

Bassler, B. L. (2002). "Small talk. Cell-to-cell communication in bacteria." Cell **109**(4): 421-424.

Boriack-Sjodin, P. A., S. M. Margarit, D. Bar-Sagi and J. Kuriyan (1998). "The structural basis of the activation of Ras by Sos." Nature **394**(6691): 337-343.

Bos, J. L., H. Rehmann and A. Wittinghofer (2007). "GEFs and GAPs: critical elements in the control of small G proteins." Cell **129**(5): 865-877.

Boykevisch, S., C. Zhao, H. Sondermann, P. Philippidou, S. Halegoua, J. Kuriyan and D. Bar-Sagi (2006). "Regulation of ras signaling dynamics by Sos-mediated positive feedback." Curr Biol **16**(21): 2173-2179.

Bremner, R. and A. Balmain (1990). "Genetic changes in skin tumor progression: correlation between presence of a mutant ras gene and loss of heterozygosity on mouse chromosome 7." Cell **61**(3): 407-417.

Brennan, C. W., R. G. Verhaak, A. McKenna, B. Campos, H. Noushmehr, S. R. Salama, S. Zheng, D. Chakravarty, J. Z. Sanborn, S. H. Berman, R. Beroukhim, B. Bernard, C. J. Wu, G. Genovese, I. Shmulevich, J. Barnholtz-Sloan, L. Zou, R. Vegesna, S. A. Shukla, G. Ciriello, W. K. Yung, W. Zhang, C. Sougnez, T. Mikkelsen, K. Aldape, D. D. Bigner, E. G. Van Meir, M. Prados, A. Sloan, K. L. Black, J. Eschbacher, G. Finocchiaro, W. Friedman, D. W. Andrews, A. Guha, M. Iacocca, B. P. O'Neill, G. Foltz, J. Myers, D. J. Weisenberger, R. Penny, R. Kucherlapati, C. M. Perou, D. N. Hayes, R. Gibbs, M. Marra, G. B. Mills, E. Lander, P. Spellman, R. Wilson, C. Sander, J. Weinstein, M. Meyerson, S. Gabriel, P. W. Laird, D. Haussler, G. Getz, L. Chin and T. R. Network (2013). "The somatic genomic landscape of glioblastoma." Cell **155**(2): 462-477.

Bunda, S., P. Heir, T. Srikumar, J. D. Cook, K. Burrell, Y. Kano, J. E. Lee, G. Zadeh, B. Raught and M. Ohh (2014). "Src promotes GTPase activity of Ras via tyrosine 32 phosphorylation." Proc Natl Acad Sci U S A **111**(36): E3785-3794.

Buss, J. E. and B. M. Sefton (1986). "Direct identification of palmitic acid as the lipid attached to p21ras." Mol Cell Biol **6**(1): 116-122.

Cancer Genome Atlas, N. (2015). "Genomic Classification of Cutaneous Melanoma." Cell **161**(7): 1681-1696.

Cancer Genome Atlas Research, N. (2012). "Comprehensive genomic characterization of squamous cell lung cancers." Nature **489**(7417): 519-525.

Cancer Genome Atlas Research, N. (2014). "Comprehensive molecular profiling of lung adenocarcinoma." Nature **511**(7511): 543-550.

Castellano, E. and J. Downward (2011). "RAS Interaction with PI3K: More Than Just Another Effector Pathway." Genes Cancer **2**(3): 261-274.

Cengel, K. A., K. R. Voong, S. Chandrasekaran, L. Maggiorella, T. B. Brunner, E. Stanbridge, G. D. Kao, W. G. McKenna and E. J. Bernhard (2007). "Oncogenic K-Ras signals through epidermal growth factor receptor and wild-type H-Ras to promote radiation survival in pancreatic and colorectal carcinoma cells." Neoplasia **9**(4): 341-348.

Chadwick, D. J. and J. Goode (2008). Mast Cells and Basophils: Development, Activation and Roles in Allergic/Autoimmune Disease, John Wiley & Sons.

Chandra, A., H. E. Grecco, V. Pisupati, D. Perera, L. Cassidy, F. Skoulidis, S. A. Ismail, C. Hedberg, M. Hanzal-Bayer, A. R. Venkitaraman, A. Wittinghofer and P. I. Bastiaens (2011). "The GDI-like solubilizing factor PDEdelta sustains the spatial organization and signalling of Ras family proteins." Nat Cell Biol **14**(2): 148-158.

Chen, X., M. Venkatachalapathy, D. Kamps, S. Weigel, R. Kumar, M. Orlich, R. Garrecht, M. Hirtz, C. M. Niemeyer, Y. W. Wu and L. Dehmelt (2017). ""Molecular Activity Painting": Switch-like, Light-Controlled Perturbations inside Living Cells." Angew Chem Int Ed Engl **56**(21): 5916-5920.

Cichowski, K., S. Santiago, M. Jardim, B. W. Johnson and T. Jacks (2003). "Dynamic regulation of the Ras pathway via proteolysis of the NF1 tumor suppressor." Genes Dev **17**(4): 449-454.

Clackson, T., W. Yang, L. W. Rozamus, M. Hatada, J. F. Amara, C. T. Rollins, L. F. Stevenson, S. R. Magari, S. A. Wood, N. L. Courage, X. Lu, F. Cerasoli, Jr., M. Gilman and D. A. Holt (1998). "Redesigning an FKBP-ligand interface to generate chemical dimerizers with novel specificity." Proc Natl Acad Sci U S A **95**(18): 10437-10442.

Cohen-Saidon, C., A. A. Cohen, A. Sigal, Y. Liron and U. Alon (2009). "Dynamics and variability of ERK2 response to EGF in individual living cells." Mol Cell **36**(5): 885-893.

Corbalan-Garcia, S., S. S. Yang, K. R. Degenhardt and D. Bar-Sagi (1996). "Identification of the mitogen-activated protein kinase phosphorylation sites on human Sos1 that regulate interaction with Grb2." Mol Cell Biol **16**(10): 5674-5682.

Daub, H., F. U. Weiss, C. Wallasch and A. Ullrich (1996). "Role of transactivation of the EGF receptor in signalling by G-protein-coupled receptors." Nature **379**(6565): 557-560.

Dharmaiah, S., L. Bindu, T. H. Tran, W. K. Gillette, P. H. Frank, R. Ghirlando, D. V. Nissley, D. Esposito, F. McCormick, A. G. Stephen and D. K. Simanshu (2016). "Structural basis of recognition of farnesylated and methylated KRAS4b by PDEdelta." Proc Natl Acad Sci U S A **113**(44): E6766-E6775.

Dougherty, M. K., J. Muller, D. A. Ritt, M. Zhou, X. Z. Zhou, T. D. Copeland, T. P. Conrads, T. D. Veenstra, K. P. Lu and D. K. Morrison (2005). "Regulation of Raf-1 by direct feedback phosphorylation." Mol Cell **17**(2): 215-224.

Downward, J. (2003). "Targeting RAS signalling pathways in cancer therapy." Nat Rev Cancer **3**(1): 11-22.

Fey, D., D. Matallanas, J. Rauch, O. S. Rukhlenko and B. N. Kholodenko (2016). "The complexities and versatility of the RAS-to-ERK signalling system in normal and cancer cells." Semin Cell Dev Biol **58**: 96-107.

Forbes, S. A., D. Beare, H. Boutselakis, S. Bamford, N. Bindal, J. Tate, C. G. Cole, S. Ward, E. Dawson, L. Ponting, R. Stefancsik, B. Harsha, C. Y. Kok, M. Jia, H. Jubb, Z. Sondka, S. Thompson, T. De and P. J. Campbell (2017). "COSMIC: somatic cancer genetics at high-resolution." Nucleic Acids Res **45**(D1): D777-D783.

Freedman, T. S., H. Sondermann, G. D. Friedland, T. Kortemme, D. Bar-Sagi, S. Marqusee and J. Kuriyan (2006). "A Ras-induced conformational switch in the Ras activator Son of sevenless." Proc Natl Acad Sci U S A **103**(45): 16692-16697.

Gideon, P., J. John, M. Frech, A. Lautwein, R. Clark, J. E. Scheffler and A. Wittinghofer (1992). "Mutational and kinetic analyses of the GTPase-activating protein (GAP)-p21 interaction: the C-terminal domain of GAP is not sufficient for full activity." Mol Cell Biol **12**(5): 2050-2056.

Giglione, C., S. Gonfloni and A. Parmeggiani (2001). "Differential actions of p60c-Src and Lck kinases on the Ras regulators p120-GAP and GDP/GTP exchange factor CDC25Mm." Eur J Biochem **268**(11): 3275-3283.

Guerrero, I., A. Villasante, V. Corces and A. Pellicer (1985). "Loss of the normal N-ras allele in a mouse thymic lymphoma induced by a chemical carcinogen." Proc Natl Acad Sci U S A **82**(23): 7810-7814.

Gureasko, J., W. J. Galush, S. Boykevisch, H. Sondermann, D. Bar-Sagi, J. T. Groves and J. Kuriyan (2008). "Membrane-dependent signal integration by the Ras activator Son of sevenless." Nat Struct Mol Biol **15**(5): 452-461.

Gureasko, J., O. Kuchment, D. L. Makino, H. Sondermann, D. Bar-Sagi and J. Kuriyan (2010). "Role of the histone domain in the autoinhibition and activation of the Ras activator Son of Sevenless." Proc Natl Acad Sci U S A **107**(8): 3430-3435.

Hall, B. E., D. Bar-Sagi and N. Nassar (2002). "The structural basis for the transition from Ras-GTP to Ras-GDP." Proc Natl Acad Sci U S A **99**(19): 12138-12142.

Hanafusa, H., S. Torii, T. Yasunaga and E. Nishida (2002). "Sprouty1 and Sprouty2 provide a control mechanism for the Ras/MAPK signalling pathway." Nat Cell Biol **4**(11): 850-858.

Hancock, J. F., A. I. Magee, J. E. Childs and C. J. Marshall (1989). "All ras proteins are polyisoprenylated but only some are palmitoylated." Cell **57**(7): 1167-1177.

Hancock, J. F., H. Paterson and C. J. Marshall (1990). "A polybasic domain or palmitoylation is required in addition to the CAAX motif to localize p21ras to the plasma membrane." Cell **63**(1): 133-139.

Harvey, J. J. (1964). "An Unidentified Virus Which Causes the Rapid Production of Tumours in Mice." Nature **204**: 1104-1105.

Ho, S. N., S. R. Biggar, D. M. Spencer, S. L. Schreiber and G. R. Crabtree (1996). "Dimeric ligands define a role for transcriptional activation domains in reinitiation." Nature **382**(6594): 822-826.

Hobbs, G. A., C. J. Der and K. L. Rossman (2016). "RAS isoforms and mutations in cancer at a glance." J Cell Sci **129**(7): 1287-1292.

Hollstein, P. E. and K. Cichowski (2013). "Identifying the Ubiquitin Ligase complex that regulates the NF1 tumor suppressor and Ras." Cancer Discov **3**(8): 880-893.

Hu, J., E. C. Stites, H. Yu, E. A. Germino, H. S. Meharena, P. J. S. Stork, A. P. Kornev, S. S. Taylor and A. S. Shaw (2013). "Allosteric activation of functionally asymmetric RAF kinase dimers." Cell **154**(5): 1036-1046.

Ikonomou, G., V. Kostourou, S. Shirasawa, T. Sasazuki, M. Samiotaki and G. Panayotou (2012). "Interplay between oncogenic K-Ras and wild-type H-Ras in Caco2 cell transformation." J Proteomics **75**(17): 5356-5369.

Ismail, S. A., Y. X. Chen, A. Rusinova, A. Chandra, M. Bierbaum, L. Gremer, G. Triola, H. Waldmann, P. I. Bastiaens and A. Wittinghofer (2011). "Arl2-GTP and Arl3-GTP regulate a GDI-like transport system for farnesylated cargo." Nat Chem Biol **7**(12): 942-949.

Jeng, H. H., L. J. Taylor and D. Bar-Sagi (2012). "Sos-mediated cross-activation of wild-type Ras by oncogenic Ras is essential for tumorigenesis." Nat Commun **3**: 1168.

John, J., I. Schlichting, E. Schiltz, P. Rosch and A. Wittinghofer (1989). "C-terminal truncation of p21H preserves crucial kinetic and structural properties." J Biol Chem **264**(22): 13086-13092.

John, J., R. Sohmen, J. Feuerstein, R. Linke, A. Wittinghofer and R. S. Goody (1990). "Kinetics of interaction of nucleotides with nucleotide-free H-ras p21." Biochemistry **29**(25): 6058-6065.

Jun, J. E., I. Rubio and J. P. Roose (2013). "Regulation of ras exchange factors and cellular localization of ras activation by lipid messengers in T cells." Front Immunol **4**: 239.

Kamioka, Y., S. Yasuda, Y. Fujita, K. Aoki and M. Matsuda (2010). "Multiple decisive phosphorylation sites for the negative feedback regulation of SOS1 via ERK." J Biol Chem **285**(43): 33540-33548.

Kenney, C. and E. Stites (2017). "Analysis of RAS as a tumor suppressor." bioRxiv.

Kidger, A. M. and S. M. Keyse (2016). "The regulation of oncogenic Ras/ERK signalling by dual-specificity mitogen activated protein kinase phosphatases (MKPs)." Semin Cell Dev Biol **50**: 125-132.

Kim, H. J. and D. Bar-Sagi (2004). "Modulation of signalling by Sprouty: a developing story." Nat Rev Mol Cell Biol **5**(6): 441-450.

Kirsten, W. H. and L. A. Mayer (1967). "Morphologic responses to a murine erythroblastosis virus." J Natl Cancer Inst **39**(2): 311-335.

Kong, G., Y. I. Chang, A. Damnernsawad, X. You, J. Du, E. A. Ranheim, W. Lee, M. J. Ryu, Y. Zhou, Y. Xing, Q. Chang, C. E. Burd and J. Zhang (2016). "Loss of wild-type Kras promotes activation of all Ras isoforms in oncogenic Kras-induced leukemogenesis." Leukemia **30**(7): 1542-1551.

Kotting, C., A. Kallenbach, Y. Suveyzdis, A. Wittinghofer and K. Gerwert (2008). "The GAP arginine finger movement into the catalytic site of Ras increases the activation entropy." Proc Natl Acad Sci U S A **105**(17): 6260-6265.

Ksionda, O., A. Limnander and J. P. Roose (2013). "RasGRP Ras guanine nucleotide exchange factors in cancer." Front Biol (Beijing) **8**(5): 508-532.

Lake, D., S. A. Correa and J. Muller (2016). "Negative feedback regulation of the ERK1/2 MAPK pathway." Cell Mol Life Sci **73**(23): 4397-4413.

Leventis, R. and J. R. Silvius (1998). "Lipid-binding characteristics of the polybasic carboxy-terminal sequence of K-ras4B." Biochemistry **37**(20): 7640-7648.

Li, J., Z. Zhang, Z. Dai, C. Plass, C. Morrison, Y. Wang, J. S. Wiest, M. W. Anderson and M. You (2003). "LOH of chromosome 12p correlates with Kras2 mutation in non-small cell lung cancer." Oncogene **22**(8): 1243-1246.

Lim, K. H., B. B. Ancrile, D. F. Kashatus and C. M. Counter (2008). "Tumour maintenance is mediated by eNOS." Nature **452**(7187): 646-649.

Liu, P., A. Calderon, G. Konstantinidis, J. Hou, S. Voss, X. Chen, F. Li, S. Banerjee, J. E. Hoffmann, C. Theiss, L. Dehmelt and Y. W. Wu (2014). "A bioorthogonal small-molecule-switch system for controlling protein function in live cells." Angew Chem Int Ed Engl **53**(38): 10049-10055.

Lowenstein, E. J., R. J. Daly, A. G. Batzer, W. Li, B. Margolis, R. Lammers, A. Ullrich, E. Y. Skolnik, D. Bar-Sagi and J. Schlessinger (1992). "The SH2 and SH3 domain-containing protein GRB2 links receptor tyrosine kinases to ras signaling." Cell **70**(3): 431-442.

Maertens, O. and K. Cichowski (2014). "An expanding role for RAS GTPase activating proteins (RAS GAPs) in cancer." Adv Biol Regul **55**: 1-14.

Magee, A. I., L. Gutierrez, I. A. McKay, C. J. Marshall and A. Hall (1987). "Dynamic fatty acylation of p21N-ras." EMBO J **6**(11): 3353-3357.

Mangoura, D., Y. Sun, C. Li, D. Singh, D. H. Gutmann, A. Flores, M. Ahmed and G. Vallianatos (2006). "Phosphorylation of neurofibromin by PKC is a possible molecular switch in EGF receptor signaling in neural cells." Oncogene **25**(5): 735-745.

Margarit, S. M., H. Sondermann, B. E. Hall, B. Nagar, A. Hoelz, M. Pirruccello, D. Bar-Sagi and J. Kuriyan (2003). "Structural evidence for feedback activation by Ras.GTP of the Ras-specific nucleotide exchange factor SOS." Cell **112**(5): 685-695.

Martin-Gago, P., E. K. Fansa, C. H. Klein, S. Murarka, P. Janning, M. Schurmann, M. Metz, S. Ismail, C. Schultz-Fademrecht, M. Baumann, P. I. Bastiaens, A. Wittinghofer and H. Waldmann (2017). "A PDE6delta-KRas Inhibitor Chemotype with up to Seven H-Bonds and Picomolar Affinity that Prevents Efficient Inhibitor Release by Arl2." Angew Chem Int Ed Engl **56**(9): 2423-2428.

McGillicuddy, L. T., J. A. Fromm, P. E. Hollstein, S. Kubek, R. Beroukhim, T. De Raedt, B. W. Johnson, S. M. Williams, P. Nghiemphu, L. M. Liau, T. F. Cloughesy, P. S. Mischel, A. Parret, J. Seiler, G. Moldenhauer, K. Scheffzek, A. O. Stemmer-Rachamimov, C. L. Sawyers, C. Brennan, L. Messiaen, I. K. Mellinghoff and K. Cichowski (2009). "Proteasomal and genetic inactivation of the NF1 tumor suppressor in gliomagenesis." Cancer Cell **16**(1): 44-54.

Min, J., A. Zaslavsky, G. Fedele, S. K. McLaughlin, E. E. Reczek, T. De Raedt, I. Guney, D. E. Strochlic, L. E. Macconaill, R. Beroukhim, R. T. Bronson, S. Ryeom, W. C. Hahn, M. Loda and K. Cichowski (2010). "An oncogene-tumor suppressor cascade drives metastatic prostate cancer by coordinately activating Ras and nuclear factor-kappaB." Nat Med **16**(3): 286-294.

Moodie, S. A., B. M. Willumsen, M. J. Weber and A. Wolfman (1993). "Complexes of Ras.GTP with Raf-1 and mitogen-activated protein kinase kinase." Science **260**(5114): 1658-1661.

Muhlhauser, W. W., A. Fischer, W. Weber and G. Radziwill (2017). "Optogenetics - Bringing light into the darkness of mammalian signal transduction." Biochim Biophys Acta **1864**(2): 280-292.

Nassar, N., G. Horn, C. Herrmann, A. Scherer, F. McCormick and A. Wittinghofer (1995). "The 2.2 A crystal structure of the Ras-binding domain of the serine/threonine kinase c-Raf1 in complex with Rap1A and a GTP analogue." Nature **375**(6532): 554-560.

Newlaczyl, A. U., J. M. Coulson and I. A. Prior (2017). "Quantification of spatiotemporal patterns of Ras isoform expression during development." Sci Rep **7**: 41297.

Nissan, M. H., C. A. Pratilas, A. M. Jones, R. Ramirez, H. Won, C. Liu, S. Tiwari, L. Kong, A. J. Hanrahan, Z. Yao, T. Merghoub, A. Ribas, P. B. Chapman, R. Yaeger, B. S. Taylor, N. Schultz, M. F. Berger, N. Rosen and D. B. Solit (2014). "Loss of NF1 in cutaneous melanoma is associated with RAS activation and MEK dependence." Cancer Res **74**(8): 2340-2350.

Osterop, A. P., R. H. Medema, G. C. vd Zon, J. L. Bos, W. Moller and J. A. Maassen (1993). "Epidermal-growth-factor receptors generate Ras.GTP more efficiently than insulin receptors." Eur J Biochem **212**(2): 477-482.

Papke, B., S. Murarka, H. A. Vogel, P. Martin-Gago, M. Kovacevic, D. C. Truxius, E. K. Fansa, S. Ismail, G. Zimmermann, K. Heinelt, C. Schultz-Fademrecht, A. Al Saabi, M. Baumann, P. Nussbaumer, A. Wittinghofer, H. Waldmann and P. I. Bastiaens (2016). "Identification of pyrazolopyridazinones as PDEdelta inhibitors." Nat Commun **7**: 11360.

Plowman, S. J., R. L. Berry, S. A. Bader, F. Luo, M. J. Arends, D. J. Harrison, M. L. Hooper and C. E. Patek (2006). "K-ras 4A and 4B are co-expressed widely in human tissues, and their ratio is altered in sporadic colorectal cancer." J Exp Clin Cancer Res **25**(2): 259-267.

Ponting, C. P. and D. R. Benjamin (1996). "A novel family of Ras-binding domains." Trends Biochem Sci **21**(11): 422-425.

Porfiri, E. and F. McCormick (1996). "Regulation of epidermal growth factor receptor signaling by phosphorylation of the ras exchange factor hSOS1." J Biol Chem **271**(10): 5871-5877.

Putyrski, M. and C. Schultz (2012). "Protein translocation as a tool: The current rapamycin story." FEBS Lett **586**(15): 2097-2105.

Qiu, W., F. Sahin, C. A. Iacobuzio-Donahue, D. Garcia-Carracedo, W. M. Wang, C. Y. Kuo, D. Chen, D. E. Arking, A. M. Lowy, R. H. Hruban, H. E. Remotti and G. H. Su (2011). "Disruption of p16 and activation of Kras in pancreas increase ductal adenocarcinoma formation and metastasis in vivo." Oncotarget **2**(11): 862-873.

Rivera, V. M., T. Clackson, S. Natesan, R. Pollock, J. F. Amara, T. Keenan, S. R. Magari, T. Phillips, N. L. Courage, F. Cerasoli, Jr., D. A. Holt and M. Gilman (1996). "A humanized system for pharmacologic control of gene expression." Nat Med **2**(9): 1028-1032.

Rocks, O., A. Peyker, M. Kahms, P. J. Verveer, C. Koerner, M. Lumbierres, J. Kuhlmann, H. Waldmann, A. Wittinghofer and P. I. Bastiaens (2005). "An acylation cycle regulates localization and activity of palmitoylated Ras isoforms." Science **307**(5716): 1746-1752.

Roose, J. P., M. Mollenauer, M. Ho, T. Kurosaki and A. Weiss (2007). "Unusual interplay of two types of Ras activators, RasGRP and SOS, establishes sensitive and robust Ras activation in lymphocytes." Mol Cell Biol **27**(7): 2732-2745.

Rost, B. R., F. Schneider-Warme, D. Schmitz and P. Hegemann (2017). "Optogenetic Tools for Subcellular Applications in Neuroscience." Neuron **96**(3): 572-603.

Rubio, I. and R. Wetzker (2000). "A permissive function of phosphoinositide 3-kinase in Ras activation mediated by inhibition of GTPase-activating proteins." Curr Biol **10**(19): 1225-1228.

Sasaki, A. T., C. Janetopoulos, S. Lee, P. G. Charest, K. Takeda, L. W. Sundheimer, R. Meili, P. N. Devreotes and R. A. Firtel (2007). "G protein-independent Ras/PI3K/F-actin circuit regulates basic cell motility." J Cell Biol **178**(2): 185-191.

Satoh, T., M. Endo, M. Nakafuku, T. Akiyama, T. Yamamoto and Y. Kaziro (1990). "Accumulation of p21ras.GTP in response to stimulation with epidermal growth factor and oncogene products with tyrosine kinase activity." Proc Natl Acad Sci U S A **87**(20): 7926-7929.

Scheffzek, K., M. R. Ahmadian, W. Kabsch, L. Wiesmuller, A. Lautwein, F. Schmitz and A. Wittinghofer (1997). "The Ras-RasGAP complex: structural basis for GTPase activation and its loss in oncogenic Ras mutants." Science **277**(5324): 333-338.

Schindelin, J., I. Arganda-Carreras, E. Frise, V. Kaynig, M. Longair, T. Pietzsch, S. Preibisch, C. Rueden, S. Saalfeld, B. Schmid, J. Y. Tinevez, D. J. White, V. Hartenstein, K. Eliceiri, P. Tomancak and A. Cardona (2012). "Fiji: an open-source platform for biological-image analysis." Nat Methods **9**(7): 676-682.

Schlessinger, J. (2000). "Cell signaling by receptor tyrosine kinases." Cell **103**(2): 211-225.

Schmick, M., A. Kraemer and P. I. Bastiaens (2015). "Ras moves to stay in place." Trends Cell Biol **25**(4): 190-197.

Schmick, M., N. Vartak, B. Papke, M. Kovacevic, D. C. Truxius, L. Rossmannek and P. I. H. Bastiaens (2014). "KRas localizes to the plasma membrane by spatial cycles of solubilization, trapping and vesicular transport." Cell **157**(2): 459-471.

Schneider, C. A., W. S. Rasband and K. W. Eliceiri (2012). "NIH Image to ImageJ: 25 years of image analysis." Nat Methods **9**(7): 671-675.

Seibel, N. M., J. Eljouni, M. M. Nalaskowski and W. Hampe (2007). "Nuclear localization of enhanced green fluorescent protein homomultimers." Anal Biochem **368**(1): 95-99.

Silvius, J. R., P. Bhagatji, R. Leventis and D. Terrone (2006). "K-ras4B and prenylated proteins lacking "second signals" associate dynamically with cellular membranes." Mol Biol Cell **17**(1): 192-202.

Sondermann, H., S. M. Soisson, S. Boykevisch, S. S. Yang, D. Bar-Sagi and J. Kuriyan (2004). "Structural analysis of autoinhibition in the Ras activator Son of sevenless." Cell **119**(3): 393-405.

Spandidos, A. and N. M. Wilkie (1988). "The normal human H-ras1 gene can act as an onco-suppressor." Br J Cancer Suppl **9**: 67-71.

Spandidos, D. A., M. Frame and N. M. Wilkie (1990). "Expression of the normal H-ras1 gene can suppress the transformed and tumorigenic phenotypes induced by mutant ras genes." Anticancer Res **10**(6): 1543-1554.

Stone, J. C. (2011). "Regulation and Function of the RasGRP Family of Ras Activators in Blood Cells." Genes Cancer **2**(3): 320-334.

Stowe, I. B., E. L. Mercado, T. R. Stowe, E. L. Bell, J. A. Oses-Prieto, H. Hernandez, A. L. Burlingame and F. McCormick (2012). "A shared molecular mechanism underlies the human rasopathies Legius syndrome and Neurofibromatosis-1." Genes Dev **26**(13): 1421-1426.

Swanson, K. D., J. M. Winter, M. Reis, M. Bentires-Alj, H. Greulich, R. Grewal, R. H. Hruban, C. J. Yeo, Y. Yassin, O. Iartchouk, K. Montgomery, S. P. Whitman, M. A. Caligiuri, M. L. Loh, D. G. Gilliland, A. T. Look, R. Kucherlapati, S. E. Kern, M. Meyerson and B. G. Neel (2008). "SOS1 mutations are rare in human malignancies: implications for Noonan Syndrome patients." Genes Chromosomes Cancer **47**(3): 253-259.

Swarthout, J. T., S. Lobo, L. Farh, M. R. Croke, W. K. Greentree, R. J. Deschenes and M. E. Linder (2005). "DHHC9 and GCP16 constitute a human protein fatty acyltransferase with specificity for H- and N-Ras." J Biol Chem **280**(35): 31141-31148.

Tape, C. J., S. Ling, M. Dimitriadi, K. M. McMahon, J. D. Worboys, H. S. Leong, I. C. Norrie, C. J. Miller, G. Poulogiannis, D. A. Lauffenburger and C. Jorgensen (2016). "Oncogenic KRAS Regulates Tumor Cell Signaling via Stromal Reciprocation." Cell **165**(4): 910-920.

To, M. D., R. D. Rosario, P. M. Westcott, K. L. Banta and A. Balmain (2013). "Interactions between wild-type and mutant Ras genes in lung and skin carcinogenesis." Oncogene **32**(34): 4028-4033.

Toettcher, J. E., O. D. Weiner and W. A. Lim (2013). "Using optogenetics to interrogate the dynamic control of signal transmission by the Ras/Erk module." Cell **155**(6): 1422-1434.

Trahey, M. and F. McCormick (1987). "A cytoplasmic protein stimulates normal N-ras p21 GTPase, but does not affect oncogenic mutants." Science **238**(4826): 542-545.

Tsai, F. D., M. S. Lopes, M. Zhou, H. Court, O. Ponce, J. J. Fiordalisi, J. J. Gierut, A. D. Cox, K. M. Haigis and M. R. Philips (2015). "K-Ras4A splice variant is widely expressed in cancer and uses a hybrid membrane-targeting motif." Proc Natl Acad Sci U S A **112**(3): 779-784.

Uhlen, M., L. Fagerberg, B. M. Hallstrom, C. Lindskog, P. Oksvold, A. Mardinoglu, A. Sivertsson, C. Kampf, E. Sjostedt, A. Asplund, I. Olsson, K. Edlund, E. Lundberg, S. Navani, C. A. Szigyarto, J. Odeberg, D. Djureinovic, J. O. Takanen, S. Hober, T. Alm, P. H. Edqvist, H. Berling, H. Tegel, J. Mulder, J. Rockberg, P. Nilsson, J. M. Schwenk, M. Hamsten, K. von Feilitzen, M. Forsberg, L. Persson, F. Johansson, M. Zwahlen, G. von Heijne, J. Nielsen and F. Ponten (2015). "Proteomics. Tissue-based map of the human proteome." Science **347**(6220): 1260419.

Uhlen, M., C. Zhang, S. Lee, E. Sjostedt, L. Fagerberg, G. Bidkhori, R. Benfeitas, M. Arif, Z. Liu, F. Edfors, K. Sanli, K. von Feilitzen, P. Oksvold, E. Lundberg, S. Hober, P. Nilsson, J. Mattsson, J. M. Schwenk, H. Brunnstrom, B. Glimelius, T. Sjoblom, P. H. Edqvist, D. Djureinovic, P. Micke, C. Lindskog, A. Mardinoglu and F. Ponten (2017). "A pathology atlas of the human cancer transcriptome." Science **357**(6352).

van der Geer, P., S. Wiley, G. D. Gish and T. Pawson (1996). "The Shc adaptor protein is highly phosphorylated at conserved, twin tyrosine residues (Y239/240) that mediate protein-protein interactions." Curr Biol **6**(11): 1435-1444.

Vartak, N., B. Papke, H. E. Grecco, L. Rossmannek, H. Waldmann, C. Hedberg and P. I. Bastiaens (2014). "The autodepalmitoylating activity of APT maintains the spatial organization of palmitoylated membrane proteins." Biophys J **106**(1): 93-105.

Verhaak, R. G., K. A. Hoadley, E. Purdom, V. Wang, Y. Qi, M. D. Wilkerson, C. R. Miller, L. Ding, T. Golub, J. P. Mesirov, G. Alexe, M. Lawrence, M. O'Kelly, P. Tamayo, B. A. Weir, S. Gabriel, W. Winckler, S. Gupta, L. Jakkula, H. S. Feiler, J. G. Hodgson, C. D. James, J. N. Sarkaria, C. Brennan, A. Kahn, P. T. Spellman, R. K. Wilson, T. P. Speed, J. W. Gray, M. Meyerson, G. Getz, C. M. Perou, D. N. Hayes and N. Cancer Genome Atlas Research (2010). "Integrated genomic analysis identifies clinically relevant subtypes of glioblastoma characterized by abnormalities in PDGFRA, IDH1, EGFR, and NF1." Cancer Cell **17**(1): 98-110.

Vetter, I. R. and A. Wittinghofer (2001). "The guanine nucleotide-binding switch in three dimensions." Science **294**(5545): 1299-1304.

Vojtek, A. B., S. M. Hollenberg and J. A. Cooper (1993). "Mammalian Ras interacts directly with the serine/threonine kinase Raf." Cell **74**(1): 205-214.

von Kriegsheim, A., D. Baiocchi, M. Birtwistle, D. Sumpton, W. Bienvenut, N. Morrice, K. Yamada, A. Lamond, G. Kalna, R. Orton, D. Gilbert and W. Kolch (2009). "Cell fate decisions are specified by the dynamic ERK interactome." Nat Cell Biol **11**(12): 1458-1464.

Voss, S., L. Klewer and Y. W. Wu (2015). "Chemically induced dimerization: reversible and spatiotemporal control of protein function in cells." Curr Opin Chem Biol **28**: 194-201.

Wan, J., H. Li, Y. Li, M. L. Zhu and P. Zhao (2006). "Loss of heterozygosity of Kras2 gene on 12p12-13 in Chinese colon carcinoma patients." World J Gastroenterol **12**(7): 1033-1037.

Wang, M. and P. J. Casey (2016). "Protein prenylation: unique fats make their mark on biology." Nat Rev Mol Cell Biol **17**(2): 110-122.

Warne, P. H., P. R. Viciana and J. Downward (1993). "Direct interaction of Ras and the amino-terminal region of Raf-1 in vitro." Nature **364**(6435): 352-355.

Wartmann, M., P. Hofer, P. Turowski, A. R. Saltiel and N. E. Hynes (1997). "Negative modulation of membrane localization of the Raf-1 protein kinase by hyperphosphorylation." J Biol Chem **272**(7): 3915-3923.

Wennerberg, K., K. L. Rossman and C. J. Der (2005). "The Ras superfamily at a glance." J Cell Sci **118**(Pt 5): 843-846.

Willumsen, B. M., A. Christensen, N. L. Hubbert, A. G. Papageorge and D. R. Lowy (1984). "The p21 ras C-terminus is required for transformation and membrane association." Nature **310**(5978): 583-586.

Wright, L. P. and M. R. Philips (2006). "Thematic review series: lipid posttranslational modifications. CAAX modification and membrane targeting of Ras." J Lipid Res **47**(5): 883-891.

Yarden, Y. and G. Tarcic (2013). Vesicle trafficking in cancer. New York, Springer.

Yoon, S. and R. Seger (2006). "The extracellular signal-regulated kinase: multiple substrates regulate diverse cellular functions." Growth Factors **24**(1): 21-44.

Young, A., D. Lou and F. McCormick (2013). "Oncogenic and wild-type Ras play divergent roles in the regulation of mitogen-activated protein kinase signaling." Cancer Discov **3**(1): 112-123.

Zhang, H., X. H. Liu, K. Zhang, C. K. Chen, J. M. Frederick, G. D. Prestwich and W. Baehr (2004). "Photoreceptor cGMP phosphodiesterase delta subunit (PDEdelta) functions as a prenyl-binding protein." J Biol Chem **279**(1): 407-413.

Zhang, X., J. Gureasko, K. Shen, P. A. Cole and J. Kuriyan (2006). "An allosteric mechanism for activation of the kinase domain of epidermal growth factor receptor." Cell **125**(6): 1137-1149.

Zhang, X. F., J. Settleman, J. M. Kyriakis, E. Takeuchi-Suzuki, S. J. Elledge, M. S. Marshall, J. T. Bruder, U. R. Rapp and J. Avruch (1993). "Normal and oncogenic p21ras proteins bind to the amino-terminal regulatory domain of c-Raf-1." Nature **364**(6435): 308-313.

Zhang, Z., S. Kobayashi, A. C. Borczuk, R. S. Leidner, T. Laframboise, A. D. Levine and B. Halmos (2010). "Dual specificity phosphatase 6 (DUSP6) is an ETS-regulated negative feedback mediator of oncogenic ERK signaling in lung cancer cells." Carcinogenesis **31**(4): 577-586.

Zhang, Z., Y. Wang, H. G. Vikis, L. Johnson, G. Liu, J. Li, M. W. Anderson, R. C. Sills, H. L. Hong, T. R. Devereux, T. Jacks, K. L. Guan and M. You (2001). "Wildtype Kras2 can inhibit lung carcinogenesis in mice." Nat Genet **29**(1): 25-33.

Zhou, B., C. J. Der and A. D. Cox (2016). "The role of wild type RAS isoforms in cancer." Semin Cell Dev Biol **58**: 60-69.

Zimmermann, G., B. Papke, S. Ismail, N. Vartak, A. Chandra, M. Hoffmann, S. A. Hahn, G. Triola, A. Wittinghofer, P. I. Bastiaens and H. Waldmann (2013). "Small molecule inhibition of the KRAS-PDEdelta interaction impairs oncogenic KRAS signalling." Nature **497**(7451): 638-642.

9 Abbreviations

A

ANOVA · analysis of variance
APS · ammonium persulfate
APT · acyl protein thioesterase
Arl · Arf-like GTPase

B

BCA · bicinchoninic acid
BFP · blue fluorescent protein
BSA · bovine serum albumine

C

CIAP · calf intestinal alkaline phosphatase
CID · chemically induced dimerization
CRafRBD · Ras binding domain of CRaf

D

DH · Dbl homology
DMEM · Dulbecco's Modified Eagle's Medium
DMSO · dimethyl sulfoxide
DNA · deoxyribonucleic acid
DTT · dithiothreitol
DUSP · dual-specificity MAP kinase phosphatase

E

E. Coli · *Escherichia coli*
eDHFR · E.Coli dihydrofolate reductase
EDTA · ethylenediaminetetraacetic acid
EGF · epidermal growth factor
EGFR · epidermal growth factor receptor
ERK · extracellular signal–regulated kinase
EYFP · enhanced yellow fluorescent protein

F

FCS · fetal calf serum
FKBP · FK506 binding protein
FRAP · fluorescence recovery after photobleaching
FRET · Förster resonance energy transfer

G

GAP · GTPase activating protein
GDP · guanosine-5'-diphosphate
GEF · guanine nucleotide exchange factor
GPCR · G-protein coupled receptor
GST · glutathione S-transferase
GTP · guanosine-5'-triphosphate

H

HF · histone-like fold
HVR · hypervariable region, hypervariable region

I

ICMT · protein-S-isoprenylcysteine O-methyltransferase
ICW · In-Cell Western
IPTG · Isopropyl β-D-1-thiogalactopyranoside

K

kb · kilobasepair
kDa · kilo Dalton

L

LB · lysogeny broth

M

M · mol·L-1
MAP · mitogen activated protein
MAPK · mitogen activated protein kinase
mCherry · monomeric Cherry
MKP · MAP kinase phosphatase
mTFP · monomeric teal fluorescent protein
mTOR · mammalian target of rapamycin

N

NA · numerical aperture
NES · nuclear export sequence
NOS · nitric oxide synthase
Nvoc · nitroveratryloxycarbonyl

O

OAc · acetate ion

P

PAGE · polyacrylamide gel electrophoresis
PBS · phosphate-buffered saline
PCR · polymerase chain reaction
PDEδ · phosphodiesterase 6 δ-subunit
PH · pleckstrin homology
P_i · phosphate ion
PI3K · phosphatidylinositide 3-kinase
PIP_2 · phosphatidylinositol 4,5-bisphosphate
PKC · protein kinase C
PLCε · phospholipase Cε
PM · plasma membrane
PVDF · polyvinylidene fluoride

R

RALGDS · RAL guanine nucleotide dissociation stimulator
Ras · rat sarcoma
RasGRF · Ras guanine nucleotide releasing factor
RasGRP · Ras guanine nucleotide releasing protein
RCE1 · Ras converting enzyme 1
REM · Ras exchange motif
RIPA · radioimmunoprecipitation assay
ROI · region of interest, region of interest
RTK · receptor tyrosine kinase

S

SDS · sodium dodecyl sulfate
SLF' · modified synthetic ligand of FKBP
SOC · super optimal broth with catabolite repression
SOS · son of sevenless
SOScat · catalytically active domains of SOS

T

TAE · Tris-acetate-EDTA
TB · terrific broth
TBS · Tris-buffered saline
TEMED · N,N,N',N'-tetramethylene-diamine
TIRF · total internal reflection fluorescence
tKRas · C-terminus ("tail") of KRas
TMP · trimethoprim
Tris · tris(hydroxymethyl)aminomethane

U

UV · ultra-violet

W

wt · wild type

10 List of figures

11 List of tables

12 Acknowledgements

Special thanks to Prof. Dr. Philippe Bastiaens for his supervision and trusting me with this exciting, but also challenging project. It was a joy to work with such a brilliant mind and I'm grateful for every bit I learnt from you.

Further, I would like to thank Dr. Leif Dehmelt for taking over the second revision.

Many thanks to the lab of Dr. Yaowen Wu, especially Dr. Laura Klewer and Dr. Xi Chen for supplying with their dimer-inducing compounds and introducing me to the technique.

Thanks to Dr. Astrid Krämer and Tanja Forck for their hard work keeping the lab organized and for their help with any minor or major issue.

I'd also like to thank all the lab technicians for their calm answers to all my thousand questions, helping with tasks when the day needed more than 24 hours, stocking supplies up and keeping the lab running.

Special thanks to Dr. Sven Müller for helping me out with all the microscopes and explaining them more than once, if needed. Also, the office grown chilies are great.

Thanks to all the past and current members of the department for all the support, helpful critique, all the on and off topic discussions. Overall, I had a great time over the years and I'm glad to have such great colleagues.

Also, I'd like to thank my family and friends who were there to enjoy the good times with me and supported me in the less good times.